Evaluation and Application of the Community Land Model for Simulating Energy and Carbon Exchange in Agricultural Ecosystems

A DISSERTATION
SUBMITTED TO THE FACULTY OF
UNIVERSITY OF MINNESOTA
BY

Ming Chen

IN PARTIAL FULFILLMENT OF THE REQUIREMENTS
FOR THE DEGREE OF
DOCTOR OF PHILOSOPHY

Adviser: Tim Griffis

June, 2016

Acknowledgements

During the past years of my Ph.D. study, I have received support and encouragement from numerous great people. First I would like to thank Dr. Tim Griffis, my advisor, for inspiring me throughout my journey, and patiently guiding me through the process of conceptualizing this research. Tim gave me a huge amount of freedom to explore various areas from land surface modeling to remote sensing to field observations. At the same time, he always challenged me to think in new ways and encouraged me to investigate deeper. I would also like to extend my gratitude to my dissertation committee: Drs. Tracy Twine, John Baker, and Marvin Bauer for their time and support over the years. I felt lucky to work with people in Tim's group: Jennifer Corcoran, Joel Fassbinder, Natalie Shultz, Zichong Chen, and Ke Xiao, who created a great atmosphere to work, discuss, and support each other. I would like to especially thank Jeff Wood for his great feedback for my first manuscript and Peter Turner for his discussion and help with this study. Thanks also go to Matt Erickson, who helped me with all kinds of lab and field work and Jeremy Smith, who provided me great suggestions during coding in Matlab.

Finally, I would like to thank my family for their support in helping me balance motherhood and studies. Without the great and selfless help from my in-laws and my parents after the birth of our two daughters Ella and Angela, I cannot have this work done. The greatest support came from my husband Zewei Song. Thank you for always being there for me, believing in me, and encouraging me to achieve my goal.

Dedication

For Zewei and our daughters, Ella and Angela.

Abstract

Land surface models (LSMs) serve as important tools for studying the interactions between the atmosphere and ecosystems, understanding biophysical feedback processes, and predicting future climate. Most state-of-the-art LSMs assessed in the fifth phase of the Coupled Model Inter-comparison project (CMIP5), however, did not include process-based crop models with comprehensive physiology and phenology. One of the most widely used LSMs, the Community Land Model (CLM), has only recently included prognostic crops (CLM4-Crop). This thesis research evaluated the CLM4-Crop LSM for corn and soybean agro-ecosystems using 54 site-years of data, improved its representation of phenology for application within the US Corn Belt, and assessed CLM's performance in simulating carbon and energy exchange for the conterminous United States.

The results indicated that CLM4-Crop has a biased phenology during the early growing season and underestimated carbon emissions from corn and soybean sites. The carbon budget for the conterminous United States estimated by CLM4-Crop showed a greater carbon sink (-0.191±0.020 PgC yr^{-1}) compared to the original CLM4-CN model (-0.139±0.034 PgC yr^{-1}). A modified model, CLM4-CropM, with improved phenology and crop physiological parameters was developed to better simulate crop gross primary production (GPP), ecosystem respiration (ER) and leaf area index (LAI). The key parameters include the maximum carboxylation rate at 25 ^{o}C (V_{cmax25}), specific leaf area at the top of the canopy (*slatop*) and a parameter determining the initial carbon allocation to leaves (*fleafi*). CLM4-CropM estimated a smaller carbon sink (-0.094±0.023 PgC yr^{-1}) than either CLM4-CN or CLM4-Crop, and the magnitude and trend of NEE was in good agreement with remote sensing-based estimates. This research has important implications for studying the long-term carbon budget of intensively cultivated regions.

Table of Contents

List of Tables

List of Figures

Chapter 1: Introduction

The United States is by far the largest producer of corn and soybean in the world, producing about 32 % and 50 % of the world's corn and soybean, respectively. Production is concentrated in the upper Midwest, where most of the fields are rainfed, rendering the crop yield in this region sensitive to climate change [*Twine et al.*, 2013; *Mourtzinis et al.*, 2015]. The crop modeling results in the IPCC AR4 showed that in mid- and high-latitude regions, rainfed crop yields may be slightly benefited from moderate-to-medium increases in temperature (1-3°C) along with increases in precipitation and CO_2. A recent study showed that in the United States, soybean yields fell by around 2.4% for every 1 °C rise in growing season temperature from 1994 to 2013 [*Mourtzinis et al.*, 2015]. Averaged across the U.S., corn planting dates advanced about 10 days from 1981 to 2005, and soybean planting dates about 12 days, which led to an increase in the latent heat flux and a decrease in the sensible heat flux in June [*Sacks and Kucharik*, 2011]. In order to estimate how future climate trends influence the agro-ecosystems and how the agro-ecosystems impact the regional energy, water, and carbon budgets, it is important to use reliable process-based climate models with prognostic crop schemes incorporated [*Betts*, 2005; *Lokupitiya et al.*, 2009; *Ma et al.*, 2012].

Historically, global climate models represented crops as grass due to the limitation of spatial crop data and crop management parameterization. Early this century, climate modelers started to introduce adaptations of complex crop schemes into land surface models to better describe managed ecosystems [*Tsvetsinskaya et al.*, 2001]. This progress

was followed by many others incorporating realistic crop processes into land surface models in order to be used in earth system models [*Kucharik*, 2003; *Bondeau et al.*, 2007; *Osborne et al.*, 2007; *Stehfest et al.*, 2007; *Gervois et al.*, 2008; *Levis et al.*, 2009; *Lokupitiya et al.*, 2009]. In this study, the Community Land Model (CLM) was chosen for it is one of the most widely used land surface schemes that has been evaluated at different scales and is ready to be coupled to regional and global atmospheric models. Compared to the unmanaged crop, the prognostic crop scheme in CLM4-Crop has more reasonable phenology over the growing season and has corrected the high bias of leaf area index (LAI) during winter in CLM3.5 with grass-like phenology for crop. However, the prognostic crop scheme in CLM has only been evaluated at limited sites [*Levis et al.*, 2012; *Drewniak et al.*, 2013] and had high LAI bias during early growing season in these studies. In general, CLM4-Crop has great potential to simulate prognostic crop over a large scale and to investigate climate-crop interactions, however, it still needs systematic testing and improvements.

During the past half century, the United States' carbon budget has been influenced by climate change, land use change, and rising CO_2. How we attribute the changes in annual flux of carbon to the different impact factors, however, remains uncertain. Reliable climate models with prognostic crop schemes can separate different climate impacts to the regional carbon budget and can provide reasonable future predictions. The regional carbon budget simulated by a process based model could be sensitive to the way we represent crop, especially in regions like the United States Corn Belt, where the agro-

ecosystem is the dominant land use type. It is important to study how sensitive the simulated regional carbon budget is to the crop schemes, before we draw conclusions from the model results.

In Chapter 2 of this Dissertation, a peer-reviewed published article, a prognostic crop phenology was added into CLM3.5 to improve its phenology simulation for corn and soybean. The phenology simulation of CLM3.5-CornSoy was evaluated and compared to another crop model, CLM4-Crop, at two Rosemount, Minnesota AmeriFlux sites. The energy, water and carbon budget simulation of CLM3.5-CornSoy and CLM4-Crop was also evaluated and compared at these sites. The performances of the two crop models at these sites were linked to the crop phenology simulation.

In Chapter 3, the CLM4-Crop and its modified version CLM4-CropM were used to simulate the energy and carbon budgets of corn and soybean at multiple AmeriFlux crop sites. CLM4-Crop was evaluated to see if its performance was reliable for the US Corn Belt and to assess if the model performance was site specific. CLM4-CropM with a new leaf emergence scheme was compared to CLM4-Crop to assess if it improved the early growing season phenology simulation and how that affects energy and carbon fluxes. Systematic model bias was identified and afterwards a calibration across sites was carried out.

In Chapter 4, the CLM model was used to diagnose changes in net ecosystem CO_2 exchange within the US Corn Belt over the period 1948 to 2004. We compared influences of different crop schemes to the regional carbon budget. The trend of the US net ecosystem CO_2 exchange over the 57 years was also analyzed.

In Chapter 5, overall conclusions of this Dissertation research are presented, along with an outline of future research directions regarding the development of CLM.

Chapter 2: Simulating crop phenology in the Community Land Model and its impact on energy and carbon fluxes[1]

2.1 Introduction

The impact of climate change on future crop system production and food security remains an important global issue [*Karl and Peterson*, 2009; *Piao et al.*, 2010; *Lobell et al.*, 2011; *Ma et al.*, 2012; *Rosenzweig et al.*, 2013; *Yin*, 2013]. Predicting the impact of future climate change on agricultural systems requires incorporation of mechanistic crop biophysical processes and interactive crop management into climate models, which remains relatively rare [*Rosenzweig et al.*, 2013]. An accurate representation of dynamic crop phenology in land surface models is crucial for predicting the energy, water and carbon budgets of these managed ecosystems [*Betts*, 2005; *Lokupitiya et al.*, 2009; *Ma et al.*, 2012]. In regions with large agricultural coverage, a reasonable estimation of crop phenology is especially important in order to simulate the regional thermodynamic properties of the atmospheric boundary layer [*Raddatz and Cummine*, 2003]. In the United States Corn Belt, soybean and corn are cultivated on approximately 600,000 km^2 of the land surface – an area greater than the entire state of California [*Griffis et al.*, 2013]. In order to predict future climate change impacts on the energy, water and carbon budgets of this region, as well as to estimate the climate impact on food production,

[1] *Chen, M., T. J. Griffis, J. Baker, J. D. Wood and K. Xiao (2015), Simulating crop phenology in the Community Land Model and its impact on energy and carbon fluxes. J. Geophys. Res. Biogeosci., 120, 310–325. doi: 10.1002/2014JG002780.*

models that can simulate crop phenology and growth under typical human management are required.

The Community Land Model (CLM) is the land surface scheme of the Community Earth System Model (CESM) and one of the most widely used land surface schemes in regional and global scale simulations [*Sacks et al.*, 2008; *Lawrence and Chase*, 2009, 2010; *Jin and Miller*, 2010; *Levis*, 2010; *Li and Zhuguo*, 2010; *Gopalakrishnan et al.*, 2011; *Sakaguchi et al.*, 2011a; *Lawrence et al.*, 2011, 2012; *Bonan et al.*, 2012; *Levis et al.*, 2012]. Since CLM is part of the Earth system model framework, it is compatible with other modeling components such as regional or global circulation models (i.e. the Weather Research and Forecasting Model and the Community Atmosphere Model) and provides an excellent platform for simulation of land surface processes of various ecosystems, including cropping systems [*Levis et al.*, 2012; *Drewniak et al.*, 2013]. CLM has been evaluated against observations across the globe over different ecosystems [*Kumar and Merwade*, 2011; *Sakaguchi et al.*, 2011b; *Wang and Zeng*, 2011; *Yuan and Liang*, 2011]. However, the model has only recently been adapted to include biophysical processes and parameters specific to major cropping systems and has been evaluated against observations at relatively few sites [*Kumar and Merwade*, 2011; *Yuan and Liang*, 2011; *Levis et al.*, 2012; *Drewniak et al.*, 2013].

The crop simulation in CLM version 3.5 [*Oleson et al.*, 2008; *Stöckli et al.*, 2008] was prescribed as grasslands (drought-stressed deciduous and unmanaged) to reduce the

constraints from limited crop management data and also to facilitate simulation of crops under future climate scenarios. The unmanaged cropland in CLM3.5 was found to underestimate leaf area index (LAI; m^2 leaf m^{-2} ground) during the growing season and simulated an unrealistically long growing season into the early winter [*Levis et al.*, 2012]. This biased crop phenology propagated into the simulations of surface albedo, soil moisture, and net ecosystem CO_2 exchange (NEE; μmol m^{-2} s^{-1}) [*Levis et al.*, 2012]. With this simplified crop parameterization, CLM3.5 was evaluated against 16 AmeriFlux sites. The simulated sensible heat flux (*H*; W m^{-2}) showed good agreement with observations, except at 9 crop sites, where CLM3.5 missed the observed two peaks of *H* during the growing season [*Kumar and Merwade*, 2011]. In another study [*Yuan and Liang*, 2011], CLM3.5 simulated daily sensible heat fluxes for two crop sites (AmeriFlux sites ARM and Bo1) were less correlated with the observations (0.50 for ARM and 0.49 for Bo1) compared to the average of 13 non-agricultural sites (0.64). [*Yuan and Liang*, 2011].

In this study we examined two versions of CLM that have cropping schemes (CLM3.5-CornSoy and CLM4-Crop) and tested them against two crop sites over a period of 4 years to evaluate their ability to simulate crop phenology, energy fluxes, and NEE. The first model, CLM3.5-CornSoy, includes phenological processes and parameters specific to corn and soybean ecosystems and simulates prognostic leaf emergence, grain filling and harvest dates. The second model, CLM4-Crop [*Lawrence et al.*, 2012; *Levis et al.*, 2012], is able to simulate prognostic corn, soybean and spring wheat for North America. Both of the crop algorithms were derived from Agro-IBIS [*Kucharik*, 2003], with some key

differences that will be described later. Here we evaluate CLM3.5-CornSoy and CLM4-Crop at two agricultural AmeriFlux sites in order to address the following questions: 1) What are the strengths and weaknesses of each model when simulating crop phenology? 2) To what extent do model errors in phenology influence the simulated energy and carbon fluxes? and 3) What are the key model deficiencies that must be addressed in order to reduce model biases in simulating phenology, energy, and carbon fluxes?

2.2 Methods

2.2.1 Phenology schemes of two crop models

CLM is the land surface scheme of CESM [*Bonan and Oleson*, 2002; *Zeng et al.*, 2002; *Dai et al.*, 2003; *Dickinson and Oleson*, 2006; *Oleson et al.*, 2008, 2010]. CLM simulates surface albedo, radiation transfer through the canopy, soil, leaf and canopy air temperature, sensible and latent heat fluxes and momentum exchange between land and atmosphere in its bio-geophysical modules. CLM simulates carbon allocation and transfer between ecosystem carbon pools (plant organs, litter and SOMs) in its biogeochemical modules. In this study, both candidate models were coupled to the CN module [*Thornton et al.*, 2007, 2009], which has demonstrated better performance in simulating photosynthesis [*Sakaguchi et al.*, 2011a].

Two versions of CLM (CLM3.5 and CLM4) are compared in this study. CLM3.5 is a transitional model from the earlier version 3.0 with an improved simulation of the hydrological cycle [*Oleson et al.*, 2004a, 2004b, 2007, 2008]. In this study, we added a crop phenology module to CLM3.5-CN. The revised model is called CLM3.5-CornSoy.

CLM4 shares similar biogeophysical and biogeochemical schemes with CLM3.5, but with modifications that have been proved to cause increased soil moisture variability, drier soils and lower soil temperature in organic-rich soils [*Oleson et al.*, 2008]. The major modifications include a revised numerical solution of the Richards equation [*Decker and Zeng*, 2009; *Zeng and Decker*, 2009], a revised ground evaporation scheme [*Sakaguchi and Zeng*, 2009] and a better representation of the hydraulic and thermal properties of organic soils [*Lawrence and Slater*, 2007]. *Levis et al.* [2012] incorporated crop-specific phenology and carbon allocation algorithms into the CLM4.0-CN [*Lawrence et al.*, 2012]. The crop plant functional type (PFT) optical properties have been parameterized according to the values presented in *Asner et al.*, [1998]. This version of the crop simulation enabled model is called CLM4-Crop.

The crop algorithms in CLM3.5-CornSoy are specific to corn and soybean, the dominant crops in the Corn Belt, and were first implemented in Agro-IBIS. Agro-IBIS has been evaluated for North American mid-latitude study sites [*Kucharik and Twine*, 2007; *Twine and Kucharik*, 2009]. Two phenological phases of crops are simulated in CLM3.5-CornSoy: phase 1 is from leaf emergence to the beginning of grain fill, and phase 2 is

from the beginning of grain fill until harvest. Before phase 1 is initiated, CLM3.5-CornSoy calculates the growing degree time (GDT, or heat unit) and tests if it reaches the leaf emergence threshold (GDT_{on}, Table 2.1). When GDT exceeds the threshold, leaf emergence occurs, assuming that land managers have already planted their fields. The timing of grain fill is simulated using GDT with a different threshold (GDT_{grain}, Table 2.1). When the crops reach the grain filling stage, the LAI stops increasing as crops begin to allocate more carbon into the reproduction pool. In CLM3.5-CornSoy, background litter fall was increased in order to represent the reduction of carbon allocated to leaves. Thus, once the grain filling is initiated, LAI will start to decrease slowly. Harvest time is estimated using day length, similar to the way leaf off is simulated for seasonal deciduous trees.

GDT is a thermal time variable similar to growing degree days (GDD), but calculated on a half-hourly model time step:

$$GDT = \int (T_{air} - T_{ref}) \cdot dt \text{ , when } T_{air} > T_{ref} \quad (2.1)$$

Here, T_{air} is the air temperature at 2 m and the reference temperature T_{ref} is 8℃.

Compared to GDD, GDT is more sensitive to temperature variations especially in early growing season. For example, during early growing season, some days have several hours above the base temperature but the daily averaged temperature is below the base temperature. In this case the temperature will accumulate in GDT but not GDD.

The harvest time is estimated using the daytime length *Day_L* as the threshold (Table 2.1). The process of harvest is simplified as a rapid "litter fall". Currently this model does not simulate the reproductive carbon pool.

The crop algorithm in CLM4-Crop also originated from the Agro-IBIS model [*Levis et al.*, 2012]. The crop types in CLM4-crop include corn, soybeans, and temperate mid-latitude cereals. In this study, only corn and soybean schemes were tested because they represent the dominant cropping system in the Corn Belt. CLM4-Crop simulates one more phenological phase than does CLM3.5-CornSoy. Phase 1 in CLM4-Crop starts at planting and ends with leaf emergence. Phase 2 and phase 3 are the same as CLM3.5-CornSoy's two phases. In CLM4-Crop, harvest commences automatically when the crops reach physiological maturity, which is defined by a GDD threshold.

Another important difference between the phenology algorithms used in these two models is that CLM4-Crop has a maximum constraint on LAI (5 for corn, 6 for soybean), while CLM3.5-CornSoy does not limit the maximum LAI. The benefit of using a maximum constraint is that the values are guaranteed to fall within a realistic range; however, such approaches are not physically-based and can result in a loss of information such as masking of inter-annual variations in maximum LAI values.

2.2.2 Crop parameterization in the two models

Two other modifications to CLM3.5 were made to better simulate corn and soybean systems. In the original model, there was a nitrogen limitation in place for all plant functional types. Here, we assume that nitrogen is not limiting since for corn it is typically applied according to guidelines developed in each state through N rate experiments by Extension Service scientists. "Safety" factors are typically built into these guidelines to virtually ensure that N will not be yield-limiting. Soybeans are legumes that derive their N from symbiotic bacteria. Thus the nitrogen limitation in the original CLM3.5-CN was removed for corn and soybean. The same approach is used in CLM4-Crop, with the nitrogen limitation disabled for corn, soybean, and temperate cereals [*Levis et al.*, 2012]. The second change we made was only for corn. The fraction of leaf nitrogen in Rubisco was modified from 0.1 to 0.05 according to previous studies on C_4 plants [*Schmitt and Edwards*, 1981; *Rowan et al.*, 1987; *Makino et al.*, 2003]. This modification was made to prevent unrealistically high photosynthetic rates.

In CLM4-Crop, the maximal carboxylation rate at 25 ^{o}C (V_{cmax25}) was set to 101 μmol CO_2 m^{-2} s^{-1} for corn, soybean and temperate cereals according to measured values for C_3 crops [*Kattge et al.*, 2009], compared to 50 μmol CO_2 m^{-2} s^{-1} in CLM3.5-CornSoy [*Wullschleger*, 1993; *Kucharik et al.*, 2000; *Oleson et al.*, 2007] (Table 2.1).

In CLM3.5-CornSoy, the leaf orientation index for corn and soybean is -0.3 (Table 2.1) which was adopted from the Simple Biosphere Model (SiB) [*Dorman and Sellers*, 1989].

The leaf orientation index describes the departure of leaf angles from a random distribution and equals +1 for horizontal leaves, 0 for random leaves, and –1 for vertical leaves. In CLM4-Crop, the leaf orientation index for corn and soybean was set to the more vertical orientation of -0.5 according to the Agro-IBIS values [*Levis et al.*, 2012]. A detailed list of CLM4-Crop parameter values can be found in Levis et al. [2012].

2.2.3 The water stress factor

Both CLM3.5 and CLM4 use a PFT-dependent water stress factor to describe the soil water constraint on the transpiration or photosynthetic rate. This water stress factor is calculated as:

$$\beta_t = \sum_i w_i r_i \qquad (2.2)$$

where w_i is a plant wilting factor for layer i and r_i is the fraction of roots in layer i. Currently, both models use a static root distribution function to describe all crop PFTs. The plant wilting factor is then calculated according to the soil water matric potential [*Oleson et al.*, 2004b, 2010]. Here the soil layer needs to be hydrologically active and in CLM4 this is defined as the upper 10 of the total 15 soil layers.

2.2.4 Model spin-up

During spin-up, CLM3.5-CornSoy and CLM4-Crop were run offline and driven by the Princeton meteorological forcing data set [*Sheffield et al.*, 2006]. The data ranged from 1948 to 2008. The spatial and temporal resolution was 1 × 1^{o} and 3-hours, respectively. The meteorological fields include solar radiation, air temperature, air humidity, air pressure, wind speed, and precipitation. To ensure the models reached a steady state (i.e. that the slowest soil storage pools of carbon had reached equilibrium), we recycled the forcing data for 4000 years for CLM3.5-CornSoy and 1000 years for CLM4-Crop [*Thornton and Rosenbloom*, 2005; *Sakaguchi et al.*, 2011a]. After spin-up, the soil organic carbon (SOC) of the field reached a steady-state value of 20.6 and 11.2 kg C m^{-2} in CLM3.5-CornSoy, and 21.7 and 10.1 kg C m^{-2} in CLM4-Crop for corn and soybean, respectively. These values are in close agreement with the National Cooperative Soil Survey values (14.2 to 22.7 kg C m^{-2}).

2.2.5 Research Sites

The AmeriFlux sites US-Ro1 and US-Ro3 are located approximately 25 km to the south of Minneapolis/St. Paul (44°41′19″ N, 93°4′22″ W; 259.7m ASL). The two sites are about 500 m apart, with US-Ro3 in the north and US-Ro1 in the south. Both sites are rain-fed rotation fields of corn (*Zea mays*) and soybean (*Glycine max*). Waukegan silt loam (fine, mixed, mesic typic hapludoll) is the major soil type in these two fields with a surface layer of high organic carbon content (2.6% average) and variable thickness (0.3-2.0 m) underlain by coarse glacial outwash sand and gravel with little water-holding

capacity. The average air temperature from 1980 to 2010 was 7.8°C with a maximum annual mean temperature of 13.0°C. The annual average precipitation for the same period was 814 mm. One major difference between the two sites is that US-Ro1 is under conventional management and US-Ro3 is managed under reduced tillage with winter cover crops [*Baker and Griffis*, 2005]. These site differences, with near identical meteorology, provide a good opportunity to evaluate the robustness of the crop scheme implemented in CLM. At site US-Ro1, corn was grown in 2007 and 2009 and soybean was grown in 2008 and 2010. At site US-Ro3, corn was grown in 2007, 2008 and 2010 and soybean was grown in 2009. These 8 site-years of data were used to test the CLM3.5-CornSoy and CLM4-crop simulations.

The meteorological forcing data were averaged over the two sites (approximately 500 m apart from each other) for every hour to get an ensemble forcing data set from 2007 to 2010. Data used to drive the model included solar radiation (Eppley PSP, The Eppley Lab, Newport, RI, USA), air temperature and humidity (HMP35C, Vaisala Inc., MA, USA), air pressure, wind speed (CSAT3, Campbell Scientific, Inc., UT, USA), and precipitation. Precipitation was measured using two instruments, a tipping bucket rain gauge (6028-B, All Weather Inc., CA, USA) with a precision of 0.25 mm for liquid precipitation, and a weighing rain gauge (Geonor T-200B, Campbell Scientific, Inc., UT, USA) for solid precipitation. We did not use the tipping bucket rain gauges in the winter because they are known to systematically under-estimate snowfall [*Groisman and Legates*, 1994; *Upton and Rahimi*, 2003]. The time attribution of the local measured

meteorological data is converted from local time to the Greenwich Mean Time (GMT) to be consistent with CESM. LAI was measured approximately once a week with an AccuPar hand-held sensor (AccuPAR, Mode PAR-80, Decagon Devices Inc., Pullman, WA, USA).

2.2.6 Model evaluation data

Eddy covariance (EC) measurements of sensible heat flux (H; W m^{-2}), latent heat flux (LE; W m^{-2}) and net ecosystem CO_2 exchange (NEE; μmol m^{-2} s^{-1}) have been ongoing at these two sites since 2004 [*Baker and Griffis*, 2005]. These fluxes were quality controlled and filtered using a friction velocity (u_*) threshold greater than 0.1 m s^{-1} (a typical value for agricultural land) to eliminate periods of weak turbulence and were gap filled. Systematic errors in EC measured *H* and *LE* due to a lack of energy balance closure were corrected by assuming the available energy (the residual of the net radiation minus the ground heat flux) and the Bowen ratio were measured correctly. *H* and *LE* were increased proportionally for each half hourly period to force energy balance closure [*Blanken et al.*, 1997; *Xiao et al.*, 2010b]. Soil heat flux (*G*) at the surface was estimated by correcting the measured heat flux at a soil depth of 10 cm (HFP01SC, HukseﬂuxUSA, Inc., NY, USA) using the calorimetric method. The required soil temperature measurements were made using thermocouples positioned above (but offset from) the heat flux plates. Other details regarding the EC measurements, data processing, and data quality assessment can be found in previous studies [*Baker and Griffis*, 2005; *Griffis et al.*, 2005].

The EC measured NEE was partitioned into gross primary production (GPP) and ecosystem respiration (ER) using the Fluxnet Canada methodology described by Barr et al. [2004]. The grain yield for each site was recorded by the Rosemount Research and Outreach Center at the University of Minnesota. Using the lab measured mean grain carbon content (45% for corn and 54% for soybean), we calculated the carbon lost through harvest each year [*Baker and Griffis*, 2005]. In order to close the annual carbon budget for cropping systems we have estimated the Net Biome Productivity (NBP) by adding the harvested grain carbon (a carbon loss) to the EC measured annual NEE:

$$NBP = NEE + C_{grain} \quad (2.3)$$

where C_{grain} is the harvested grain carbon calculated from the yield data at the sites.

2.2.7 Evaluation of model performance

In our simulations, only one crop is growing in the entire grid cell. No other PFTs are growing in the grid cell. The footprint of the NEE measurement is also within the field. Thus we can compare the measured and simulated fluxes.

The metrics used for evaluating model performance were the correlation coefficient and bias.

The correlation coefficient (r) of a variable X was calculated as:

$$r = \frac{\sum_{i-1}^{n}(X_{mi} - \overline{X_m})(X_{oi} - \overline{X_o})}{\sqrt{\sum_{i-1}^{n}(X_{mi} - \overline{X_m})}\sqrt{\sum_{i-1}^{n}(X_{oi} - \overline{X_o})}} \quad (2.4)$$

where X_m and X_o are the modeled and observed values, respectively, and over-bars represent means.

Model bias was calculated as the mean of the model-observation residuals [*Schaefer et al.*, 2012]:

$$b = \overline{(X_{mi} - X_{oi})} \qquad (2.5)$$

A positive bias indicates that the model overestimated the observations.

The ideal model will have r=1 and b=0. If the modeled values yield a correlation coefficient close to 1, but a large bias, we can conclude that the model has captured the dynamics of the processes, but that relevant parameter values need further optimization. If the modeled values yield a bias close to 0, but a low correlation coefficient with the observations, we can conclude that the model does not adequately capture the dynamics of the processes. In this situation, a more realistic mechanism needs to be developed to improve the simulation.

2.3 Results and Discussion

2.3.1 Phenology

The seasonal patterns of LAI are provided in Figure 1.1. The correlation coefficient between simulated and observed corn LAI for CLM3.5-CornSoy was 0.71 (b=1.60) and for soybean, 0.81 (b=2.54). CLM4-Crop simulations yielded LAI correlation coefficients of 0.35 (b=1.39) for corn and 0.22 (b=2.71) for soybean. Overall, both models overestimated LAI during the growing season. The CLM4-Crop simulated LAI was less correlated with the observations because of unrealistically high LAI values during the early growing season in all modeled years. This overestimated LAI in the early growing season in CLM4-Crop was also observed in previous studies [*Levis et al.*, 2012; *Drewniak et al.*, 2013], where they suggested that the planting date was biased earlier. In this study, CLM4-Crop predicted planting dates were within 10 days of the actual planting dates. Thus, the timing of leaf emergence seems to be predicted early after planting in CLM4-Crop. Further, it is likely that using the observed crop V_{cmax25} value of 101 μmol CO_2 m^{-2} s^{-1} [*Kattge et al.*, 2009] in the present canopy radiative transfer scheme also contributed to the amplified growth rate. *Bonan et al.* [2012] found that the use of leaf-level measured values of V_{cmax25} within the sunlit-shaded big-leaf framework of CLM resulted in higher photosynthetic rates when nitrogen was non-limiting (i.e. for cropping systems). Although currently CLM4-Crop uses the maximum LAI constraint to limit corn and soybean LAI under 5 and 6, respectively, this early growing season offset represents an important model bias that propagates into energy and carbon flux simulations that needs to be corrected.

Compared to CLM4-Crop, CLM3.5-CornSoy displayed more year-to-year LAI variability. For example, in 2007, the U.S. Drought Monitor classified the study region in the moderate drought category due to below normal rainfall in June and July. This caused a significant depletion of soil water content. This phenomenon was captured by CLM3.5-CornSoy as a lower maximum LAI for 2007 than other years for both corn and soybean (maximum LAI of corn for 2007 was about 5, while in other corn years it reached 7 to 8). CLM4-Crop did not capture this inter-annual variability because the simulated LAI reached the model's maximum LAI limit every year (Figure 1.1). On the other hand, CLM3.5-CornSoy overestimated corn maximum LAI in 2008 and 2010 by 2. These uncertainties are diagnosed further in section 3.3.

Both models predicted the timing of grain-filling (peak LAI) very well for all years. The harvest dates were simulated earlier than the real harvest dates in both models. This is because in the model, harvest happens when the crops reached physiological maturity and in practice, farmers often delay harvest to allow the grain to dry in the field (e.g., moisture content lower than 20%) to minimize or eliminate fossil fuel-based drying prior to storage or shipping. The simulated harvest date was usually in September, while the actual corn and soybean harvest in the Upper Midwest typically occurs from late October to mid-November.

The overall need to improve the understanding of environmental controls on vegetation phenology was highlighted by *Richardson et al.* [2012]. They examined the simulation of phenology in 14 land surface schemes at 10 forested sites. Their results indicate that it is a major challenge for state-of-the-art models to predict how phenology responds to future climate change. For example, simulations of deciduous forest phenology misrepresent the critical transition periods in nearly all cases. They found that the simulations were biased with longer growing seasons and over-estimation of gross ecosystem photosynthesis by $+160 \pm 145$ g C m^{-2} yr^{-1} in spring and $+75 \pm 130$ g C m^{-2} yr^{-1} in fall. In the next sections, we examine the extent to which bias in crop phenological simulation impacts the energy and carbon flux simulations.

2.3.2 Energy fluxes

The two models share identical schemes for simulating the energy balance. All of the energy flux related differences we report in this section can be attributed to the differences in phenological and hydrological schemes, as well as the different parameterizations in crop optical properties.

The modeled hourly net radiation (R_n) was highly correlated with the observations ($r>0.92$) but was slightly overestimated by both models (1.2). The averaged CLM3.5-CornSoy R_n bias was 6.7 W m^{-2} for corn and 17.6 W m^{-2} for soybean. The averaged CLM4-Crop R_n bias was 9.1 W m^{-2} for corn and 18.9 W m^{-2} for soybean. Further, the

simulated R_n was consistently biased higher for the soybean canopy than the corn canopy in both models. There are two major differences in the parameterization of crop leaf optical properties in the two models. First, CLM4-Crop defines a more vertically oriented leaf distribution adopted from Agro-IBIS than CLM3.5-CornSoy (see section 2.1.2). Leaf orientation depends on species and can vary as a function of season (phenology) [*Ross*, 1975]. *Ross and Ross* (1969) provided leaf angle distribution formulae, and summarized data for the leaf angle distribution factor for different crops. The value for corn ranged from -0.13 to 0.46. The authors did not report parameter values for soybean. Instead, they provided estimates for another bean crop (*Vicia faba*), that ranged from 0.30 to 0.39 [*Ross and Ross*, 1969; *Ross*, 1975]. The CLM3.5-CornSoy leaf angle distribution factor of -0.3 and the CLM4-Crop leaf angle distribution factor of -0.5 for crops are too vertical compared to these observations. Our field data and analyses [*Baker and Griffis*, 2008, 2012] show that both corn and soybean leaves have a close to spherical distribution, but more horizontal than vertical (see Figure S1 S2). The typical leaf angle distribution factors at our sites from leaf emergence to grain fill (maximum LAI) and from grain fill to harvest are 0.17 and 0.12 for corn and 0.17 and 0.18 for soybean. Our sensitivity tests indicate that the more horizontal distribution will amplify the net radiation bias. The parameterization scheme for the optical properties of crops are different in the two models. CLM3.5-CornSoy adopted parameters of crop leaf and stem reflectance, transmittance from *Dorman and Sellers* [1989]. CLM4-Crop uses parameters from *Asner and Wessman* [1998], which have a significantly lower reflectance and higher transmittance for crops. That partly explains why CLM4-Crop has higher net radiation

simulated for both crops. However, the parameters used in CLM4-Crop are closer to the documented values in previous studies [*Walter-Shea et al.*, 1989; *Walter-Shea and Norman*, 1991; *Schepers et al.*, 1996]. Thus we examined the monthly bias of R_n and LAI. The linear regression showed positive correlations between monthly LAI bias and monthly net daytime and nighttime long wave radiation biases (r^2=0.20, 0.36, respectively; both p value less than 0.01, see Figure S3 S4). These analyses indicate that high LAI is associated with a lower canopy temperature and, therefore, less outgoing long wave radiation, both during daytime and nighttime. These results highlight that in order to improve the R_n bias, a better crop phenology (LAI) simulation is needed. This is a challenging task because of the feedbacks among LAI, radiation balance, photosynthesis, and leaf growth.

Although the total energy received by the canopy only had a bias within 20 W m^{-2}, there were important deficiencies when partitioning the total energy into *H*, *LE*, and *G*.

CLM4-Crop exhibited less bias in simulated *H* than CLM3.5-CornSoy. The correlation coefficient for *H* between CLM4-Crop simulation and observation was 0.64 (*b*=6.8 W m^{-2}) for corn and 0.52 (*b*=8.1 W m^{-2}) for soybean. For CLM3.5-CornSoy the correlation coefficient for *H* was 0.70 (*b*=-31.4 W m^{-2}) for corn and 0.70 (*b*=-9.9 W m^{-2}) for soybean. The monthly averaged biases of *H* simulations for corn and soybean are shown in Figure 2.1. Both models underestimated *H* (-40 to -60 Wm^{-2}) in May. During the mid-growing season (July and August), *H* was generally over-estimated by both models (Figure 2.1

b,c,d), except for corn in CLM3.5-CornSoy (Figure 2.1 a). CLM4-Crop showed more pronounced high bias of *H* during mid-growing season for both crops. This indicates that CLM4-Crop likely overestimated leaf temperature during the mid-growing season. The leaf temperature data in Table 2.2 show that this was the case. This bias is examined further below by considering the model *LE* simulations.

CLM3.5-CornSoy performed slightly better in simulating *LE.* The correlation coefficient between simulated and observed corn *LE* for CLM3.5-CornSoy was 0.89 (b=8.1 W m^{-2}) and for soybean, 0.83 (b=9.6 W m^{-2}). CLM4-Crop simulations gave an *LE* correlation coefficient of 0.79 (b=-27.3 W m^{-2}) for corn and 0.68 (b=-15.2 W m^{-2}) for soybean. These results indicated that *LE* was overall underestimated for both corn and soybean by CLM4-Crop. This *LE* deficiency is pronounced during middle and late growing season (July to September) when transpiration becomes a major fraction of evapotranspiration (Figure 2.1).

To determine what caused the underestimation of *LE* and the over-estimation of *H* from July to September in CLM4-Crop, we examined the soil water content (SWC) along with the root distribution for crops (Figure 2.2). The trends are the same in all years. As an example, Figure 2. shows the evaluation of SWC in 2008 at site US_Ro1. CLM3.5-CornSoy and CLM4-Crop performed similarly when simulating SWC in layers above -5 cm and -15 cm. The amplitude of inter-annual SWC variation was captured well to the depth of -15 cm, however, both models have a slightly earlier (about 7 days) onset of

SWC increase caused by earlier snowmelt. CLM4-Crop overestimated SWC at depth of 5 cm from Mid-April to late June by about 10%. From July to September, CLM4-Crop underestimated SWC in all layers. The most pronounced underestimation (around 20%) is from -15 cm to -50 cm, where most of the crop roots are located. CLM3.5-CorySoy also underestimated SWC from -5 cm to -50cm during this period, with the amplitude less than CLM4-Crop (around 10%). At the depth of -100 cm, CLM3.5-CornSoy simulated a wetter soil than observed. In contrast, CLM4-Crop simulated a much drier soil than observed (SWC close to 0). The simulated drier soil in CLM4-Crop led to a higher than normal water stress, which was calculated in the model as a smaller β_t (see section 2.1.3). This biased water stress factor further constrains transpiration and caused the underestimation of *LE* in CLM4-Crop. Overall, both models significantly underestimated SWC (around 20%) during mid growing season at soil layers above -50 cm, and CLM4-Crop underestimated SWC to the depth of 100cm. Therefore, additional work is needed to improve soil water dynamics especially at deeper soil layers. Further, when calculating water stress for crops, a reasonable root distribution is very important. Currently in both models, the root distribution for all crop PFTs is a static equation and the roots in CLM4-Crop are distributed towards shallower soil than CLM3.5-CornSoy. Root distribution can vary substantially depending on soil type, soil water availability, crop type and other management factors like tillage and fertilization. Maximum rooting depths, reported in previous studies, ranged from 90 to 240 cm, and 70 to 180 cm for corn and soybean, respectively [*Allmaras et al.*, 1973; *Dwyer et al.*, 1988; *Keller and Bliesner*, 1990; *Laboski et al.*, 1998]. *Drewniak et al.* [2013] incorporated a dynamic rooting

scheme into CLM4-Crop to estimate plant root growth and response to environmental conditions. A similar approach could improve the SWC simulation and biases associated with crop water stress.

The simulated *G* had the lowest correlation with observations (0.30-0.64) of all energy fluxes. Since *G* is calculated as the residual of the surface energy balance in both models, errors in *H* and *LE* propagate into *G*. *G* was biased high in almost all years for both models (Figure 2.3 as an example), indicating that the simulated sums of *H* and *LE* were biased low. In a number of previous studies, eddy covariance measurements of *H* and *LE* were used directly in model parameterization and evaluations [*Stöckli et al.*, 2008] before energy balance closure corrections were applied. Eddy covariance measured *H* and *LE* typically represent about 80% of the available energy (R_n-*G*) [*Wilson et al.*, 2002], so parameterizing the model in this way might result in systematically underestimated sum of *H* and *LE*. This may be one reason contributing to the large bias in *G*. Other energy storage terms (i.e. canopy storage, photosynthesis, etc) that have not been calculated explicitly for this comparison may also contribute to the bias, but these terms are expected to be relatively small for corn and soybean.

2.3.3 Carbon fluxes

Overall, both models simulated the amplitude of seasonal NEE reasonably well. The average correlation coefficients were 0.87, 0.88 and 0.59 for NEE, GPP and ER for

CLM3.5-CornSoy and 0.55, 0.68 and 0.29 for CLM4-Crop (Table 2.3). The lower correlation coefficients for CLM4-Crop were due to three reasons:

First, the accuracy of the NEE and GPP simulations are intimately connected to the phenology simulations. The overestimated LAI during the early growing season in CLM4-Crop led to positive NEE and GPP biases during this period. From May to June, CLM3.5-CornSoy performed better at simulating GPP (r=0.93, b=3.73 μmol m^{-2} s^{-1}) and NEE (r=0.83, b=-1.18 μmol m^{-2} s^{-1}). CLM4-Crop always overestimated GPP (r=0.77, b=8.25 μmol m^{-2} s^{-1}) and underestimated NEE (r=0.66, b=-6.44 μmol m^{-2} s^{-1}) for all modeled early growing seasons, due to its overestimated early growing season LAI.

Second, the approach adopted by CLM4-Crop to account for the carbon flux (loss) associated with harvested grain is to "dump" the harvested biomass into the litter pool within a single time step. This obviously results in an unrealistic CO_2 emission when compared to the observations and thus lower correlations between the EC measured and modeled NEE and ER. However, for a global simulation, using this approach over the long term is a valid assumption and closes the carbon budget. For CLM3.5-CornSoy, this simplified model only considers crop phenology and there is no reproductive carbon pool currently. Thus CLM3.5-CornSoy does not simulate the decomposition of the harvested grain carbon, it only simulates the decomposition of the above ground biomass as litter fall, and the result agrees well with the EC measurement.

Third, unrealistic water stress in CLM4-Crop caused biased GPP for soybean. CLM4-Crop captured some of the water stress events for corn, when the GPP of corn was reduced due to limited soil water (Figure 2.4b). However, for soybean, the CLM4-Crop simulations were too sensitive to soil moisture. GPP was overestimated when there was sufficient SWC and underestimated when there was a deficiency in SWC. This simulation problem arises from the bias in soil water content (i.e. too dry for all of the soil layers during mid and late growing season) simulated in CLM4-Crop that led to an overestimation of water stress in July, August and September. CLM3.5-CornSoy performed better at simulating both GPP and ER for soybean.

CLM4-Crop did a better job of simulating the amplitude of GPP for the corn years, largely due to its restriction of maximum LAI. Although CLM3.5-CornSoy performed well in simulating the seasonal pattern of GPP, the maximum values of GPP for corn were significantly overestimated (Figure 2.4b) due to high bias in LAI during late growing season (Figure 1.1). Currently, the assumption of no nitrogen limitation all-year-round for crops might need further investigation. Since growth respiration was calculated in CLM as a fraction of GPP, ER was also overestimated in CLM3.5-CornSoy for corn, which offset GPP in simulating a reasonable corn NEE in CLM3.5-CornSoy. For soybean, CLM3.5-CornSoy captured the timing of leaf emergence and grain filling very well. The peak GPP was also captured by the model but GPP during early and late growing season was overestimated. This indicated that the model had a good estimation of the photosynthesis rate during peak season, but one single value of V_{cmax25} is not suitable for

early and late growing season. In the newly released CLM version 4.5, a day length dependent V_{cmax25} was introduced to include the seasonal variation of V_{cmax25} [*Bonan et al.*, 2012; *Oleson et al.*, 2013]. The upscaling of photosynthesis from leaf level to canopy level was also improved by considering the change of V_{cmax25} with depth in the canopy. This change has the potential to improve the early growing season bias of GPP simulated by CLM4-Crop.

Based on our NEE EC measurements, the corn field was a carbon sink (-0.49 ± 0.12 kg C m^{-2} yr^{-1}. The uncertainty presented here was calculated as the standard error of the annual NEE.). After adding the harvested grain carbon of 0.60 ± 0.09 kg C m^{-2} yr^{-1} to the annual NEE, the corn fields became a small carbon source, releasing approximately 0.07 ± 0.10 kg C m^{-2} yr^{-1} into the atmosphere (Figure 2.5). The CLM4-Crop estimated annual NBP was -0.39 ± 0.05 kg C m^{-2} yr^{-1}, representing a carbon sink, mainly caused by the high bias in GPP during the early growing season. CLM3.5-CornSoy currently does not simulate the reproductive pool. The NEE in CLM3.5-CornSoy of -0.57±0.05 kg C m^{-2} yr^{-1} was in close agreement with NEE measured by eddy covariance. When we added the measured yield carbon to CLM3.5-CornSoy results, the estimated NBP was 0.04 ± 0.11 kg C m^{-2} yr^{-1}, and in excellent agreement with the observed values.

Soybean was almost carbon neutral with an averaged NEE of 0.02 ± 0.02 kg C m^{-2} yr^{-1} carbon released into the atmosphere based on the EC measurement. After we added the harvested carbon of 0.21 ± 0.02 kg C m^{-2} yr^{-1} into the annual carbon budget, the soybean

fields became a carbon source of 0.22 ± 0.04 kg C m^{-2} yr^{-1} (Figure 2.5). CLM4-Crop estimated annual soybean NBP was 0.10 ± 0.07 kg C m^{-2} yr^{-1}. However, based on the previous analyses we know that photosynthesis was biased high in the model, but that the unrealistic water stress offset this bias. CLM3.5-CornSoy, without considering harvested carbon, gave a more negative NEE of -0.31 ± 0.04 kg C m^{-2} yr^{-1}. After we added the observed harvested carbon to the CLM3.5-CornSoy budget it brings the annual NBP to -0.10 ± 0.06 kg C m^{-2} yr^{-1}. This value is more negative than the observed value, due to the overestimated GPP during early and late growing season (Figure 2.4b).

If we assume corn and soybean are equally distributed (each take up 50% of the total 60 million ha cultivated area) in the corn belt, and assume that the productivities observed at these two fields are typical for the corn belt, then the total annual NEE in the corn belt area would be -141 ± 99 Tg C yr^{-1}, without considering carbon removed through harvest. In an atmospheric inversion study using 8 tall towers (100 m CO_2 measurement level) over the corn belt region (100 million ha), the NEE was derived to be -178 ± 35 Tg C yr^{-1} from June to December, 2007 [*Lauvaux et al.*, 2011]. These studies took a flux measurement point of view and did not consider the decomposition of the harvested grain (CO_2 leakage) outside of the flux tower footprint. If we add the harvested carbon and calculate the annual NBP, the Corn Belt becomes a carbon source of 89 ± 41 Tg C yr^{-1}. The CLM4-Crop estimated value was -87 ± 36 Tg C yr^{-1}. This negative offset is largely due to the bias of early growing season phenology simulated in CLM4-Crop. CLM3.5-CornSoy also estimated a carbon sink with an annual NBP of -18 ± 94 Tg C yr^{-1}

presumably because of the overestimation of soybean GPP during the early and late growing season.

2. 4 Conclusion

This study evaluated two models, CLM3.5-CornSoy and CLM4-Crop at two different corn-soybean AmeriFlux sites from 2007 to 2010. Our analyses indicate that:

1. The two models with their prognostic crop phenology captured the seasonal pattern of LAI reasonably well. CLM4-Crop overestimated LAI during the early growing season, due to earlier estimation of leaf emergence and a V_{cmax25} value that does not have seasonal variation. Both models showed positive LAI bias for both corn and soybeans for all of the growing seasons. The LAI bias of CLM3.5-CornSoy was 1.6 for corn and 2.5 for soybean. CLM4-Crop gave an LAI bias of 1.4 for corn and 2.7 for soybean. These LAI biases propagated into the energy and carbon flux simulations. Future work is needed to improve the crop phenology simulation, especially during the early growing season. For example, a V_{cmax25} with seasonal variation should help to reduce the early growing season growth rate and thus assimilate less carbon during this period. Future studies should focus on the driving mechanisms of seasonal variations of crop photosynthesis and carbon allocation associated with leaf growth and should work to eliminate the need for setting a maximum LAI constraint.

2. Net radiation was biased high in both models and was especially pronounced for soybeans. This bias was partially compensated by using a leaf angle distribution value that was too vertical compared to field observations. The bias is likely to be more pronounced if the leaf angle distribution parameter is modified towards a more realistic value (0.17-0.12 and 0.17-0.18) as observed for corn and soybean, respectively. Here, we propose that the bias in LAI (phenology) is the main cause of the net radiation bias, because higher LAI leads to a lower surface temperature and thus a positive net long wave radiation bias. This bias has important implications for radiation balance, energy partitioning, and carbon cycling.

3. CLM4-Crop showed higher *H* and lower *LE* than observations from July to September, which we attribute to the underestimated SWC of all soil layers during this period. CLM3-Crop performed similar to CLM4-Crop to the depth of -50cm, but predicted a much wetter soil at a depth of -100 cm. This overestimated deeper soil SWC in CLM3.5-CornSoy partly offset the dry bias in the upper soil layers. Future work should focus on the mechanism of soil water dynamics especially for the deeper soil layers (lower than -15cm).

4. Field observations indicated that both corn and soybean systems were carbon sources. However, both models underestimated the carbon emissions. Corn in CLM4-Crop and soybean in CLM3.5-CornSoy are even predicted as carbon sinks. These biases emphasize the need to improve the crop phenology simulation in earth system models.

Chapter 3: Can CLM4-Crop accurately simulate the long-term carbon budget across agricultural sites?

3.1 Introduction

LSMs serve as important tools for studying the interactions between the atmosphere and ecosystems, understanding biophysical feedback processes, and predicting future climate. Most state-of-the-art LSMs assessed in the fifth phase of the Coupled Model Inter-comparison project (CMIP5), however, did not include process-based crop models with comprehensive physiology and phenology. The development and evaluation of land surface models (LSMs) with prognostic agricultural schemes remains an active and important topic of inquiry [*Tsvetsinskaya et al.*, 2001; *Kucharik*, 2003; *Bondeau et al.*, 2007; *Osborne et al.*, 2007; *Stehfest et al.*, 2007; *Gervois et al.*, 2008; *Lokupitiya et al.*, 2009; *Levis et al.*, 2012; *Song et al.*, 2013; *Wu et al.*, 2015; *Chen et al.*, 2015]. Such advances are important for achieving realistic simulations of weather and climate, and increasing our capacity to develop sound policies regarding the impacts of climate change on agricultural systems and the potential impacts of land management on climate [*Levis et al.*, 2012].

The first attempt to incorporate explicit crop simulations into a land surface model (name here) was made early this century by *Tsvetsinskaya et al.*, [2001]. The Biosphere-Atmosphere Transfer Scheme (BATS) was modified to include plant growth functions

for corn. The modified model showed improved simulation of surface fluxes and temperature over an agricultural region in dry, normal and wet years in central and eastern Nebraska and eastern Kansas. Since then, there have been numerous advances in developing and improving the representation of agricultural systems within LSMs.

Kucharik and Brye [2003] incorporated phenology, carbon allocation, and a corn-specific parameterization into the Integrated Biosphere Simulator (IBIS). The model was further developed to include other crops (soybean, winter and spring wheat). Its ability to simulate crop yields, water and energy balance, and impacts of climate change on agro-ecosystems in the United States were investigated at multiple sites and scales [*Donner and Kucharik*, 2003; *Kucharik*, 2003; *Twine et al.*, 2004, 2013; *Kucharik and Twine*, 2007; *Twine and Kucharik*, 2009; *Webler et al.*, 2012; *Xu et al.*, 2016].

Gervois et al. [2004] incorporated a crop simulation model (STICS) into the French LSM ORCHIDEE to simulate winter wheat and maize and evaluated the model at two sites in Western Europe and two sites in the United States for single years. They identified a systematic overestimation of corn water stress at the AmeriFlux Bondville site in response to rain deficit, which led to a substantial underestimate in the carbon sink strength (2 gC m^{-2} day^{-1}). *Bondeau et al.*, [2007] introduced a dynamic representation of crop phenology, carbon allocation, and management practices for 13 crop functional types into the Lund-Potsdam-Jena (LPJ) Dynamic Global Vegetation Models (DGVMs), and evaluated the coupled model LPJmL at two agricultural sites in the United States

(Bondville, Illinois and Ponca, Oklahoma) and one in Europe (Jokioinen, Finland). The LPJmL model did not explicitly represent the conventional corn and soybean rotation that is common in the US Corn Belt. This resulted in a pronounced corn-phase simulation bias with unrealistic high-cumulated soil carbon and a substantial overestimation of ecosystem respiration (ER) (i.e. up to 200 gC m^{-2} $month^{-1}$).

Van den Hoof et al., [2011] introduced a crop model for simulating winter wheat into the Australia LSM JULES (JULES-SUCROS). This model was evaluated at six European FLUXNET crop sites. They showed that JULES-SUCROS significantly improved the correlation between simulated and observed fluxes over cropland compared to the default grass-like treatment of crops. *Song et al.* [2013] developed a dynamic crop scheme for corn and soybean and implemented them into the Integrated Science Assessment Model (ISAM). The model was calibrated and evaluated using AmeriFlux observations (Mead Nebraska and Bondville Illinois). They demonstrated that when using dynamic carbon allocation and root distribution processes, the estimated gross primary production (GPP) and latent heat flux (LE) were in much better agreement with the observational data than for the static root distribution simulation. Most recently, *Wu et al.* [2015] developed a generic crop phenology and harvest module and a parameterization of nitrogen fertilization into the LSM ORCHIDEE to simulate the responses of temperate crops to changing climate and CO_2. This model (ORCHIDEE-CROP) was evaluated at seven winter wheat and maize sites in Europe over 10 site years. They showed that by increasing the number and resolution of the soil layers that the model substantially

reduced the bias in NEE at corn sites and also improved the simulation of sensible heat fluxes across all sites.

The Community Land Model (CLM) is the land component of the widely used Community Earth System Model (CESM) [*Oleson et al.,* 2010]. Recent inclusion of the prognostic crop scheme into CLM (called CLM4-Crop) has the potential to provide better spatial and temporal information of climate-crop interactions and improved weather and climate prediction [*Levis et al.,* 2012]. For example, when CLM4-Crop was coupled to an atmospheric model (i.e. the Community Atmosphere Model, version 4 [CAM4.0] [*Neale et al.,* 2010]), forecasted precipitation during the peak growing season was significantly improved over Midwestern North America. Further improvements in CLM4-crop are needed in order to advance its carbon forecast capability. For example, recent efforts have examined the phenology and the seasonality of net ecosystem CO_2 exchange (NEE) related to cropping systems over multiple years at three AmeriFlux sites and demonstrated high sensitivity of energy balance and carbon simulations to biases in phenology [*Levis et al.,* 2012; Chen et al., 2015].

While the above studies have demonstrated considerable progress in representing agricultural processes within LSMs, few studies have quantified the accuracy of the simulations over relatively long time scales (>10 years) and at multiple sites. Soil and plant biophysical properties and climate vary considerably among sites (*Fulton et al.,* 1996; *Mzuku et al.,* 2005; *Loescher et al.,* 2014; *Mourtzinis et al.,* 2015). An important

consideration, therefore, is the evaluation of these models across a broad range of sites to determine if the parameterizations are sufficiently general, while also providing reasonably good performance across space and time. Evaluation of models over relatively long time scales can be used to help identify model deficiencies. For example, the ability of models to capture long-term variations in plant phenology and energy and carbon fluxes remains an important challenge [*Richardson et al.*, 2007; *Schwalm et al.*, 2010; *Wang et al.*, 2012; *Piao et al.*, 2013]. Depending on the inter-annual variation of climate, it is suggested that 10 to 20 years of meteorological forcing data is generally necessary for reliable estimates of mean yield potential of crops and its inter-annual variability [*Van Wart et al.*, 2015]**.** Flux observations from networks such as AmeriFlux are just now providing long-term records approaching these important timescales and provide an opportunity for decadal-scale model assessment.

Here, we examine the performance of two versions of CLM4-Crop (CLM4-Crop and CLM4-CropM) at 9 agricultural sites with a focus on the ability of the model to capture seasonal and inter-annual variations in leaf area index (LAI), NEE, ER, and GPP. We use a total of 54 site-years of data to diagnose some of the key model deficiencies in CLM4-Crop and address the following questions:

1. Is the new phenology scheme reliable for simulating inter-annual variations in early growing season crop phenology at multiple sites across a climate gradient?
2. Are biases in simulated phenology across sites random, or are there systematic deficiencies that can be addressed with objective model tuning?

3. Are the models reliable for simulating the intra-annual and inter-annual variations in energy and carbon exchange?

4. Do the models adequately capture the long-term (>10 years) dynamics of NEE at agricultural sites?

3.2 Methods

3.2.1 Meteorology and biological data

The models were evaluated at nine AmeriFlux sites in the US Corn Belt located within latitude and longitude ranges of 40–45°N and 88–97°W, respectively (Fig. 1). These sites represent cropland systems in the northern (US-Ro1, US-Ro3), western (US-Ne1, US-Ne3), southern (US-Bo1, US-Bo2) and central (US-IB1, US-Br1, US-Br3) US Corn Belt. Climate and cropping information for these sites are provided in Table 3.1.

AmeriFlux level 2 gap-filled meteorological data were used because they represent the longest available time series. The biological data included LAI and yield/harvested grain carbon (Level 1 AmeriFlux data). The US-Bo1, US-Ne1 and US-Ne3 sites have the longest available time series of LAI and were thus chosen for the LAI evaluation. The yield/harvest grain data were converted to gC m^{-2} y^{-1} to compare with model simulations, assuming grain carbon content is 45% for corn and 54% for soybean based on laboratory measured mean values [*Baker and Griffis*, 2005].

3.2.2 CLM4-Crop and CLM4-CropM

CLM is the land surface component of CESM [*Bonan and Oleson*, 2002; *Zeng et al.*, 2002; *Dai et al.*, 2003; *Dickinson and Oleson*, 2006; *Oleson et al.*, 2008, 2010]. CLM simulates biophysical and biochemical processes between soil, plant, and the atmosphere. In this study, the fourth version of CLM with the crop scheme activated (CLM4-Crop) was used [*Levis et al.*, 2012].

The crop algorithms in CLM4-Crop originated from the Agro-IBIS model [*Levis et al.*, 2012]. The crop types simulated in CLM4-crop include corn, soybean, and temperate cereals. Here we evaluate the simulation of corn and soybean since they represent the dominant crops in the United States Corn Belt. CLM4-Crop simulates three phenological phases: 1) planting to emergence, 2) leaf emergence to the beginning of grain fill, and 3) from the beginning of grain fill until harvest.

CLM4-Crop is known to overestimate LAI during early growing season [*Levis et al.*, 2012; *Chen et al.*, 2015]. Planting occurs when three thresholds are met in CLM4-Crop: a GDD threshold with the base temperature 8℃, a threshold of 10-day running mean of air temperature and a threshold of daily minimum air temperature. When each of the three thresholds is met, planting starts. To improve the early growing season phenology simulated in CLM4-Crop, in this study we modified the model and simulated the planting

date using growing degree time (GDT). The modified model is called CLM4-CropM. GDT is a thermal time variable similar to growing degree days (GDD), but calculated on a half-hourly model time step [*Chen et al.*, 2015]:

$$GDT = \int (\mathrm{T}_{air} - \mathrm{T}_{ref}) \cdot \mathrm{dt} \text{ , when } T_{air} > T_{ref} \quad (1)$$

Here, T_{air} is the air temperature at 2 m and the reference temperature T_{ref} is 8℃.

As shown by *Chen et al.*, (2015), GDT is more sensitive to temperature variations compared to GDD, especially in the early growing season. The modified model is called CLM4-CropM.

3.2.3 Model simulations

The models were forced by hourly meteorological fields (solar radiation, air temperature, precipitation, air humidity, air pressure and wind speed) at each site (Table 3.1). Mineral soil texture data were extracted from a global data set [*Oleson et al.*, 2010]. To ensure that model soil carbon pools were at steady state, each model was spun up for 1000 years by re-cycling the available site meteorological data [*Thornton and Rosenbloom*, 2005]. Afterwards, the models were forced by the meteorological data at the site for the available years and the hourly output of results was evaluated against measurements.

The model is run in single site mode so that there is one PFT that matches the land cover type in which the flux tower is located [*Stöckli et al.*, 2008; *Yuan and Liang*, 2011; *Chen et al.*, 2015]. The metrics used for evaluating model performance were the correlation coefficient, standard deviation and root mean square error. These three indices were summarized and plotted as Taylor diagrams [*Taylor*, 2001].

3.2.4 Model parameterization

There are more than 80 plant physiological parameters in CLM4. Here only some of the key parameters that determined from previous sensitivity analysis that control carbon sequestration of crop PFTs are discussed [*Sargsyan et al.*, 2014; *Bilionis et al.*, 2015]. CLM4 uses a PFT-dependent water stress factor to describe the soil water constraint on the transpiration and photosynthetic rate. This water stress factor is calculated as:

$$\beta_t = \sum_i w_i r_i \qquad (2)$$

where w_i is a plant wilting factor for layer i and r_i is the fraction of roots in layer i. The water stress factor β_t in CLM4-Crop was multiplied by 1.25 for increased drought tolerance of soybean [*Levis et al.*, 2012].

To calculate the optical depth of the canopy as well as the fraction of sunlit and shaded leaves in the canopy, a leaf angle distribution factor (χl) is used in the model. This

parameter ranges from -1 to 1. Here -1 indicates vertically distributed leaves, 1 indicates horizontally distributed leaves and 0 indicates a random distribution. The default leaf angle distribution factor for corn and soybean was set to -0.4. With the two-big-leaf approximation in CLM, a more planophile canopy will reflect more short wave radiation upward, and thus have less fraction of sunlit leaf. The reduced fraction of sunlit leaf will reduce the canopy photosynthesis rate. Further sensitivity tests are discussed in section 3.4.

The maximum carboxylation rate of rubisco at 25 $^{\circ}C$ (V_{cmax25}) was set to 100.7 μmol m^{-2} s^{-1} in CLM4-Crop for both corn and soybean [*Kattge et al.*, 2009; *Bonan et al.*, 2012; *Levis et al.*, 2012]. This value is the mean V_{cmax25} derived for C_3 crops using a plant trait database (https://www.try-db.org/TryWeb/Home.php). Here we note that the V_{cmax25} value for C_3 crops has a relatively large standard deviation of 36.6 μmol m^{-2} s^{-1}.

3.2.5 Model evaluation

In previous CLM-Crop model evaluation studies, data were extracted from global simulations at individual grid cells where the towers were located to compare against site observations at two AmeriFlux sites [*Levis et al.*, 2012; *Drewniak et al.*, 2013]. This is a method used in *Randerson et al.*, [2009] and a mismatch of the scale of a model grid cell and flux tower footprint was noted. In the large grid cell, multiple PFTs co-exist, while usually the flux tower footprint represents a single PFT. To eliminate the scale mismatch,

the model can be run at a single point with only one PFT, which permits a more objective comparison with tower observations [*Stöckli et al.*, 2008; *Yuan and Liang*, 2011; *Chen et al.*, 2015].

The long term carbon budget was calculated using the NBP approach [*Baker and Griffis*, 2005; *Suyker and Verma*, 2010; *Chen et al.*, 2015]. The yield grain carbon was added to the EC measured annual NEE to account for the carbon removed during harvest and to close the carbon budget.

The metrics used for evaluating model performance were the correlation coefficient, standard deviation and root mean square error. These three indexes were summarized and plotted as Taylor diagrams [*Taylor*, 2001].

The correlation coefficient (r) of a variable X was calculated as:

$$r = \frac{\sum_{i-1}^{n}(\mathrm{X}_{mi} - \overline{X_m})(\mathrm{X}_{oi} - \overline{X_o})}{\sqrt{\sum_{i-1}^{n}(\mathrm{X}_{mi} - \overline{X_m})}\sqrt{\sum_{i-1}^{n}(\mathrm{X}_{oi} - \overline{X_o})}} \qquad (3.3)$$

where X_m and X_o are the modeled and observed values, respectively, and over-bars represent means.

The standard deviation (s) was calculated as:

$$s = \sqrt{\frac{1}{N}\sum_{i=1}^{N}(X_i - \overline{X})^2} \quad (3.4)$$

where X_i is the hourly modeled or observed values.

The root mean square error (RMS) was calculated as:

$$RMS = \sqrt{\frac{1}{N}\sum_{i=1}^{N}(X_{mi} - X_{oi})^2} \quad (3.5)$$

Where X_{mi} and X_{oi} are the modeled and observed values, respectively.

3.3 Results and Discussion

3.3.1 Phenology simulation across crop sites

Our assessment of simulated crop phenology were restricted to comparisons with observations from sites with the longest and most complete LAI records (>10 years): US-Bo1, US-Ne1 and US-Ne3 (Figures 3.2-3.4) and that they represent different geographical regions and climate conditions in the Corn Belt (Table 3.1). Therefore, these sites constitute good boundaries on parameter space with respect to the coupled carbon cycle and interactions with climate and the hydrologic cycle.

US-Bo1 (Bondville, IL)

The simulated phenology was evaluated against observations over a period of 11 years (1997-2007) at this site. In general, both models captured the seasonal pattern and amplitude of LAI at site US-Bo1 (Figure 3.3); however, emergence was biased early up to around 30 days in all years for CLM4-Crop simulations. In a previous global scale study, CLM4-Crop simulated 20-year averaged monthly LAI at the grid cell where US-Bo1 was located (other PFTs coexisted in the grid cell) also showed over-estimated LAI during the first half of the growing season and an over-estimated length of growing season [*Levis et al.*, 2012]. This multi-year comparison at site US-Bo1 confirmed that the agricultural system contributed to this bias.

The simulated inter-annual variability in early growing season phenology based on CLM4-CropM showed a notable improvement. In some years when CLM-Crop simulated emergence times that were close to the observations, CLM-CropM did similarly well (e.g., 1997, 2000, 2004). In other years when CLM-Crop estimated earlier emergence, CLM-CropM gave better estimations (e.g., 1998-1999, 2001-2003, 2005-2007). This indicates that that CLM4-CropM phenology scheme has greater skill at capturing the observed inter-annual variability of the onset of the growing season compared to CLM4-Crop.

The maximum LAI assumptions in CLM4 of 5 m^2 m^{-2} for corn and 6 m^2 m^{-2} for soybean worked well for seven years out of the eleven (1997, 2001-2002, 2004-2007). However for the other years, the maximum LAI threshold was either underestimated for corn (1999,

2003) and soybean (1998) or overestimated (2000). Thus, there is still a need to improve the photosynthesis and carbon allocation processes in the model to eliminate the need for an upper limit of LAI, and to make the model fully prognostic so that it can capture the inter-annual variability in LAI. When the crops start the grain filling process, usually more of the fixed carbon will be allocated to the reproduction pool, and the LAI will start to decline. The timing of grain fill (the point when LAI begins to decrease) was well simulated by both models.

US-Ne3 (Mead, NE)

US-Ne3 is rainfed with corn and soybean rotation. This site has the lowest annual precipitation (784 mm) among the nine sites (Table 3.1). Using EF=LE/(H+LE) as an index for dryness, for soybean, major dry periods occurred during the vegetative and reproductive growth phase in 2002. For corn, major dry periods occurred during silking and/or reproductive stages in 2003 and during vegetative/silking growth stages in 2005 [*Suyker and Verma*, 2012]. From the observations we can see that limited water at this site did adversely affect the maximum LAI, especially for soybean (Fig 3). The maximum LAI for soybean reached 4 m^2 m^{-2}, while the simulated maximum LAI for both models reached the maximum constraint of 6 m^2 m^{-2}.

Based on LAI observations at US-Ne3, soybean displayed slower growth rates compared to corn between leaf emergence and grain filling. However, both models simulated

growth rates that were too fast in this early stage and LAI soon reached the maximum constraint of 6 m^2 m^{-2}. This resulted in an overestimated LAI for soybean during the early growing season for both models at this site. Multiple factors contribute to the model estimation of LAI including photosynthetic rate, canopy structure, and allocation of assimilated carbon to leaves. The sensitivity of LAI to the parameters used in these processes were explored further in section 3.4.

Similar to the site US-Bo1, the estimated timing of emergence was biased early in CLM4-Crop up to 50 days. CLM4-CropM simulated emergence time aligned well with the observed emergence especially for corn (Fig 3). For soybean, CLM4-CropM predicted a reasonable emergence time in most of the years (e.g., 2002, 2006, 2008, 2010) but was biased early in 2004 (performed better than CLM4-Crop) and 2012 (similar to CLM4-Crop) by about 10 days. The timing of grain fill was well simulated by both models in all years (Fig 3).

US-Ne1 (Mead, NE)

The Mead site US-Ne1 is an irrigated corn field. Irrigation at this site provided about 40–50% of the total water received [*Suyker and Verma*, 2010]. Due to irrigation, the maximum LAI of corn at this site was higher than the rainfed Mead site US-Ne3, with some years reaching about 6 m^2 m^{-2} (Figure 3.4). Since CLM4-Crop and CLM4-CropM use a rainfed assumption and do not simulate irrigation, we expected a lower simulated LAI (i.e. similar to the value of 5 m^2 m^{-2} at the rainfed site US-Ne3) in the model

estimation. The maximum LAI constraint of 5 m^2 m^{-2} for corn in the models contributed to the under-estimated maximum LAI for seven years out of the eleven (e.g., 2002-2003, 2007-2009, 2010-2011) and smoothed out the inter-annual LAI variability.

Similar to the site US-Bo1 and US-Ne3, CLM4-CropM performed better in estimating the timing of emergence, which largely reduced the early growing season LAI bias in CLM4-Crop. The onset of emergence simulated by CLM4-Crop was biased earlier by around 50 days in each year at this site while the CLM4-CropM simulated emergence time was within a 2-day range of the observations. Similar to the sites US-Bo1 and US-Ne3, the timing of grain fill and harvest time were well simulated by both models. This is also consistent with a previous study at Rosemount, Minnesota [*Chen et al.,* 2015]. Although CLM4-Crop did not simulate the first half of the phenology well, the model at all four sites captured the timing of grain fill.

Based on the cross-site analysis over multiple years, CLM4-Crop had consistent earlier onset of growing season at all three sites. This systematic model error was unacceptably large with a mean onset bias of 17 days. The GDT method delayed the leaf emergence date and largely reduced the high LAI bias during the early growing season in the CLM4-Crop model at US-Bo1, US-Ne1 and US-Ne3. CLM4-CropM did a better job capturing the inter-annual and across-site variation of leaf emergence time. The phenology for corn was better simulated than soybean by both models in terms of the early growing season growth rate. For soybean, the leaf growth rate during the early growing season was biased

high in both models, especially in drier conditions. The maximum soybean LAI assumption of 6 m^2 m^{-2} was biased high by about 30% in the water-limited Mead site US-Ne3. One thing to notice is that the Agro-IBIS, which used the same mechanism to simulate crop phenology, did not show earlier onset of growing season or overestimated LAI during the early growing season [*Webler et al.*, 2012; *Twine et al.*, 2013]. This suggests that Agro-IBIS incorporated a different set of crop physiological parameters such as GDD and V_{cmax25}.

Those phenology biases are going to propagate into the energy and NEE fluxes [*Chen et al.*, 2015].

3.3.2 Evaluation of energy fluxes and NEE

The simulated hourly energy and NEE fluxes were evaluated against site observations and presented as Taylor diagrams (Fig 3.5) with summary statistics provided in Table 3.2. Note that these evaluations were performed using the default generic corn and soybean physiological parameterization in CLM4-Crop. The only difference between CLM4-Crop and CLM4-CropM is the timing of planting date. The models were not tuned to any site-specific observations to optimize the results.

Among the energy fluxes, R_n was the best-simulated variable (Fig 5). The averaged correlation coefficient was 0.94 for the nine sites (54 site-years) for both models. US-Ro1

and US-Ro3 had comparatively lower correlation coefficients for R_n (0.93 for both sites and both models). The correlation coefficient of R_n was lower at these two sites because during winter, a small bias in the estimation of the snow cover caused a large change in ground albedo, which affected the R_n simulation, especially at these two sites because they are located at higher latitudes. In a previous study, R_n during growing season was evaluated at these two sites and the correlation coefficient was from 0.98 to 0.99 for the same years [*Chen et al.*, 2015].

The simulated latent heat flux (*LE*) had a standard deviation that was closer to the observations and a higher correlation coefficient (0.76 for CLM4-Crop and 0.77 for CLM4-CropM) compared to the observed sensible heat flux (*H*) at all of the crop sites (0.60 for CLM4-Crop and 0.65 for CLM4-CropM) (Fig 3.5). This phenomenon was also found in a previous study when CLM3.5 simulated daily mean energy fluxes were evaluated at 15 AmeriFlux sites [*Yuan and Liang*, 2011]. In their study, simulated *LE* had a higher correlation with the observations compared to simulated *H* at 11 sites, including 2 crop sites. The simulated *H* generally had less variation (standard deviation) than the observations among all sites (Fig 3.5). Ground heat flux (*G*), as the residual of R_n-*H*-*LE* [*Oleson et al.*, 2010], had a standard deviation 2 times or greater than the standard deviation of the observed ground heat flux (Fig 3.5). This was consistent among all sites. This bias has been reported for other process based models which calculate *G* as a residual [*Webler et al.*, 2012]. The skill of both models when simulating hourly energy fluxes were similar, however, CLM4-CropM generally had higher correlation coefficients

and lower RMSDs with the observations when compared to CLM4-Crop. The modified phenological scheme improved the sensible heat flux simulations notably, because the improved early growing season phenology resulted in more realistic canopy canopy temperature, which helped reduce the *H* bias in this period..

The model performance of simulating NEE was similar among sites. Compared to the energy fluxes, the simulated NEE was generally less correlated with the observations (r=0.54 for CLM4-Crop and r=0.62 for CLM4-CropM). To close the carbon budget at crop sites the CLM4-Crop model assumes the harvested biomass is decomposed on site following harvest in one time step [*Levis et al.*, 2012; *Chen et al.*, 2015]. This results in an unrealistic carbon flux from the field into the atmosphere after harvest, which lowered the correlation coefficient of simulated and observed NEE. The correlation coefficients of the hourly NEE simulated by CLM4-Crop ranged from 0.45 (US-Bo2) to 0.66 (US-IB1) for the nine sites. The correlation coefficients of NEE simulated by CLM4-CropM ranged from 0.51 (US-Bo2) to 0.76 (US-IB1). The standard deviation of the simulated NEE is close to the observations, indicating the amplitude of NEE was well simulated by both models. CLM4-Crop generally had higher standard deviation than the observations (from 1.04 at US-Ro1 to 1.22 at US-Br1), except for the site US-Ne1 (0.98). CLM4-CropM reduced the standard deviation of CLM4-Crop at all sites and had the NEE variation closer to observation (from 1.00 at US-Ro1 to 1.12 at US-Br1).

The annual "NEE" simulated by the two crop models is actually net biome production (NBP) [*Baker and Griffis*, 2005; *Suyker and Verma*, 2010; *Chen et al.*, 2015], which considered the decomposition of the harvested carbon. On average, CLM4-CropM gave more positive annual NBP value at all sites (Fig 6). At the five sites where yield data are available (US-Ro1, US-Ro3, US-Bo1, US-Ne1 and US-Ne3), the observed NBP is shown along with the modeled values. We can see both observation and models show substantial inter-annual variation of NBP. In seven out of the nine sites, NBP was estimated positive (C source). However, there are two sites where the annual NBP is negative, indicating carbon sinks (US-IB1 and US-Br3).

In general, CLM4-CropM improved the NEE simulation, with increased correlation coefficient and standard deviation closer to observations. Since the photosynthetic processes are the same in both models, the improved NEE skill is directly linked to the simulations of phenology. The simulated annual NEE differs across the nine sites: seven sites were estimated as carbon sources while two sites were estimated as carbon sinks.

3.3.3 Long-term carbon budget simulation

The long-term carbon budget simulations were evaluated over 10 years at site US-Bo1, and over 11 years at US-Ne1 and US-Ne3. The measured and modeled accumulated carbon budgets at these three sites are shown in Figures 3.7-3.9, respectively.

US-Bo1

From 1997 to 2006, the EC measured cumulative NEE was -3026 gC m^{-2} (Fig 7). After accounting for the yield carbon to close the carbon budget, the total NBP was 1543 gC m^{-2}, indicating a net carbon emission rate of 154.3 gC m^{-2} yr^{-1} over the 10-year period. Here we assume that grain carbon is the only carbon taken from the field and that the above ground biomass remains as residue. At this site, CLM4-Crop estimated a carbon source of 86 gC m^{-2} with the carbon emission rate of 8.6 gC m^{-2} yr^{-1}. CLM4-CropM also predicted a carbon source of 516 gC m^{-2} - a carbon emission rate of 51.6 gC m^{-2} yr^{-1}. Although both models significantly underestimated carbon emissions at US-Bo1, the CLM-CropM simulated long-term carbon budget is closer to the observations compared to CLM4-Crop.

To better understand what contributes to the underestimated carbon emissions at US-Bo1, the 10-year accumulative GPP and ER[2] simulations were also examined (Fig 7). GPP and ER were substantially overestimated by 10902 and 9431 gC m^{-2}, respectively, using CLM4-Crop. CLM4-CropM also overestimated both GPP and ER, but reduced the bias for GPP by 17% and reduced the bias for ER by 16%. The simulated GPP and ER for soybean was biased higher compared to corn. This was partly attributed to the fact that early growing season LAI of soybean was substantially overestimated compared to corn (Fig 2). The GPP bias of the 5 soybean years contributed to 68% and 75% of the total

[2] Here the yield carbon was added to the ecosystem respiration term to account for the total carbon released from the agro-ecosystem.

GPP bias from CLM4-Crop and CLM4-CropM, respectively. ER bias of the 5 soybean years contributed to 58% and 64% of the total ER bias from CLM4-Crop and CLM4-CropM, respectively. Overall, due to the larger bias in simulated GPP compared to ER, the NEE (and NBP) values estimated by both models were more negative compared to the flux tower derived values.

US-Ne1

From 2002 to 2012, the EC measured carbon budget at site US-Ne1 showed a carbon sink of -3860 gC m^{-2} (Fig 8). After accounting for the harvested grain carbon, this site was a carbon source of 1009 gC m^{-2} over the 11 years. On average, the carbon emission rate from this system was approximately 91.7 gC m^{-2} per year. The CLM4-Crop simulated carbon budget for the 11 years was 69 gC m^{-2} with the carbon emission rate of 6.3 gC m^{-2} yr^{-1}. CLM4-CropM simulated carbon budget was 897 gC m^{-2} with the carbon emission rate of 81.5 gC m^{-2} yr^{-1}. The CLM4-CropM simulation was in closer agreement with the observations largely because CLM4-CropM simulated a more realistic growing season length.

The 11-year accumulative GPP and ER were overestimated by both models (Fig 3.9). However, the biases were smaller compared to US-Bo1 (Fig 3.6). GPP and ER were overestimated by 6325 and 5470 gC m^{-2} (575 and 497 gC m^{-2} yr^{-1}) using CLM4-Crop. CLM4-CropM with better phenology simulation reduced the bias of GPP by 67% and reduced the bias of ER by 63%.

US-Ne3

The EC measured NEE showed that US-Ne3 was a carbon sink of -2468 gC m^{-2} from 2002 to 2012 with an NBP of a moderate carbon source of 504 gC m^{-2}. The carbon emission rate was 45.8 gC m^{-2} yr^{-1}, about half of the irrigated Mead site US-Ne1 or one third of the Bondville site US-Bo1. CLM4-Crop estimated the 11-year NBP at 244 gC m^{-2}, with a carbon emission rate of 22.2 gC m^{-2} yr^{-1}. CLM4-CropM predicted a NBP of 636 gC m^{-2} with a carbon emission rate of 57.8 gC m^{-2} yr^{-1}.

Similar to the sites US-Bo1 and US-Ne1, both GPP and ER were overestimated at US-Ne3 (Fig 8). GPP and ER were overestimated by 12176 and 11933 gC m^{-2} (1107 and 1085 gC m^{-2} yr^{-1}) using CLM4-Crop. CLM4-CropM reduced the overestimations of GPP by 51% and 13% for corn and soybean, respectively. Using CLM4-CropM, the overestimations of ER were reduced by 39% and 12% for corn and soybean, respectively.

The average NBP of the three sites under consideration was estimated to be a carbon source of 97.3±54.5 gC m^{-2} yr^{-1} (the uncertainty is calculated as standard error). This value is comparable with a European study over seven crop sites from 2004 to 2007 [*Kutsch et al.*, 2010], which estimated an annual carbon loss of 95±87 gC m^{-2} yr^{-1} from the seven European sites. The CLM4-Crop value was 12.4±8.6 and the CLM4-CropM value was 63.6±15.8 gC m^{-2} yr^{-1}. The response of ecosystems to regionally heterogeneous stimuli such as historical land use, or rainfall and temperature anomalies and their effects

on carbon fluxes is an important aspect for estimating large scale carbon sinks and sources [*Schimel et al.*, 2001]. In this case, comparing the three sites we can see large differences in the annual NBP. It also emphasizes the importance of evaluating a model across different sites before applying it to the region. The modified model CLM4-CropM improved the carbon budget estimation and the estimated value is within the range of measured value. However, the model still needs improvement to represent the variability of carbon budgets across sites.

3.3.4 Sensitivity tests and model calibration

The results above illustrate that the over-estimated GPP is one of the major model deficiencies that needs to be resolved in order to perform reliable long-term simulations. Here we note that the model simulated ER is intimately connect to the GPP simulation because plant maintenance respiration (MR) is simulated proportional to plant biomass, growth respiration is currently simulated as 0.3 of the available GPP (GPP-MR), and heterotrophic respiration is proportional to litter and soil carbon pools, which are also related to plant biomass. Thus our sensitivity tests focus on the impact of the simulated GPP. First we compared the model simulated GPP for corn and soybean across sites (Fig 10). The poor simulation of soybean GPP is consistent across sites and contributed to the overall GPP bias we observed in the long-term accumulate GPP flux. The model-observation mismatch in soybean GPP can be separated into two groups. The first group is site/year specific errors. For example, we observed unrealistic variations in simulated

GPP during the 2008 growing season at US-Ro1 and during 2009 growing season at US-Ro3. This error was eliminated by reverting to the original calculation of β_t (i.e. by eliminating the 1.25 soybean drought tolerance factor). This factor was recently introduced to increase soybean drought tolerance [*Levis et al.*, 2012].

The second group is systematic bias across all sites. For example, the soybean leaf growth rate during the early growing season was overestimated across all sites. The estimated harvest time was also biased late, resulting in a longer growing season for soybean across all sites. Further, accumulative GPP and ER for soybean were consistently over-estimated at all sites. Here our goal is to improve the model by reducing the systematic bias across sites to provide more reliable carbon simulations for corn-soybean systems.

A series of sensitivity tests were carried out across sites to diagnose the potential factors that contributed to the high bias of GPP simulation for soybean, as well as to diagnose the most sensitive parameters to carbon flux simulations across sites. Global sensitivity analyses have been carried out previously for CLM in which 80 parameters were investigated with respect to their influence on LAI and carbon simulations [*Sargsyan et al.*, 2014]. However, for crop PFTs in CLM4, the nitrogen limitation has been turned off and, therefore, previous sensitivity tests will differ from those carried out here.

Based on previous analyses on CLM model physiological parameters [*Sargsyan et al.*, 2014; *Bilionis et al.*, 2015], five parameters were chosen to carry out the sensitivity tests because of their large impact on the simulation of LAI, GPP, and ER. Note here the nitrogen related parameters were not tested because this version of the model assumes no nitrogen limit for cropping systems. The parameters included: leaf angle distribution factor (χl), specific leaf area at the top of plant canopy (*slatop*), initial carbon allocation to leaf (*fleafi*), the maximum carboxylation rate of rubisco at 25 $^{\circ}C$ (V_{cmax25}), and growing degree days required to reach plant maturity (GDD_{mat}). Each parameter value was increased and decreased by 20% (except χl, which was 0 in the control run. It was increased and decreased by 0.2). The corresponding changes in LAI, and the carbon fluxes compared to the control run are shown in Table 3.3.

The sensitivity tests revealed that among the five parameters, V_{cmax25}, *slatop* and *fleafi* are the parameters that LAI, GPP and ER are most sensitive to. This is consistent among the four sites (US-Bo1, US-Ne3, US-Ro1 and US-Ro3). The sensitivity of NEE to those parameters varies greatly (Table 3.3) because NEE is the very small difference between the large opposing fluxes of GPP and ER. Thus when describing model sensitivity to changing parameter values we refer to the gross fluxes.

A 20% reduction of GDD_{mat} at US-Bo1 and US-Ne3 shortened the length of the growing season and therefore had a substantial influence on LAI, GPP and ER simulations. However, at the two Rosemount sites, a 20% reduction in GDD_{mat} had very little impact

on LAI or the carbon fluxes. This is because at Rosemount the model reached another important threshold (the number of days past planting) before GDD_{mat} was reached. This indicates that the current use of a universal GDD_{mat} is not sufficiently general across site locations. For example, at higher latitudes, soybean cultivars were selected to better adapt to cooler temperatures and thus require less GDD to reach plant maturity. A dynamic GDD_{mat} that changes with annual mean temperature could represent this cultivar selection at different latitudes and better predict the harvest time. Selecting crop cultivars for better adaption to local environment and climate is a process similar to acclimation however in a shorter time scale. When simulating crops at the global scale, it is impossible to parameterize each crop cultivar, thus a dynamic parameterization scheme that considers the cultivar selection will provide more reasonable estimations of the crop phenology and regional carbon budget.

Following the sensitivity tests, the model was calibrated and validated using the site-years that have yield information available (for the purpose of evaluating ER. see Table 3.4). Half of the site-years were used to calibrate the model and the other half were used to validate the model. Based on a previous CLM-Crop model calibration study [*Bilionis et al.*, 2015], the specific leaf area at top of the canopy (*slatop*) was reduced from 0.07 to 0.06 $m^2\ gC^{-1}$. The initial fraction of carbon allocated to leaves (*fleafi*) was reduced from 0.85 to 0.68 (The range of this parameter in previous literature is from 0.85 [*Levis et al.*, 2012] to 0.47 [*Twine et al.*, 2013]). GDD_{mat} was reduced to 80% of the calculated value. The threshold of days past planting which is a second constraint on harvest time was also

reduced by 80%, in order to improve the simulation at sites located at higher latitudes like Rosemount.

Finally, the V_{cmax25} was reduced by one half of its observed standard deviation from100.7 $\mu mol\ m^{-2}\ s^{-1}$ to 80 $\mu mol\ m^{-2}\ s^{-1}$. There are two reasons for this downward adjustment. First, directly implementing leaf trait V_{cmax25} values into big leaf models like CLM have been shown to cause overestimated canopy level GPP [*Bonan et al.*, 2012]. Second, most estimates of V_{cmax25} ignore the importance of the wall resistance of the cell and assume that the intercellular CO_2 concentration is equal to CO_2 concentration at the sites of carboxylation. This can lead to an overestimation of V_{cmax} by up to 20% [*Long and Bernacchi*, 2003; *June*, 2011].

The calibrated CLM4-CropM simulations of LAI, NEE, GPP and ER over the 14 soybean years across sites were compared with the default CLM4-CropM results in Figure 3.11. After calibration the simulated seasonal variation and magnitude of those variables was greatly improved. The correlation coefficients and biases of modeled and observed weekly LAI, NEE, GPP and ER values are shown in Table 3.4. Based on this calibration, the average correlation coefficient of LAI across 14 site-years for soybean increased from 0.75 to 0.87 while the bias of LAI reduced from 1.28 to 0.08 $m^2\ m^{-2}$. Further, the simulation of the gross carbon fluxes GPP and ER were also improved with increased correlation coefficients and reduced bias across site years (Table 3.4). The correlation coefficient of NEE increased from 0.58 to 0.76. The bias of NEE remained

about the same magnitude before and after the calibration. Again, this is because NEE is a small difference between two much larger gross carbon fluxes acting in opposite directions.

3. 4 Conclusions

This study used data from nine American sites (54 site-years) to examine the performance of two versions of CLM4-Crop (CLM4-Crop and CLM4-CropM) capturing seasonal variations in leaf area index (LAI), NEE, ER, and GPP, as well as long term carbon budgets for agro-ecosystems. Some key parameters were analyzed and the model was calibrated across sites for soybean simulations. Our analyses indicate that:

1. The model-simulated crop phenology has been evaluated at US-Bo1, US-Ne1 and US-Ne3 where long-term LAI data were available. Results show that compared to the default GDD algorithm currently used in CLM4-Crop, the GDT approach improved the early growing season phenology, with better timing of leaf emergence across all sites. The high bias in early growing season LAI that was found in CLM4-Crop simulations has been largely reduced using the GDT approach and this is consistent across sites. However, in both models LAI of soybean was generally overestimated, especially in drier conditions.

2. *LE* was better simulated by both models (r=0.76 and 0.77 for CLM4-Crop and CLM4-CropM, respectively) than *H* (r=0.60 and 0.65 for CLM4-Crop and CLM4-CropM,

respectively) at all sites. The GDT method improved sensible heat flux simulation notably.

3. The observed and modeled long-term simulations of carbon fluxes showed that for corn years, NBP, GPP and ER are well estimated in CLM4-CropM. For soybean, the NBP budgets were reasonably estimated in CLM4-CropM but GPP and ER were overestimated. This is consistent over the sites. CLM4-Crop has a longer growing season for both corn and soybean, thus gave more negative NEE as well as higher GPP and ER for long term simulations.

4. V_{cmax25}, *slatop* and *fleafi* were the parameters that LAI, GPP and ER are mostly sensitive to. GDD_{mat} largely affects the length of the simulated growing season at lower latitude sites but did not affect the phenology simulation at Rosemount with higher latitude. The calibrated CLM4-CropM model generally had shorter growing season, reduced GPP and ER than CLM4-Crop, and also gave more positive carbon budgets, which were closer to the observations. The overestimation of annual GPP and ER for soybean was reduced by 84.7 % and 72.7%, respectively, in the calibrated CLM4-CropM model.

In general, the calibrated CLM4-CropM had shown robust estimation of crop phenology, energy and carbon fluxes at all the sites. Although it still has some deficiencies (i.e.,

slightly overestimation of the early growing season GPP), we expect it to give reasonable estimations over the US Corn Belt.

Chapter 4: Diagnosing changes in net ecosystem CO_2 exchange in the conterminous United States using the Community Land Model

4.1 Introduction

The spatial and temporal variability of terrestrial carbon sources and sinks are dictated by the interactions between the biosphere and the atmosphere. Quantifying carbon sinks and sources is required to inform climate change adaptation and mitigation strategies. Previous studies have used Satellite data combined with simple models to derive net primary production (NPP) [*Hicke et al.*, 2002; *Lobell et al.*, 2002] or gross primary production (GPP) [*Xiao et al.*, 2010a; *Guanter et al.*, 2014; *Yebra et al.*, 2015] but did not explicitly account for heterotrophic or ecosystem respiration. Others have used land use change data [*Houghton et al.*, 1999; *Houghton*, 2003], atmospheric CO_2 observations [*Peters et al.*, 2007] or combined satellite data with eddy covariance flux towers and models to derive net ecosystem exchange (NEE) [*Potter et al.*, 2007; *Xiao et al.*, 2008, 2011; *West et al.*, 2010; *Chen et al.*, 2011]. Further, isotopes and inverse modeling have been used to constrain the terrestrial carbon sinks and sources [*Ciais et al.*, 2010]. Although there is a consensus that U.S. terrestrial ecosystems represent a carbon sink, the magnitude and pattern of the carbon sinks/sources remains highly uncertain [*Houghton*, 1999; *Pacala et al.*, 2001]. The total carbon budget for the conterminous United States ranges from -0.110 [*Houghton*, 2003] to -0.681 PgC yr^{-1} [*SOCCR*,

http://cdiac.ornl.gov/SOCCR/final.html]. Several studies have indicated that croplands, with higher GPP compared to natural vegetation, contribute to nearly half of the total carbon sink of the conterminous United States [*Chen et al.*, 2011; *Xiao et al.*, 2011]. Those studies did not take into account the consumption of crop production and the amount of carbon released into the atmosphere through this process.

The Corn Belt, concentrated in the Midwestern United States, is one of the world's most intensively cultivated regions. It accounts for more than 40% of the world's grain production and has been shown to be one of the most productive locations on the planet [*Guanter et al.*, 2014]. Cropland in this region has a profound impact on the regional energy, water, and carbon budgets. The impact of climate change and the CO_2 fertilization effect on this important agricultural region remains uncertain. The phenology of crops is subject to climate conditions such as temperature and precipitation. The atmospheric CO_2 level has increased from 280 ppmv in the 1860s to around 400 ppmv globally (GLOBALVIEW-CO_2) as a result of anthropogenic activities' emission (i.e. fossil fuel combustion, deforestation, and cement manufacture) and is expected to have an important influence on photosynthesis and transpiration. Air temperature and precipitation have been increasing over the past half-century with pronounced warming at night in the northern hemisphere. The impact of these environmental changes on photosynthesis, respiration, and productivity remain important questions. Especially in terms of projected climate change.

Climate models serve as important tools to test our current understanding of the terrestrial carbon budget, to predict future trends, and to inform climate policy decisions. Within the past decade, global climate models have incorporated process based prognostic schemes to simulate crops [*Bondeau et al.*, 2007; *Osborne et al.*, 2007; *Stehfest et al.*, 2007; *Gervois et al.*, 2008; *Levis et al.*, 2009; *Lokupitiya et al.*, 2009; *Wu et al.*, 2015]. However, different schemes, assumptions, and processes considered in the model can have large impacts on the model estimation of the regional energy, water, and carbon budgets. Therefore, it is of great interest to see how sensitive the estimated regional carbon budget is to the representation of crops in these models.

In this study we addressed the following questions:

1. How sensitive is the carbon budget of the conterminous United States to the way crops are represented within the community land model (CLM)?
2. What is the estimated aggregate carbon budget of the conterminous United States?
3. How has the carbon budget of the conterminous United States changed over the past half century in response to climate change? Is there a notable trend?
4. How has the CO_2 fertilization effect impacted the carbon budget?

4.2 Methods

4.2.1 Community Land Model 4.0

The fourth version of the Community Land Model (CLM4.0) is the land surface component of the Community Earth System Model (CESM1.0). Spatial land surface heterogeneity in CLM is represented as a nested sub-grid hierarchy. The model grid cells are composed of multiple land units (i.e. glacier, urban, lake, wetland, and vegetated land unit). The vegetated land unit can be further divided into unique soil columns. To allow natural vegetation and crops to coexist in a model grid cell and be handled with different management, the vegetated land unit is divided into two parts. Natural vegetation PFTs are in the unmanaged land unit where they share the same soil conditions. Crop PFTs occupy different soil columns in the managed land unit, where they do not share soil conditions thus do not compete for water and nutrients [*Levis et al.*, 2012]. The vegetation on a soil column is represented using a percentage composition of bare ground and different Plant Functional Types (PFTs). There are fourteen natural PFTs and three crop PFTs (corn, soybean and temperate cereals) in CLM4.0. Biogeochemistry is simulated using CLM4.0-CN, which combines the carbon (C) and nitrogen (N) cycle to model fluxes from vegetation, litter and soil organic matter. Crops in CLM4.0-CN are unmanaged, which has the same water-stress deciduous phenology as natural grass [*Oleson et al.*, 2010]. *Levis et al.* [2012] incorporated prognostic crops into CESM, in which corn, soybean and temperate wheat were treated as special crop PFTs. A high bias in the early growing season LAI simulated by CLM4-Crop was identified at multiple sites [*Levis et al.*, 2012; *Chen et al.*, 2015]. In order to improve the early growing season crop phenology of CLM4-Crop, a new method that uses growing degree time (GDT) to

predict the timing of leaf emergence was introduced into CLM4-Crop (see section 2.2.1). The modified model was called CLM4-CropM (See chapter 3).

4.2.2 Photosynthesis and respiration

Carbon assimilated during photosynthesis is distributed among twenty vegetation carbon pools, three litter pools, four soil organic matter pools and the atmosphere [*Oleson et al.*, 2010]. The photosynthesis, maintenance respiration, growth respiration, decomposition, and allocation are calculated on the radiation time step (half-hourly).

Leaf gross photosynthesis is calculated as:

$$A = \min(w_c, w_j, w_e) \tag{4.1}$$

Where ω_c is the RuBP carboxylase (Rubisco) limited rate of carboxylation, ω_j is the maximum rate of carboxylation allowed by the capacity to regenerate RuBP, and ω_e is the export limited rate of carboxylation for C_3 plants and the PEP carboxylase limited rate of carboxylation for C_4 plants. Photosynthesis in C_3 plants is based on the model of *Collatz et al.* [1991] and photosynthesis in C_4 plants is calculated based on the model of *Collatz et al.* [1992]. When atmospheric CO_2 increases, the gradient of CO_2 from the atmosphere to the plant intercellular space increases. More CO_2 will diffuse into the intercellular space. Theoretically, the plant is able to assimilate more CO_2, but is still constrained by the three limitations in equation 4.1.

Ecosystem respiration is partitioned into autotrophic respiration (A_R) and heterotrophic respiration (H_R).

$$E_R = A_R + \mathrm{H}_R \tag{4.2}$$

The A_R component is the sum of growth (G_R) and maintenance (M_R) respiration.

$$A_R = G_R + M_R \tag{4.3}$$

Growth respiration is calculated as a portion (α) of the total available carbon that could be allocated to different carbon pools. Here $\alpha = 0.3$.

$$G_R = C_{allocated} \cdot \alpha \tag{4.4}$$

The maintenance respiration is divided into leaf and fine root maintenance respiration. If it is a woody PFT, the maintenance respiration also includes live stem and live coarse root maintenance respiration.

$$M_R = \begin{cases} M_{R-leaf} + M_{R-froot}, & non-woody \\ M_{R-leaf} + M_{R-froot} + M_{R-livecroot}, & woody \end{cases} \tag{4.5}$$

All of the maintenance respirations are calculated based on a temperature depended Q_{10} equation. The leaf maintenance respiration is calculated as:

$$M_{R-leaf} = N_{leaf} \cdot br \cdot tc \tag{4.6}$$

Here N_{leaf} is the leaf nitrogen. The base respiration rate $br = 2.525 \times 10^{-6} gC \cdot gN^{-1} \cdot s^{-1}$, tc is a temperature scalar factor, which is calculated based on a Q_{10} equation: $tc = Q_{10}\left(\frac{T_{2m} - 20}{10}\right)$. Here Q_{10} is a parameter (currently Q_{10} =2.0) and T_{2m} is the 2 m air temperature. $20^{o}C$ is the base temperature.

The fine root maintenance respiration is calculated as:

$$M_{R\text{-}foot} \mu \sum_{i=1}^{n} Q_{10}^{\frac{T_i - 25}{10}} \times fr_i \quad (4.7)$$

Here i stands for different layer depth, Q_{10} is set to 1.5. 25^oC is the base temperature assumed for all seasons, and fr_i is the fraction of root in the soil layer i .

All of the autotrophic respiration components are calculated at the PFT level. The carbon flux for a column is then averaged over different PFTs on this column. In contrast, the heterotrophic respiration is calculated at the column level.

Heterotrophic respiration fluxes are calculated as fractions of the mass flow from the litter pools to soil organic matter (SOM) pools and the mass loss from SOM pools (part of the decomposition processes). The decomposition is soil temperature and moisture dependent, and also based on the size of the littler pools and SOM pools.

$$HR = HR_{lit} + HR_{SOM} \quad (4.8)$$

$$HR_{lit} = HR_{lit1} + HR_{lit2} + HR_{lit3} \quad (4.9)$$

$$HR_{SOM} = HR_{SOM1} + HR_{SOM2} + HR_{SOM3} + HR_{SOM4} \quad (4.10)$$

The heterotrophic respiration of each soil carbon pool is calculated as:

$$HR_{cpooli} = f_{cpooli} \cdot Cpooli_{loss} \quad (4.11)$$

Where f_{cpooli} is the respiration fraction of the carbon flux from the upstream carbon pool due to decomposition [*Thornton and Rosenbloom*, 2005], $Cpooli_{loss}$ is the carbon loss from the carbon pool i (Here refers to the litter pools and the SOM pools). $Cpooli_{loss}$ is calculated based on the decomposition rate (d_{cpooli}) of the pool:

$$Cpooli_{loss} = Cpooli \cdot d_{cpooli} \tag{4.12}$$

Here d_{lit1} is calculated as a PFT dependent base decomposition rate, which assume no water and nitrogen limitation at 25ºC, modified on each time step by functions of soil temperature and soil water potential [*Thornton and Rosenbloom*, 2005].

4.2.3 Data available to drive CLM4.0-CN

The land surface data is the 0.5º×0.5º plant functional types (PFTs) data released by NCAR [*Oleson et al.*, 2010]. The plants were classified into 20 PFTs (Table 4.1). Within each grid cell, the coverage of each PFT is described as a percentage of the grid cell.

The model is forced by global reanalysis meteorological forcing NetCDF data sets from 1948 to 2004 [*Qian et al.*, 2007] that includes incoming short wave radiation, precipitation, specific humidity, air temperature at 2m, wind speed and air pressure at the lowest layer.

4.2.4 Model experiment design

In order to distinguish the impact of different crop models, climate change, and CO_2 fertilization on the regional carbon cycle, we designed six different models runs:

1. Three control runs

Under the control condition, three models (CLM4-CN, CLM4-Crop and CLM4-CropM) were branched from an initial file of current soil carbon condition and forced by the Qian data set from 1948 to 2004. The CO_2 level was increasing based on the observed historical CO_2 concentration over the period 1948 to 2004 [*Oleson et al.*, 2010]. A global land cover map from *Oleson et al.*, [2010] was used during the modeled period.

During the control run, only the meteorological forcing data is changing with time. For example, the solar radiation, precipitation, air temperature, humidity, air pressure, and wind velocity are changing based on their historical values (Figure 4.1). For the past 50 years, the solar radiation over the United States has been generally decreasing at a rate of 10 to 20 W m^{-2} per century. Precipitation is increasing, especially northwest to the Gulf of Mexico. The 2m air temperature is increasing as well, and more pronounced for higher latitude area. The increasing trend of temperature is greater in western United States than eastern. Nighttime air temperature has a more pronounced increasing trend than daytime temperature. Relative humidity has also been increasing, with the fastest trend centered in Colorado, where the altitude is higher.

2. Three steady CO_2 runs

In the steady CO_2 runs, CLM4-CN, CLM4-Crop and CLM4-CropM were branched from the same initial condition and were forced by the same atmospheric data set as the control run. However, we assumed that the CO_2 mixing ratio remained at the pre-industrial revolution value of 284.7 ppmv.

4.3 Results and Discussion

4.3.1 Impacts of crop schemes on NEE

Simulated NEE values for the period 1948 to 2004 are shown in Figure 4.3. The upper left plot shows the crop simulated as "unmanaged" grassland in CLM4-CN. The 57-year averaged NEE over the United States was -0.138±0.034 PgC yr^{-1} (uncertainty was calculated as standard error of the 57-year values). The Corn Belt region was estimated close to carbon neutral (-0.007±0.004 PgC yr^{-1}). The southeast part of the United States was identified as the major carbon sink. The magnitude of carbon sink in this region ranged from -30 to -90 gC m^{-2} yr^{-1}. The 57-year averaged GPP was highest in the southeastern corner of the United States (Figure 4.4). In north Florida and south Alabama, Georgia and South Carolina, the averaged annual GPP ranged up to 3000 gC m^{-2} yr^{-1}. This is consistent with previous studies that identified the forest along the east coast as a major carbon sink of the United States [*Peters et al.*, 2007; *Xiao et al.*, 2011]. The

southwestern part of the United States was identified as the major carbon source. The magnitude ranged from 0 to 40 gC m^{-2} yr^{-1}.

When crop was simulated as "managed" crop (including corn, soybean, and wheat explicitly) in CLM4-Crop, the averaged NEE over the United States was -0.191±0.020 PgC yr^{-1}. The Corn Belt region became the major carbon sink over the United States (-0.021±0.002 PgC yr^{-1}). The NEE over the Upper Midwest ranged from -40 to -90 gC m^{-2} yr^{-1}. Despite the shorter growing season of managed crop in CLM4-Crop, the Corn Belt region was estimated as a larger carbon sink over the period. This was because the managed crop simulated in CLM4-Crop has a higher photosynthesis capacity than the original model that used grassland as a surrogate for crops. The V_{cmax25} value for unmanaged crop was 57 in CLM4-CN; for managed crops, it was changed to 101 based on the C_3 crop value given in *Kattge et al.* [2009]. In the southeast region, the change from unmanaged crop to managed crop reduced the carbon assimilation. This area has sufficient precipitation and higher temperature. Under these conditions the unmanaged crop with "grass-like" phenology had a long growing season and fixed more carbon than the managed crop. In general, the managed crop simulated in CLM4-Crop contributed to greater sink in the United States compared to the unmanaged crop simulated in CLM4-CN. However, the direction of change varies spatially.

When the new phenology scheme for crops was introduced (CLM4-CropM, see chapter two), the averaged NEE over the United States became more positive (-0.094±0.024 PgC

yr^{-1}). The Corn Belt region was no longer the major carbon sink; the central part of it even became a carbon source (0.005±0.002 PgC yr^{-1}). The range of NEE was from -10 to 20 gC m^{-2} yr^{-1}. Based on the multiple sites evaluation in chapter 2, we attributed this to the fact that CLM4-CropM simulates later emergence date and generally shorter growing seasons than CLM4-Crop. Besides that, the photosynthetic rate for soybean simulated in CLM4-CropM was lower than the default CLM4-Crop and closer to observations based on our site evaluations. Thus the managed crop simulated in CLM4-CropM contributed to smaller sink in the United States compared to the unmanaged crop simulated in CLM4-CN.

The simulated NEE over the United States was sensitive to the different crop schemes embedded in CLM. The 57-year averaged NEE for the conterminous United States was -0.138±0.030, -0.191±0.020 and -0.094±0.023 PgC yr^{-1} simulated by CLM4-CN, CLM4-Crop and CLM4-CropM respectively. All three models estimated that the conterminous United States is a carbon sink, which is in agreement with previous remote sensing and modeling studies [*Potter et al.*, 2007; *Xiao et al.*, 2008, 2011; *West et al.*, 2010; *Chen et al.*, 2011]. However, CLM4-Crop estimated a greater carbon sink while CLM4-CropM estimated a smaller carbon sink compared with CLM4-CN. Over the Corn Belt region, CLM4-CropM even estimated a carbon source while CLM4-Crop predicted carbon sink. Previous studies have suggested that forests and savannas are the major carbon sinks in North America [*Peters et al.*, 2007; *Xiao et al.*, 2011]. The default CLM4-Crop predicted the Corn Belt region and northeast region as the major carbon sinks over the United

States, while CLM4-CropM, with calibrated parameters (see section 3.3.4), estimated a pattern of NEE that was similar to previous studies with the East Coast region identified as a greater carbon sink. The magnitude of the estimated GPP was smaller in CLM4-CropM (-8.15±0.06 PgC yr^{-1}) compared to CLM4-CN and CLM4-Crop (Table 4.2) and is in better agreement with previous estimates [*Lobell et al.*, 2002; *Xiao et al.*, 2010a, 2011; *Chen et al.*, 2011]. With the consumption of crops and release of carbon considered in these crop models, the NEE estimated in this study (-0.094±0.024 PgC yr^{-1}) is more neutral compared to previous estimates which ranges from -0.110 to -0.681 PgC yr^{-1}. This study emphasized the importance of incorporating calibrated crop specific modules in global climate models[*Guanter et al.*, 2014].

4.3.2 Trends in NEE

There was no significant trend of NEE over the conterminous United States simulated by CLM4-CN (-0.22 TgC yr^{-2}, p=0.92). However, there were NEE trends over different regions in the United States in different directions (Figure 4.4). Colorado, New Mexico, Louisiana and the region east to the Corn Belt had the most pronounced increasing trend of carbon uptake. The Corn Belt region, which was predicted to be the major carbon sink in CLM4-CN, with positive NEE trends of 20 to 100 gC m^{-2} $century^{-1}$. This indicated decreasing carbon uptake over the crop region during the simulated 57 years. According to the models, the climate trends are causing both increased GPP and increased ER in the United States, especially in the boundary area of South West and South East regions,

where the slightly reduced air temperature combined with increased precipitation have enhanced both photosynthesis and ecosystem respiration (Figure 4.4).

Based on the CLM4-Crop model simulations there were no significant trends of NEE over the conterminous United States (-0.19 TgC yr^{-2}, p=0.87). However, the regional differences increased. For the Corn Belt region, the NEE trend became more positive (40 to160 gC m^{-2} $century^{-1}$). Combining this with the averaged NEE over the 57 years, we know that although CLM4-Crop predicted the Corn Belt as the major carbon sink, the size of the sink has been shrinking during the past half century. Colorado, New Mexico and Louisiana still had the most pronounced increasing trend of carbon uptake (-40 to -120 gC m^{-2} $century^{-1}$).

When the new crop phenology (CLM4-CropM) was introduced, the simulated NEE trend for the Corn Belt region changed direction, which made the entire conterminous United States an increasing carbon sink (-2.95 TgC yr^{-2}, p=0.04) (Figure 4.5). Thus although CLM4-CropM estimated a carbon source for the Corn Belt region, this carbon source has been shrinking. This indicated that different crop schemes do not only affect the averaged NEE simulated by the models, but also affect how sensitive the crop system is to climate change. CLM4-CropM had shorter growing season and less GPP estimated for soybean compared to CLM4-Crop, which was proved to be closer to observations. This contributed to the moderate carbon sink estimation. At the same time, CLM4-CropM is

more sensitive to early spring temperature due to the introduction of GDT [*Chen et al.*, 2015], thus it is more sensitive to climate change.

4.3.2 The influence of increasing CO_2

The same models were run under steady CO_2 condition to compare with the transient CO_2 runs (Table 4.2). Calculating the NEE difference between the two scenarios gave us an estimate of the CO_2 fertilization effect. Estimated annual NEE for the United States with steady CO_2 were -0.091±0.034, -0.135±0.020 and -0.037±0.024 PgC yr^{-1}, while the estimated annual NEE under increasing CO_2 were -0.214±0.030, -0.191±0.020 and -0.136±0.022 PgC yr^{-1} simulated by CLM4-CN, CLM4-Crop and CLM4-CropM, respectively. The net CO_2 fertilization effect in the three schemes were calculated as -0.123, -0.056 and -0.099 PgC yr^{-1}. The CO_2 effect increased GPP by 3.9%, 4.5% and 5.0%, respectively, and those contributed to 135.2%, 41.5% and 267.6% increase of net carbon assimilation compared to the steady CO_2 scenario. One thing to notice is that the model does not consider the CO_2 acclimation of plants [*Long et al.*, 2004], thus the amount of CO_2 fertilization effect we discussed here can be considered as the maximum potential CO_2 fertilization effect.

4.4 Conclusions

This study investigated the NEE of the conterminous United States and its trend over 57 years (1948-2004) using three models: CLM4-CN, CLM4-Crop and CLM4-CropM. Our analysis indicated that:

1. The estimation of the United States carbon budget was sensitive to different crop schemes embedded in the land surface model. With unmanaged crop scheme, the NEE budget was estimated to be -0.138 ± 0.034 PgC yr^{-1}. With the default managed crop scheme, the NEE budget became -0.191 ± 0.020 PgC yr^{-1}. A modified crop phenology reduced the estimated carbon sink to -0.094 ± 0.024 PgC yr^{-1}. The modified crop model reduced the estimated NEE budget by 50.8% compared to the default crop model.

2. Consistent with previous studies, all three models simulated carbon sinks over the United States. Compared to the NEE range estimated in previous study (-0.110 PgC yr^{-1} to -0.681 PgC yr^{-1}), the magnitude of the conterminous United States' carbon sink estimated using the calibrated crop model was smaller (-0.094 ± 0.023 PgC yr^{-1}). However, most of the previous studies that use the flux tower data to train remote sensing models did not consider the carbon released during the consumption of crop yields. In this study, CLM4 model considered the decomposition of harvested biomass on site when calculating NEE (see Chapter 1).

3. CLM4-CN and the default crop model CLM4-Crop predicted no significant NEE trend over the United States. However, after using the calibrated crop model CLM4-CropM, we observed a significant decreasing NEE trend over the United States (-2.95 TgC yr^{-2}, p=0.04). In CLM4-CropM the Corn Belt was estimated to be an increasing carbon sink with averaged 0.005±0.002 PgC yr^{-1}, instead of a decreasing carbon sink estimated in CLM4-Crop with averaged value of -0.021±0.002 PgC yr^{-1}.

4. The maximum potential net CO_2 fertilization effects were calculated as -0.123, -0.056 and -0.099 PgC yr^{-1} by CLM4-CN, CLM4-Crop and CLM4-CropM, respectively.

Chapter 5: Conclusions

In order to estimate how future climate trends influence the agro-ecosystems and how the agro-ecosystems impact the regional energy, water, and carbon budgets, it is important to use reliable process-based climate models with prognostic crop schemes incorporated [*Betts*, 2005; *Lokupitiya et al.*, 2009; *Ma et al.*, 2012]. The crop phenology in CLM4-Crop was modified to better simulate corn and soybean phenology within the United States Corn Belt. In Chapter 2 two models, CLM3.5-CornSoy and CLM4-Crop, were evaluated against eight model-years of observations at two different AmeriFlux corn-soybean rotation sites. Our analyses indicated that the GDT method largely improved the estimation of leaf emergence of crops and thus has great potential to further improve energy, water, and carbon budget simulations over larger regions.

Although CLM3.5-CornSoy had better crop phenology than CLM4-Crop, CLM3.5 overestimated deep soil water. Thus in Chapter 3 we incorporated the new phenology into CLM4 (CLM4-CropM) and evaluated the two models (CLM4-Crop and CLM4-CropM) across multiple AmeriFlux sites. The improvement of CLM4-CropM simulated early growing season phenology was consistent over the sites (US-Bo1, US-Ne1, US-Ne3, US-Ro1 and US-Ro3) that have LAI data available. The correlation coefficients for R_n, H, LE and G were 0.94, 0.60, 0.76, and 0.57 for CLM4-Crop, and were 0.94, 0.65, 0.77, and 0.61, respectively, for CLM4-CropM. With better phenology, the CLM4-CropM model improved simulated sensible heat flux notably. The carbon budget was greatly improved using CLM4-CropM. The CLM4-CropM simulated long-term carbon budgets were closer

to observations at all three sites we investigated. An overestimated soybean GPP and ER was found in this study and a calibration/validation was carried out based on 14 soybean site years of data. After calibration, the correlation coefficient of simulated and observed LAI, NEE, GPP and ER were increased from 0.75, 0.58, 0.78 and 0.66 to 0.87, 0.76, 0.89 and 0.80. The overestimated GPP and ER were reduced by 84.7 % and 72.7%, respectively.

In Chapter 4 we investigated the carbon budget over the United States using three models: CLM4-CN, CLM4-Crop and the calibrated CLM4-CropM. Our results indicated that, the regional carbon budget was sensitive to how we represent crops in the land surface models. CLM4-Crop predicted the greatest carbon sink of -0.191 PgC m^{-2} yr^{-1} over the conterminous United States while the CLM4-CropM predicted the most moderate carbon sink of -0.094 PgC m^{-2} yr^{-1}. The pattern of carbon sources and sinks predicted in CLM4-CropM with calibrated parameters was similar to previous studies with the East Coast region identified as the major carbon sink. The maximum potential CO_2 fertilization effect on the conterminous United States was calculated as -0.123, -0.056 and -0.099 PgC yr^{-1} by CLM4-CN, CLM4-Crop and CLM4-CropM, respectively. Simulations using the calibrated CLM4-CropM indicate that the US Corn Belt carbon sink strength has increased over the past 57 years. The magnitude and trend of NEE estimated by CLM4-CropM was in relatively close agreement with remote sensing-based estimates. This study emphasized the importance of using calibrated crop models to improve the regional carbon budget estimations. It also highlighted that different crop schemes do not only

affect the averaged carbon budget estimated by the models, but also affect our prediction of how sensitive the crop system is to climate change.

Possible future work:

This study provided the capability of using land surface model combined with prognostic crop modules to study site to regional energy, water and carbon budgets. Our study also revealed some important model deficiencies. For example, CLM4-Crop used the same optical and photosynthesis parameterization for all crop types. The crop allocation scheme of CLM does not react to environmental stresses such as light, water and nutrient limitations, caused overly estimated productivity of crops. CLM4-Crop has a fixed rooting depth that does not have seasonal development and does not react to environmental factors. The maximum crop LAI constraints in the model might smooth out inter-annual dynamics and lead to overlooked model deficiencies in reasonably simulating photosynthesis and carbon allocation. Possible future model development includes the following aspects:

1. Reasonable seasonal crop root depth development [*Drewniak et al.*, 2013]
2. Allocation scheme that reacts to environmental stresses (e.g., light, water, nutrient)
3. Specific parameterization for different crops
4. Dynamic crop traits that changes along with climate conditions (i.e. GDD_{max})
5. Eliminating the maximum LAI constraint
6. Improve CLM canopy radiation transfer scheme.

References

Allmaras, R. R., W. W. Nelson, and W. B. Voorhees (1973), Soybean and corn rooting in Southwestern Minnesota : II . root distributions, *Soil Sci. Soc. Am. J.*, *39*, 771–777.

Asner, G., and C. Wessman (1998), Variability in leaf and litter optical properties: Implications for BRDF model inversions using AVHRR, MODIS, and MISR, *Remote Sens. Environ.*, *257*(January 1997), 243–257.

Baker, J. M., and T. J. Griffis (2005), Examining strategies to improve the carbon balance of corn/soybean agriculture using eddy covariance and mass balance techniques, *Agric. For. Meteorol.*, *128*(3-4), 163–177, doi:10.1016/j.agrformet.2004.11.005.

Baker, J. M., and T. J. Griffis (2008), How to build an inexpensive diffuse PAR sensor, in *28th Conference on Agricultural and Forest Meteorology, American Meteorological Society, April 28-May 2, 2008*, Orlando, Florida, USA.

Baker, J. M., and T. J. Griffis (2012), A device for continuous, in situ measurement of leaf area index, in *Soil Science Society of America Meeting, October 21-24, 2012*, Cincinnati, Ohio, USA.

Barr, A. G., T. A. Black, E. H. Hogg, N. Kljun, K. Morgenstern, and Z. Nesic (2004), Inter-annual variability in the leaf area index of a boreal aspen-hazelnut forest in relation to net ecosystem production, *Agric. For. Meteorol.*, *126*(3-4), 237–255, doi:10.1016/j.agrformet.2004.06.011.

Betts, R. A. (2005), Integrated approaches to climate-crop modelling: needs and challenges., *Philos. Trans. R. Soc. Lond. B. Biol. Sci.*, *360*(1463), 2049–2065, doi:10.1098/rstb.2005.1739.

Bilionis, I., B. a. Drewniak, and E. M. Constantinescu (2015), Crop physiology calibration in the CLM, *Geosci. Model Dev.*, *8*(4), 1071–1083, doi:10.5194/gmd-8-1071-2015.

Blanken, P. D., T. A. Black, P. C. Yang, H. H. Neumann, Z. Nesic, R. Staebler, G. den Hartog, M. D. Novak, and X. Lee (1997), Energy balance and canopy conductance of a boreal aspen forest: Partitioning overstory and understory components, *J. Geophys. Res.*, *102*(D24), 28915, doi:10.1029/97JD00193.

Bonan, G., and K. Oleson (2002), The Land Surface Climatology of the Community Land Model Coupled to the NCAR Community Climate Model, *J. Clim.*, *94*, 3123–3150.

Bonan, G., K. Oleson, R. Fisher, G. Lasslop, and M. Reichstein (2012), Reconciling leaf physiological traits and canopy flux data: Use of the TRY and FLUXNET databases in the Community Land Model version 4, *J. Geophys. Res.*, *117*, G02026, doi:10.1029/2011JG001913.

Bondeau, A. et al. (2007), Modelling the role of agriculture for the 20th century global

terrestrial carbon balance, *Glob. Chang. Biol.*, *13*(3), 679–706, doi:10.1111/j.1365-2486.2006.01305.x.

Chen, M., Q. Zhuang, D. R. Cook, R. Coulter, M. Pekour, R. L. Scott, J. W. Munger, and K. Bible (2011), Quantification of terrestrial ecosystem carbon dynamics in the conterminous United States combining a process-based biogeochemical model and MODIS and AmeriFlux data, *Biogeosciences*, *8*(9), 2665–2688, doi:10.5194/bg-8-2665-2011.

Chen, M., T. J. Griffis, J. Baker, J. D. Wood, and K. Xiao (2015), Simulating crop phenology in the Community Land Model and its impact on energy and carbon fluxes, *J. Geophys. Res. Biogeosciences*, *120*(2), 310–325, doi:10.1002/2014JG002780.

Ciais, P., P. Rayner, F. Chevallier, P. Bousquet, M. Logan, P. Peylin, and M. Ramonet (2010), Atmospheric inversions for estimating CO2 fluxes: methods and perspectives, *Clim. Change*, *103*(1-2), 69–92, doi:10.1007/s10584-010-9909-3.

Collatz, G., M. Ribas-Carbo, and J. Berry (1992), Coupled Photosynthesis-Stomatal Conductance Model for Leaves of C 4 Plants, *Aust. J. Plant Physiol.*, *19*(5), 519, doi:10.1071/PP9920519.

Collatz, G. J., J. T. Ball, C. Grivet, and J. A. Berry (1991), Physiological and environmental regulation of stomatal conductance, photosynthesis and transpiration: a model that includes a laminar boundary layer, *Agric. For. Meteorol.*, *54*(2-4), 107–136, doi:10.1016/0168-1923(91)90002-8.

Dai, Y. et al. (2003), The Common Land Model, *Bull. Am. Meteorol. Soc.*, *84*(8), 1013–1023, doi:10.1175/BAMS-84-8-1013.

Decker, M., and X. Zeng (2009), Impact of modified Richards equation on global soil moisture simulation in the Community Land Model (CLM3.5), *J. Adv. Model. Earth Syst.*, *1*, 1–22, doi:10.3894/JAMES.2009.1.5.

Dickinson, R., and K. Oleson (2006), The Community Land Model and its climate statistics as a component of the Community Climate System Model, *J. Clim.*, 2302–2324.

Donner, S. D., and C. J. Kucharik (2003), Evaluating the impacts of land management and climate variability on crop production and nitrate export across the Upper Mississippi Basin, *Global Biogeochem. Cycles*, *17*(3), doi:10.1029/2001GB001808.

Dorman, J., and P. Sellers (1989), A global climatology of albedo, roughness length and stomatal resistance for atmospheric general circulation models as represented by the simple biosphere model, *J. Appl. Meteorol.*, *28*, 833–855.

Drewniak, B., J. Song, J. Prell, V. R. Kotamarthi, and R. Jacob (2013), Modeling agriculture in the Community Land Model, *Geosci. Model Dev.*, *6*(2), 495–515, doi:10.5194/gmd-6-495-2013.

Dwyer, L., D. Stewart, and D. Balchin (1988), Rooting characteristics of corn, soybeans and barley as a function of available water and soil physical characteristics, *Can. J. Soil Sci.*, *68*, 121–132.

Fulton, J. P., L. G. Wells, and R. . Barnhisel (1996), Spatial Variation of Soil Physical Properties: A Precursor to Precision Tillage., in *ASAE Paper No. 961002*, Phoenix, Arizona.

Gervois, S., N. de Noblet-Ducoudré, N. Viovy, P. Ciais, N. Brisson, B. Seguin, and A. Perrier (2004), Including Croplands in a Global Biosphere Model: Methodology and Evaluation at Specific Sites, *Earth Interact.*, *8*(16), 1–25, doi:10.1175/1087-3562(2004)8<1:ICIAGB>2.0.CO;2.

Gervois, S., P. Ciais, N. de Noblet-Ducoudré, N. Brisson, N. Vuichard, and N. Viovy (2008), Carbon and water balance of European croplands throughout the 20th century, *Global Biogeochem. Cycles*, *22*(2), n/a–n/a, doi:10.1029/2007GB003018.

Gopalakrishnan, R., G. Bala, M. Jayaraman, L. Cao, R. Nemani, and N. H. Ravindranath (2011), Sensitivity of terrestrial water and energy budgets to CO2 -physiological forcing: an investigation using an offline land model, *Environ. Res. Lett.*, *6*(4), 1–7, doi:10.1088/1748-9326/6/4/044013.

Griffis, T., J. Baker, and J. Zhang (2005), Seasonal dynamics and partitioning of isotopic CO_2 exchange in a C_3/C_4 managed ecosystem, *Agric. For. Meteorol.*, *132*(1-2), 1–19, doi:10.1016/j.agrformet.2005.06.005.

Griffis, T. J., X. Lee, J. M. Baker, M. P. Russelle, X. Zhang, R. Venterea, and D. B. Millet (2013), Reconciling the differences between top-down and bottom-up estimates of nitrous oxide emissions for the U.S. Corn Belt, *Global Biogeochem. Cycles*, *27*(3), 746–754, doi:10.1002/gbc.20066.

Groisman, P., and D. Legates (1994), The accuracy of United States precipitation data, *Bull. Am. Meteorol. Soc.*, *75*(3), 215–227.

Guanter, L. et al. (2014), Global and time-resolved monitoring of crop photosynthesis with chlorophyll fluorescence., *Proc. Natl. Acad. Sci. U. S. A.*, *111*(14), E1327–33, doi:10.1073/pnas.1320008111.

Hicke, J. A., G. P. Asner, J. T. Randerson, C. Tucker, S. Los, R. Birdsey, J. C. Jenkins, C. Field, and E. Holland (2002), Satellite-derived increases in net primary productivity across North America, 1982–1998, *Geophys. Res. Lett.*, *29*(10), 1998–2001, doi:10.1029/2001GL013578.

Van den Hoof, C., E. Hanert, and P. L. Vidale (2011), Simulating dynamic crop growth with an adapted land surface model - JULES-SUCROS: Model development and validation, *Agric. For. Meteorol.*, *151*(2), 137–153, doi:10.1016/j.agrformet.2010.09.011.

Houghton, B. R. A., T. Woods, P. O. Box, and W. Hole (1999), The annual net flux of carbon to the atmosphere from changes in land use 1850 – 1990 *, *Tellus, 51B*, 298–

313, doi:10.1034/j.1600-0889.1999.00013.x.

Houghton, R. A. (1999), The U.S. Carbon Budget: Contributions from Land-Use Change, *Science (80-.).*, *285*(5427), 574–578, doi:10.1126/science.285.5427.574.

Houghton, R. A. (2003), Revised estimates of the annual net flux of carbon to the atmosphere from changes in land use and land management 1850-2000, *Tellus B*, *55*(2), 378–390, doi:10.1034/j.1600-0889.2003.01450.x.

Jin, J., and N. L. Miller (2010), Regional simulations to quantify land use change and irrigation impacts on hydroclimate in the California Central Valley, *Theor. Appl. Climatol.*, *104*(3-4), 429–442, doi:10.1007/s00704-010-0352-1.

June, T. (2011), Analysis of CO2 Fluxes: Inclusion of Wall Conductance (Gw) on the Estimation of Rubisco Activity, VCMAX of Soybean Leaves, *HAYATI J. Biosci.*, *18*(1), 43–50, doi:10.4308/hjb.18.1.43.

Karl, T. R., and T. C. Peterson (2009), *Global Climate Change Impacts in the United States*, Cambridge University Press.

Kattge, J., W. Knorr, T. Raddatz, and C. Wirth (2009), Quantifying photosynthetic capacity and its relationship to leaf nitrogen content for global-scale terrestrial biosphere models, *Glob. Chang. Biol.*, *15*(4), 976–991, doi:10.1111/j.1365-2486.2008.01744.x.

Keller, J., and R. D. Bliesner (1990), *Sprinkle and Trickle Irrigation*, Van Nostrand Reinhold, New York.

Kucharik, C., and T. Twine (2007), Residue, respiration, and residuals: Evaluation of a dynamic agroecosystem model using eddy flux measurements and biometric data, *Agric. For. Meteorol.*, *146*(3-4), 134–158, doi:10.1016/j.agrformet.2007.05.011.

Kucharik, C. J. (2003), Evaluation of a Process-Based Agro-Ecosystem Model (Agro-IBIS) across the U.S. Corn Belt: Simulations of the Interannual Variability in Maize Yield, *Earth Interact.*, *7*(14), 1–33, doi:10.1175/1087-3562(2003)007<0001:EOAPAM>2.0.CO;2.

Kucharik, C. J., and K. R. Brye (2003), Integrated BIosphere Simulator (IBIS) yield and nitrate loss predictions for Wisconsin maize receiving varied amounts of nitrogen fertilizer., *J. Environ. Qual.*, *32*(1), 247–268, doi:10.2134/jeq2003.2470.

Kucharik, C. J., J. a. Foley, C. Delire, V. a. Fisher, M. T. Coe, J. D. Lenters, C. Young-Molling, N. Ramankutty, J. M. Norman, and S. T. Gower (2000), Testing the performance of a dynamic global ecosystem model: Water balance, carbon balance, and vegetation structure, *Global Biogeochem. Cycles*, *14*(3), 795–825, doi:10.1029/1999GB001138.

Kumar, S., and V. Merwade (2011), Evaluation of NARR and CLM3.5 outputs for surface water and energy budgets in the Mississippi River Basin, *J. Geophys. Res.*, *116*(D8), 1–21, doi:10.1029/2010JD014909.

Kutsch, W. L. et al. (2010), The net biome production of full crop rotations in Europe, *Agric. Ecosyst. Environ.*, *139*(3), 336–345, doi:10.1016/j.agee.2010.07.016.

Laboski, C., R. Dowdy, R. Allmaras, and J. Lamb (1998), Soil strength and water content influences on corn root distribution in a sandy soil, *Plant Soil*, 239–247.

Lauvaux, T. et al. (2011), Constraining the CO_2 budget of the corn belt: exploring uncertainties from the assumptions in a mesoscale inverse system, *Atmos. Chem. Phys. Discuss.*, *11*(7), 20855–20898, doi:10.5194/acpd-11-20855-2011.

Lawrence, D. M., and A. G. Slater (2007), Incorporating organic soil into a global climate model, *Clim. Dyn.*, *30*(2-3), 145–160, doi:10.1007/s00382-007-0278-1.

Lawrence, D. M. et al. (2011), Parameterization improvements and functional and structural advances in Version 4 of the Community Land Model, *J. Adv. Model. Earth Syst.*, *3*(3), 1–27, doi:10.1029/2011MS000045.

Lawrence, D. M., K. W. Oleson, M. G. Flanner, C. G. Fletcher, P. J. Lawrence, S. Levis, S. C. Swenson, and G. B. Bonan (2012), The CCSM4 Land Simulation, 1850–2005: Assessment of Surface Climate and New Capabilities, *J. Clim.*, *25*(7), 2240–2260, doi:10.1175/JCLI-D-11-00103.1.

Lawrence, P. J., and T. N. Chase (2009), Climate Impacts of Making Evapotranspiration in the Community Land Model (CLM3) Consistent with the Simple Biosphere Model (SiB), *J. Hydrometeorol.*, *10*(2), 374–394, doi:10.1175/2008JHM987.1.

Lawrence, P. J., and T. N. Chase (2010), Investigating the climate impacts of global land cover change in the community climate system model, *Int. J. Climatol.*, *30*(13), 2066–2087, doi:10.1002/joc.2061.

Levis, S. (2010), Modeling vegetation and land use in models of the Earth System, *Adv. Rev.*, *1*, 840–856.

Levis, S., P. Thornton, G. Bonan, and C. Kucharik (2009), Modeling land use and land management with the Community Land Model, *iLeaps Newsl.*, *7*, 10–12.

Levis, S., G. B. Bonan, E. Kluzek, P. E. Thornton, A. Jones, W. J. Sacks, and C. J. Kucharik (2012), Interactive Crop Management in the Community Earth System Model (CESM1): Seasonal Influences on Land–Atmosphere Fluxes, *J. Clim.*, *25*(14), 4839–4859, doi:10.1175/JCLI-D-11-00446.1.

Li, M., and M. Zhuguo (2010), Comparisons of Simulations of Soil Moisture Variations in the Yellow River Basin Driven by Various Atmospheric Forcing Data Sets, *Adv. Atmos. Sci.*, *2*, 1–40, doi:10.1007/s00376-010-9155-7.1.

Lobell, D. B., J. A. Hicke, G. P. Asner, C. B. Field, C. J. Tucker, S. O. Los, and J. a H. D.B. Lobell G,P Asner, C.B. Field, C.J. Tucker and S.O. Los (2002), Satellite estimates of productivity and light use efficiency in United States agriculture, 1982-98, *Glob. Chang. Biol.*, *8*(8), 722–735, doi:10.1046/j.1365-2486.2002.00503.x.

Lobell, D. B., W. Schlenker, and J. Costa-Roberts (2011), Climate trends and global crop

production since 1980., *Science*, *333*(6042), 616–20, doi:10.1126/science.1204531.

Loescher, H., E. Ayres, P. Duffy, H. Luo, and M. Brunke (2014), Spatial variation in soil properties among North American ecosystems and guidelines for sampling designs, *PLoS One*, *9*(1), doi:10.1371/journal.pone.0083216.

Lokupitiya, E., S. Denning, K. Paustian, I. Baker, K. Schaefer, S. Verma, T. Meyers, C. J. Bernacchi, A. Suyker, and M. Fischer (2009), Incorporation of crop phenology in Simple Biosphere Model (SiBcrop) to improve land-atmosphere carbon exchanges from croplands, *Biogeosciences*, *6*(6), 969–986, doi:10.5194/bg-6-969-2009.

Long, S. P., and C. J. Bernacchi (2003), Gas exchange measurements, what can they tell us about the underlying limitations to photosynthesis? Procedures and sources of error, *J. Exp. Bot.*, *54*(392), 2393–2401, doi:10.1093/jxb/erg262.

Long, S. P., E. A. Ainsworth, A. Rogers, and D. R. Ort (2004), RISING ATMOSPHERIC CARBON DIOXIDE: Plants FACE the Future, *Annu. Rev. Plant Biol.*, *55*(1), 591–628, doi:10.1146/annurev.arplant.55.031903.141610.

Ma, S., G. Churkina, and K. Trusilova (2012), Investigating the impact of climate change on crop phenological events in Europe with a phenology model., *Int. J. Biometeorol.*, *56*(4), 749–63, doi:10.1007/s00484-011-0478-6.

Makino, A., H. Sakuma, E. Sudo, and T. Mae (2003), Differences between maize and rice in N-use efficiency for photosynthesis and protein allocation., *Plant Cell Physiol.*, *44*(9), 952–6.

Mourtzinis, S. et al. (2015), Climate-induced reduction in US-wide soybean yields underpinned by region- and in-season- speci fi c responses, *Nat. plants*, *1*(February), 8–11, doi:10.1038/nplants.2014.26.

Mzuku, M., R. Khosla, R. Reich, D. Inman, F. Smith, and L. MacDonald (2005), Spatial Variability of Measured Soil Properties across Site-Specific Management Zones, *Soil Sci. Soc. Am. J.*, *69*(5), 1572, doi:10.2136/sssaj2005.0062.

Neale, R. B. et al. (2010), Description of the NCAR Community Atmosphere Model (CAM 4.0), *Ncar/Tn-485+Str*, (April).

Oleson, K. W., G. B. Bonan, S. Levis, and M. Vertenstein (2004a), Effects of land use change on North American climate: impact of surface datasets and model biogeophysics, *Clim. Dyn.*, *23*(2), 117–132, doi:10.1007/s00382-004-0426-9.

Oleson, K. W. et al. (2004b), *Technical description of the community land model (CLM)*, National Center for Atmospheric Research, Boulder, Colorado.

Oleson, K. W., G. Y. Niu, Z. L. Yang, D. M. Lawrence, P. E. Thornton, P. J. Lawrence, R. Stockli, R. E. Dickinson, G. B. Bonan, and S. Levis (2007), *CLM3. 5 documentation*, Boulder, Colorado.

Oleson, K. W. et al. (2008), Improvements to the Community Land Model and their impact on the hydrological cycle, *J. Geophys. Res.*, *113*(G1), G01021,

doi:10.1029/2007JG000563.

Oleson, K. W. et al. (2010), *Technical description of version 4.0 of the Community Land Model (CLM)*, National Center for Atmospheric Research, Boulder, Colorado.

Oleson, K. W. et al. (2013), *Technical Description of version 4.5 of the Community Land Model (CLM)*, National Center for Atmospheric Research, Boulder, Colorado.

Osborne, T. M., D. M. Lawrence, A. J. Challinor, J. M. Slingo, and T. R. Wheeler (2007), Development and assessment of a coupled crop-climate model, *Glob. Chang. Biol.*, *13*(1), 169–183, doi:10.1111/j.1365-2486.2006.01274.x.

Pacala, S. W. et al. (2001), Consistent land- and atmosphere-based U.S. carbon sink estimates., *Science*, *292*(5525), 2316–20, doi:10.1126/science.1057320.

Peters, W. et al. (2007), An atmospheric perspective on North American carbon dioxide exchange: CarbonTracker., *Proc. Natl. Acad. Sci. U. S. A.*, *104*(48), 18925–18930, doi:10.1073/pnas.0708986104.

Piao, S. et al. (2010), The impacts of climate change on water resources and agriculture in China., *Nature*, *467*(7311), 43–51, doi:10.1038/nature09364.

Piao, S. et al. (2013), Evaluation of terrestrial carbon cycle models for their response to climate variability and to CO2 trends, *Glob. Chang. Biol.*, *19*(7), 2117–2132, doi:10.1111/gcb.12187.

Potter, C., S. Klooster, A. Huete, and V. Genovese (2007), Terrestrial carbon sinks for the United States Predicted from MODIS satellite data and ecosystem modeling, *Earth Interact.*, *11*(13), doi:10.1175/EI228.1.

Qian, T., A. Dai, and K. E. Trenberth (2007), Hydroclimatic Trends in the Mississippi River Basin from 1948 to 2004, *J. Clim.*, *20*(18), 4599–4614, doi:10.1175/JCLI4262.1.

Raddatz, R. L., and J. D. Cummine (2003), Inter-annual variability of moisture flux form the prairie agro-ecosystem: impact of crop phenology on the seasonal pattern of tornado days, *Boundary-Layer Meteorol.*, *106*, 283–295.

Randerson, J. T. et al. (2009), Systematic assessment of terrestrial biogeochemistry in coupled climate-carbon models, *Glob. Chang. Biol.*, *15*(10), 2462–2484, doi:10.1111/j.1365-2486.2009.01912.x.

Richardson, A. D., D. Y. Hollinger, J. D. Aber, S. V. Ollinger, and B. H. Braswell (2007), Environmental variation is directly responsible for short- but not long-term variation in forest-atmosphere carbon exchange, *Glob. Chang. Biol.*, *13*(4), 788–803, doi:10.1111/j.1365-2486.2007.01330.x.

Richardson, A. D. et al. (2012), Terrestrial biosphere models need better representation of vegetation phenology: results from the North American Carbon Program Site Synthesis, *Glob. Chang. Biol.*, *18*(2), 566–584, doi:10.1111/j.1365-2486.2011.02562.x.

Rosenzweig, C. et al. (2013), Assessing agricultural risks of climate change in the 21st century in a global gridded crop model intercomparison., *Proc. Natl. Acad. Sci. U. S. A.*, (14), 1–6, doi:10.1073/pnas.1222463110.

Ross, J. (1975), Radiative transfer in plant communities, in *Vegetation and the Atmosphere*, vol. 1, edited by J. L. Monteith, pp. 13–55, Academic Press.

Ross, J., and V. Ross (1969), Produktunost' fotosinteza v zavisimost' ot gustoty rastenii, photosynthetic Productivity of Plant Stand, pp. 44–59, IPA, Tartu.

Rowan, F. S., W. P. Robert, and R. S. Jeffrey (1987), The Nitrogen Use Efficiency of C_3 and C_4 Plants: II leaf nitrogen effects on the gas exchange characteristics of chenopodium albun (L.) and amaranthus retroflexus (L.), *Plant Physiol.*, *84*, 959–963.

Sacks, W. J., and C. J. Kucharik (2011), Crop management and phenology trends in the U.S. Corn Belt: Impacts on yields, evapotranspiration and energy balance, *Agric. For. Meteorol.*, *151*(7), 882–894, doi:10.1016/j.agrformet.2011.02.010.

Sacks, W. J., B. I. Cook, N. Buenning, S. Levis, and J. H. Helkowski (2008), Effects of global irrigation on the near-surface climate, *Clim. Dyn.*, *33*(2-3), 159–175, doi:10.1007/s00382-008-0445-z.

Sakaguchi, K., and X. Zeng (2009), Effects of soil wetness, plant litter, and under-canopy atmospheric stability on ground evaporation in the Community Land Model (CLM3.5), *J. Geophys. Res.*, *114*(D1), D01107, doi:10.1029/2008JD010834.

Sakaguchi, K., X. Zeng, B. J. Christoffersen, N. Restrepo-Coupe, S. R. Saleska, and P. M. Brando (2011a), Natural and drought scenarios in an east central Amazon forest: Fidelity of the Community Land Model 3.5 with three biogeochemical models, *J. Geophys. Res.*, *116*(G1), 1–25, doi:10.1029/2010JG001477.

Sakaguchi, K., X. Zeng, B. J. Christoffersen, N. Restrepo-Coupe, S. R. Saleska, and P. M. Brando (2011b), Natural and drought scenarios in an east central Amazon forest: Fidelity of the Community Land Model 3.5 with three biogeochemical models, *J. Geophys. Res.*, *116*(G1), G01029, doi:10.1029/2010JG001477.

Sargsyan, K., C. Safta, H. N. Najm, B. J. Debusschere, D. Ricciuto, and P. Thornton (2014), Dimensionality Reduction for Complex Models Via Bayesian Compressive Sensing, *Int. J. Uncertain. Quantif.*, *4*(1), 63–93, doi:10.1615/Int.J.UncertaintyQuantification.2013006821.

Schaefer, K. et al. (2012), A model-data comparison of gross primary productivity: Results from the North American Carbon Program site synthesis, *J. Geophys. Res.*, *117*(G3), G03010, doi:10.1029/2012JG001960.

Schepers, J., T. Blackmer, W. Wilhelm, and M. Resende (1996), Transmittance and Reflectance Measurements of CornLeaves from Plants with Different Nitrogen and Water Supply, *J. Plant Physiol.*, *148*, 523–529.

Schimel, D. S. et al. (2001), Recent patterns and mechanisms of carbon exchange by terrestrial ecosystems., *Nature*, *414*(6860), 169–172, doi:10.1038/35102500.

Schmitt, M. R., and G. E. Edwards (1981), Photosynthetic capacity and nitrogen use efficiency of maize, wheat and rice: A Comparison Between C_3 and C_4 Photosynthesis, *J. Exp. Bot.*, *32*(3), 459–466.

Schwalm, C. R. et al. (2010), A model-data intercomparison of CO 2 exchange across North America: Results from the North American Carbon Program site synthesis, *J. Geophys. Res.*, *115*, G00H05, doi:10.1029/2009JG001229.

Sheffield, J., G. Goteti, and E. F. Wood (2006), Development of a 50-Year High-Resolution Global Dataset of Meteorological Forcings for Land Surface Modeling, *J. Clim.*, *19*(13), 3088–3111, doi:10.1175/JCLI3790.1.

Song, Y., A. K. Jain, and G. F. McIsaac (2013), Implementation of dynamic crop growth processes into a land surface model: evaluation of energy, water and carbon fluxes under corn and soybean rotation, *Biogeosciences*, *10*(12), 8039–8066, doi:10.5194/bg-10-8039-2013.

Stehfest, E., M. Heistermann, J. A. Priess, D. S. Ojima, and J. Alcamo (2007), Simulation of global crop production with the ecosystem model DayCent, *Ecol. Modell.*, *209*(2-4), 203–219, doi:10.1016/j.ecolmodel.2007.06.028.

Stöckli, R., D. M. Lawrence, G.-Y. Niu, K. W. Oleson, P. E. Thornton, Z.-L. Yang, G. B. Bonan, A. S. Denning, and S. W. Running (2008), Use of FLUXNET in the Community Land Model development, *J. Geophys. Res.*, *113*(G1), 1–19, doi:10.1029/2007JG000562.

Suyker, A. E., and S. B. Verma (2010), Coupling of carbon dioxide and water vapor exchanges of irrigated and rainfed maize–soybean cropping systems and water productivity, *Agric. For. Meteorol.*, *150*(4), 553–563, doi:10.1016/j.agrformet.2010.01.020.

Suyker, A. E., and S. B. Verma (2012), Gross primary production and ecosystem respiration of irrigated and rainfed maize-soybean cropping systems over 8 years, *Agric. For. Meteorol.*, *165*, 12–24, doi:10.1016/j.agrformet.2012.05.021.

Taylor, K. (2001), Summarizing multiple aspects of model performance in a single diagram, *J. Geophys. Res*, *106*, 7183–7192.

Thornton, P. E., and N. A. Rosenbloom (2005), Ecosystem model spin-up: Estimating steady state conditions in a coupled terrestrial carbon and nitrogen cycle model, *Ecol. Modell.*, *189*(1-2), 25–48, doi:10.1016/j.ecolmodel.2005.04.008.

Thornton, P. E., J.-F. Lamarque, N. A. Rosenbloom, and N. M. Mahowald (2007), Influence of carbon-nitrogen cycle coupling on land model response to CO2 fertilization and climate variability, *Global Biogeochem. Cycles*, *21*(4), GB4018, doi:10.1029/2006GB002868.

Thornton, P. E., S. C. Doney, K. Lindsay, J. K. Moore, N. Mahowald, J. T. Randerson, I. Fung, J.-F. Lamarque, J. J. Feddema, and Y.-H. Lee (2009), Carbon-nitrogen interactions regulate climate-carbon cycle feedbacks: results from an atmosphere-ocean general circulation model, *Biogeosciences*, *6*(10), 2099–2120, doi:10.5194/bg-6-2099-2009.

Tsvetsinskaya, E. A., L. O. Mearns, and W. E. Easterling (2001), Investigating the Effect of Seasonal Plant Growth and Development in Three-Dimensional Atmospheric Simulations. Part I: Simulation of Surface Fluxes over the Growing Season, *J. Clim.*, *14*(5), 692–709, doi:10.1175/1520-0442(2001)014<0692:ITEOSP>2.0.CO;2.

Twine, T. E., and C. J. Kucharik (2009), Climate impacts on net primary productivity trends in natural and managed ecosystems of the central and eastern United States, *Agric. For. Meteorol.*, *149*(12), 2143–2161, doi:10.1016/j.agrformet.2009.05.012.

Twine, T. E., C. J. Kucharik, and J. A. Foley (2004), Effects of Land Cover Change on the Energy and Water Balance of the Mississippi River Basin, *J. Hydrometeorol.*, *5*(1982), 640–655, doi:10.1175/1525-7541(2004)005<0640:EOLCCO>2.0.CO;2.

Twine, T. E., J. J. Bryant, K. T Richter, C. J. Bernacchi, K. D. McConnaughay, S. J. Morris, and A. D. B. Leakey (2013), Impacts of elevated CO2 concentration on the productivity and surface energy budget of the soybean and maize agroecosystem in the Midwest USA., *Glob. Chang. Biol.*, *19*(9), 2838–52, doi:10.1111/gcb.12270.

Upton, G. J. G., and a. R. Rahimi (2003), On-line detection of errors in tipping-bucket raingauges, *J. Hydrol.*, *278*(1-4), 197–212, doi:10.1016/S0022-1694(03)00142-2.

Walter-Shea, E., and J. Norman (1991), Leaf reflectance and transmittance in soybean and corn, *Agron. J.*, *83*, 631–636.

Walter-Shea, E., J. Norman, and B. Blad (1989), Leaf bidirectional reflectance and transmittance in corn and soybean, *Remote Sens. Environ.*, *29*, 161–174.

Wang, A., and X. Zeng (2011), Sensitivities of terrestrial water cycle simulations to the variations of precipitation and air temperature in China, *J. Geophys. Res.*, *116*(D2), 1–11, doi:10.1029/2010JD014659.

Wang, T. et al. (2012), State-dependent errors in a land surface model across biomes inferred from eddy covariance observations on multiple timescales, *Ecol. Modell.*, *246*(C), 11–25, doi:10.1016/j.ecolmodel.2012.07.017.

Van Wart, J., P. Grassini, H. Yang, L. Claessens, A. Jarvis, and K. G. Cassman (2015), Creating long-term weather data from thin air for crop simulation modeling, *Agric. For. Meteorol.*, *209-210*, 49–58, doi:10.1016/j.agrformet.2015.02.020.

Webler, G., D. R. Roberti, S. V. Cuadra, V. S. Moreira, and M. H. Costa (2012), Evaluation of a Dynamic Agroecosystem Model (Agro-IBIS) for Soybean in Southern Brazil, *Earth Interact.*, *16*(12), 1–15, doi:10.1175/2012EI000452.1.

West, T. O. et al. (2010), Cropland carbon fluxes in the United States: Increasing

geospatial resolution of inventory-based carbon accounting, *Ecol. Appl.*, *20*(4), 1074–1086, doi:10.1890/08-2352.1.

Wilson, K. et al. (2002), Energy balance closure at FLUXNET sites, *Agric. For. Meteorol.*, *113*(1-4), 223–243, doi:10.1016/S0168-1923(02)00109-0.

Wu, X. et al. (2015), ORCHIDEE-CROP (v0), a new process based Agro-Land Surface Model: model description and evaluation over Europe, *Geosci. Model Dev. Discuss.*, *8*(6), 4653–4696, doi:10.5194/gmdd-8-4653-2015.

Wullschleger, S. (1993), Biochemical limitations to carbon assimilation in C3 plants—a retrospective analysis of the A/Ci curves from 109 species, *J. Exp. Bot.*, *44*(262), 907–920.

Xiao, J. et al. (2008), Estimation of net ecosystem carbon exchange for the conterminous United States by combining MODIS and AmeriFlux data, *Agric. For. Meteorol.*, *148*(11), 1827–1847, doi:10.1016/j.agrformet.2008.06.015.

Xiao, J. et al. (2010a), A continuous measure of gross primary production for the conterminous United States derived from MODIS and AmeriFlux data, *Remote Sens. Environ.*, *114*(3), 576–591, doi:10.1016/j.rse.2009.10.013.

Xiao, J. et al. (2011), Agricultural and Forest Meteorology Assessing net ecosystem carbon exchange of U . S . terrestrial ecosystems by integrating eddy covariance flux measurements and satellite observations, *Agric. For. Meteorol.*, *151*(1), 60–69, doi:10.1016/j.agrformet.2010.09.002.

Xiao, W., X. Lee, T. J. Griffis, K. Kim, L. R. Welp, and Q. Yu (2010b), A modeling investigation of canopy-air oxygen isotopic exchange of water vapor and carbon dioxide in a soybean field, *J. Geophys. Res.*, *115*(G1), 1–17, doi:10.1029/2009JG001163.

Xu, H. et al. (2016), Climate Change and Maize Yield in Iowa, edited by W. Wang, *PLoS One*, *11*(5), e0156083, doi:10.1371/journal.pone.0156083.

Yebra, M., A. I. J. M. Van Dijk, R. Leuning, and J. P. Guerschman (2015), Global vegetation gross primary production estimation using satellite-derived light-use efficiency and canopy conductance, *Remote Sens. Environ.*, *163*, 206–216, doi:10.1016/j.rse.2015.03.016.

Yin, X. (2013), Improving ecophysiological simulation models to predict the impact of elevated atmospheric CO_2 concentration on crop productivity., *Ann. Bot.*, *112*(3), 465–75, doi:10.1093/aob/mct016.

Yuan, X., and X.-Z. Liang (2011), Evaluation of a Conjunctive Surface–Subsurface Process Model (CSSP) over the Contiguous United States at Regional–Local Scales, *J. Hydrometeorol.*, *12*(4), 579–599, doi:10.1175/2010JHM1302.1.

Zeng, X., and M. Decker (2009), Improving the Numerical Solution of Soil Moisture–Based Richards Equation for Land Models with a Deep or Shallow Water Table, *J.*

Hydrometeorol., *10*(1), 308–319, doi:10.1175/2008JHM1011.1.

Zeng, X., M. Shaikh, and Y. Dai (2002), Coupling of the common land model to the NCAR community climate model, *J. Clim.*, *15*, 1832–1854.

Table 2.1 Parameters used in CLM3.5-CornSoy

	GDT_{on}[a]	GDT_{grain}[b]	Day_L[c]	χ_L[d]	F_{LNR}[e]	V_{cmax25}[f]
Corn	**450**	**1105**	**45000**	-0.30	**0.05**	*50*
Soybean	**400**	**1330**	**40800**	-0.30	0.10	*50*

[a]Leaf emergence threshold of growing degree time.
[b]Grain fill threshold of growing degree time.
[c]Typical day length when harvest begins in seconds.
[d]Leaf orientation index (-1 for vertical distribution and 1 for horizontal distribution).
[e]Fraction of leaf nitrogen in Rubisco.
[f]Maximum rate of carboxylation at 25˚C (μmol CO_2 m^{-2} s^{-1}).
[g]New parameters or new values in this study are presented in bold.

Table 2.2 Growing season (May to September) correlation coefficients and bias ($W\ m^{-2}$, in parenthesis) of the two model simulated hourly net radiation (R_n), sensible heat flux (H), latent heat flux (LE), ground heat flux (G) and leaf temperature (T_v).

		R_n		H		LE		G		T_v	
Year	Crop	CLM3.5-CornSoy	CLM4-Crop	CLM3.5-CornSoy	CLM4-Crop	CLM3.5-CornSoy	CLM4-Crop	CLM3.5-CornSoy	CLM4-Crop	CLM3.5-CornSoy	CLM4-Crop
						US_Ro1					
2007	corn	0.98 (12.3)	0.98 (12.7)	0.62 (-34.2)	0.65 (5.9)	0.90 (9.2)	0.81 (-26.6)	0.50 (6.5)	0.49 (4.4)	0.90 (-0.9)	0.91 (0.2)
2008	soybean	0.98 (21.5)	0.98 (21.5)	0.74 (-25.9)	0.47 (-2.8)	0.75 (-5.8)	0.52 (-11.1)	0.39 (9.0)	0.49 (1.3)	0.93 (0.2)	0.89 (1.0)
2009	corn	0.98 (12.8)	0.92 (18.0)	0.80 (-35.1)	0.52 (-2.0)	0.86 (-1.6)	0.65 (-23.2)	0.37 (7.3)	0.41 (4.6)	0.86 (-0.1)	0.86 (0.6)
2010	soybean	0.98 (26.2)	0.98 (31.0)	0.54 (20.5)	0.56 (18.6)	0.85 (29.3)	0.86 (-16.5)	0.31 (-12.5)	0.30 (-16.6)	0.89 (-0.2)	0.94 (0.4)
						US_Ro3					
2007	corn	0.99 (-0.4)	0.98 (-0.1)	0.68 (-43.5)	0.72 (-3.2)	0.91 (12.3)	0.83 (-24.0)	0.50 (8.3)	0.48 (6.2)	0.93 (-0.8)	0.93 (0.3)
2008	corn	0.99 (5.7)	0.98 (9.0)	0.73 (-36.2)	0.76 (10.9)	0.86 (13.3)	0.80 (-30.5)	0.54 (9.1)	0.51 (1.3)	0.92 (-0.2)	0.94 (1.5)
2009	soybean	0.98 (5.1)	0.93 (4.3)	0.83 (-24.3)	0.54 (8.5)	0.90 (5.4)	0.67 (-18.1)	0.5 (6.7)	0.55 (0.1)	0.92 (-0.1)	0.89 (0.7)
2010	corn	0.99 (2.9)	0.98 (6.0)	0.69 (-8.2)	0.55 (22.2)	0.92 (7.1)	0.85 (-32.4)	0.64 (3.8)	0.64 (2.8)	0.92 (-0.2)	0.92 (0.7)
						Average					
Corn		0.99(6.7)	0.97 (9.1)	0.70 (-31.4)	0.64 (6.8)	0.89(8.1)	0.79 (-27.3)	0.51 (7.0)	0.51 (3.9)	0.91 (-0.4)	0.91 (0.7)
Soybean		0.98 (17.6)	0.96 (18.9)	0.70 (-9.9)	0.52 (8.1)	0.83 (9.6)	0.68 (-15.2)	0.40 (1.1)	0.45 (-5.1)	0.91 (-0.0)	0.91 (0.7)
All		0.98 (10.8)	0.97 (12.8)	0.70 (-23.4)	0.60 (7.3)	0.87 (8.7)	0.75 (-22.8)	0.47 (4.8)	0.48 (0.5)	0.91 (-0.3)	0.91 (0.7)

[a]All P values ≤ 0.01.

Table 2.3 Correlation coefficients and bias (μmol·m^{-2}s^{-1}, in parenthesis) of the two model simulated hourly net ecosystem exchange (NEE), gross primary production (GPP), and ecosystem respiration (ER).

Year	Crop	NEE		GPP		ER	
		CLM3.5-CornSoy	CLM4-Crop	CLM3.5-CornSoy	CLM4-Crop	CLM3.5-CornSoy	CLM4-Crop
				US_Ro1			
2007	Corn	0.89 (-2.8)	0.59 (-0.5)	0.91 (6.0)	0.68 (2.2)	0.54 (3.1)	0.35 (1.7)
2008	Soybean	0.92 (-3.0)	0.70 (-1.4)	0.92 (6.2)	0.75 (3.3)	0.58 (3.1)	0.52 (1.9)
2009	Corn	0.85 (-2.5)	0.48 (-2.0)	0.85 (3.2)	0.47 (3.5)	0.51 (0.6)	0.12 (1.4)
2010	Soybean	0.89 (-0.9)	0.66 (1.6)	0.91 (8.0)	0.82 (3.5)	0.72 (7.1)	0.28 (5.1)
				US_Ro3			
2007	Corn	0.89 (-3.0)	0.66 (-0.7)	0.92 (5.5)	0.75 (1.8)	0.62 (2.4)	0.39 (1.0)
2008	Corn	0.82 (-2.0)	0.35 (-0.8)	0.83 (2.8)	0.41 (4.0)	0.54 (0.7)	0.23 (3.1)
2009	Soybean	0.90 (-1.1)	0.73 (-0.8)	0.90 (5.8)	0.74 (2.4)	0.46 (4.6)	0.37 (1.6)
2010	Corn	0.77 (-1.8)	0.27 (-3.1)	0.79 (3.0)	0.81 (6.9)	0.71 (1.1)	0.04 (3.7)
				Average			
Corn		0.84 (-2.4)	0.47 (-1.4)	0.86 (4.1)	0.62 (3.7)	0.59 (1.6)	0.23 (2.2)
Soybean		0.90 (-1.7)	0.69 (-0.2)	0.91 (6.7)	0.77 (3.1)	0.59 (4.9)	0.39 (2.8)
All		0.87 (-2.2)	0.55 (-1.0)	0.88 (5.1)	0.68 (3.4)	0.59 (2.9)	0.29 (2.4)

[a]All P values ≤ 0.01.

Table 3.1 AmeriFlux crop sites

ID	Site Name	Site Description	State	Latitude	Longitude	Elevation	Mean Annual Temp	Mean Annual Precip.	Years	Corn phase	Soybean phase
1	US-Ro1	Rosemount	MN	44.7143	-93.0898	260m	6.86 ˚C	806 mm	2007-2010	2007, 2009	2008, 2010
2	US-Ro3	Rosemount alternative management	MN	44.7217	-93.0893	260m	6.86 ˚C	806 mm	2007-2010	2007, 2008, 2010	2009
3	US-Bo1	Bondville	IL	40.0062	-88.2904	219m	11.02 ˚C	991 mm	1997-2007	odd years 1997-2007	even years 1998-2006
4	US-Bo2	Bondville Companion Site	IL	40.0061	-88.2918	219m	11.02 ˚C	991 mm	2005-2006	2006	2005
5	US-IB1	Fermi Agricultural	IL	41.8593	-88.2227	225m	9.18 ˚C	929 mm	2006-2008	2006, 2008	2007
6	US-Br1	Brooks Field Site 10	IA	41.9749	-93.6914	275m	8.95 ˚C	842 mm	2007-2010	2007, 2009	2008, 2010
7	US-Br3	Brooks Field Site 11	IA	41.9747	-93.6936	314m	8.95 ˚C	842 mm	2007-2010	2008, 2010	2007, 2009
8	US-Ne1	Mead Irrigated	NE	41.1650	-96.4766	361m	10.07 ˚C	784 mm	2002-2012	2002-2012	NA
9	US-Ne3	Mead Rainfed	NE	41.1797	-96.4396	363m	10.11 ˚C	784 mm	2002-2012	odd years 2003-2011	even years 2002-2012

Table 3.2. Correlation coefficients of the simulated and observed hourly energy and NEE fluxes.

Model	R_n	H	LE	G	NEE
		US-Bo1			
CLM4-Crop	0.95	0.64	0.77	0.63	0.58
CLM4-Crop_Modified	0.95	0.67	0.77	0.65	0.62
		US-Bo2			
CLM4-Crop	0.84	0.51	0.60	0.22	0.45
CLM4-Crop_Modified	0.85	0.59	0.65	0.24	0.51
		US-Br1			
CLM4-Crop	0.96	0.62	0.83	0.59	0.50
CLM4-Crop_Modified	0.95	0.67	0.82	0.63	0.56
		US-Br3			
CLM4-Crop	0.96	0.62	0.78	0.56	0.52
CLM4-Crop_Modified	0.96	0.67	0.77	0.62	0.58
		US-Ne1			
CLM4-Crop	0.98	0.57	0.80	0.68	0.58
CLM4-Crop_Modified	0.98	0.60	0.83	0.75	0.74
		US-Ne3			
CLM4-Crop	0.98	0.60	0.83	0.75	0.74
CLM4-Crop_Modified	0.98	0.67	0.83	0.70	0.66
		US-Ro1			
CLM4-Crop	0.93	0.64	0.74	0.72	0.50
CLM4-Crop_Modified	0.93	0.68	0.75	0.75	0.53
		US-Ro3			
CLM4-Crop	0.93	0.55	0.70	0.45	0.50
CLM4-Crop_Modified	0.93	0.59	0.72	0.47	0.57
		US-IB1			
CLM4-Crop	0.97	0.65	0.80	0.64	0.66
CLM4-Crop_Modified	0.97	0.73	0.83	0.67	0.76
		Average			
CLM4-Crop	0.94	0.60	0.76	0.57	0.54
CLM4-Crop_Modified	0.94	0.65	0.77	0.61	0.62

[a]All P values ≤ 0.01.

Table 3.3 Sensitivity tests for soybean simulations across sites. There are 5 years at US-Bo1, 6 years at US-Ne3, 2 years at US-Ro1 and 1 year at US-Ro3. The values of the parameters showed in the table are the default values. The left 4 columns and the right 4 columns showed the model responses after 20% increase and decrease of the parameter, respectively. Here *xl* is leaf angle distribution factor; *slatop* is specific leaf area at top of the canopy ($m^2\ gC^{-1}$); *feafi* is a dimensionless parameter for calculating initial carbon allocation to leaf; V_{cmax25} is the maximum carboxylation rate of rubisco ($\mu mol\ m^{-2}\ s^{-1}$); GDD_{mat} is the growing degree days required to reach plant maturity, in another word to reach crop harvest.

	-20%				+20%			
	Δ NEE	Δ GPP	Δ ER	Δ LAI	Δ NEE	Δ GPP	Δ ER	Δ LAI
				xl=0				
US-Bo1	1.0%	-0.1%	0.0%	-0.3%	1.1%	-0.6%	-0.4%	0.1%
US-Ne3	-13.9%	1.1%	0.8%	0.3%	26.1%	-1.8%	-1.2%	-0.6%
US-Ro1	-50.1%	1.4%	0.8%	-0.1%	19.1%	-1.3%	-1.1%	-0.1%
US-Ro3	4.4%	0.6%	0.8%	0.1%	0.7%	-0.7%	-0.6%	-0.1%
				slatop=0.07				
US-Bo1	9.1%	-3.7%	-2.3%	-5.4%	-5.1%	2.1%	1.4%	3.2%
US-Ne3	47.6%	-4.2%	-3.1%	-8.5%	-26.7%	2.2%	1.6%	3.8%
US-Ro1	116.3%	-4.1%	-2.7%	-4.8%	-97.5%	2.7%	1.6%	2.9%
US-Ro3	11.2%	-2.6%	-1.8%	-5.6%	-4.0%	1.4%	1.0%	3.0%
				fleafi=0.85				
US-Bo1	6.2%	-2.7%	-1.7%	-4.3%	-3.7%	1.7%	1.1%	2.6%
US-Ne3	28.7%	-3.0%	-2.4%	-6.5%	-19.3%	1.8%	1.3%	3.1%
US-Ro1	73.4%	-2.9%	-2.1%	-3.8%	-71.2%	2.0%	1.2%	2.3%
US-Ro3	8.1%	-2.0%	-1.4%	-4.3%	-3.3%	1.0%	0.8%	2.5%
				$V_{cmax25}=100$				
US-Bo1	13.0%	-8.0%	-5.7%	-2.8%	-4.7%	4.3%	3.3%	1.4%
US-Ne3	130.1%	-10.9%	-8.0%	-5.3%	-66.9%	5.6%	4.1%	2.2%
US-Ro1	279.6%	-12.4%	-9.1%	-3.2%	-208.9%	7.8%	5.3%	1.5%
US-Ro3	20.7%	-8.7%	-6.9%	-3.6%	-2.9%	5.0%	4.6%	0.9%
				GDD_{mat} *(dynamic)*				
US-Bo1	-2.3%	-9.6%	-8.9%	-26.3%	-2.5%	2.0%	1.5%	7.6%
US-Ne3	343.5%	-20.0%	-12.4%	-29.7%	-52.4%	2.9%	1.8%	9.8%
US-Ro1	-43.6%	0.7%	0.2%	-0.9%	11.6%	-0.8%	-0.7%	-0.4%
US-Ro3	5.7%	0.9%	1.1%	-2.5%	5.7%	-0.8%	-0.4%	-0.6%

Table 3.4 Calibration of soybean simulation, part one. Numbers in the table are correlation coefficients and bias (μmol·m^{-2}s^{-1}, in parenthesis) of the simulated weekly leaf area index (LAI), net ecosystem exchange (NEE), gross primary production (GPP), and ecosystem respiration (ER).

Model run	LAI	NEE	GPP	ER
Control run: gddmat=default vcmx=100 slatop=0.07 fleafi=0.85				
Control 1:				
US-Bo1(1998,2000)	0.85 (0.89)	0.51 (-98.70)	0.77 (1117.50)	0.55 (961.70)
US-Ne3(2002,2004,2006)	0.77 (1.40)	0.55 (-178.38)	0.72 (784.47)	0.67 (605.04)
US-Ro1(2008,2010)	0.62 (1.34)	0.79 (-196.21)	0.88 (822.78)	0.78 (625.72)
Control 1 average	0.75 (1.24)	0.61 (-160.71)	0.78 (890.57)	0.67 (712.85)
Control 2:				
US-Bo1(2002,2004,2006)	0.78 (1.18)	0.64 (53.11)	0.84 (577.65)	0.68 (629.94)
US-Ne3(2008,2010,2012)	0.72 (1.46)	0.47 (-125.23)	0.71 (936.9)	0.7 (809.69)
US-Ro3(2009)	0.67 (1.28)	0.52 (61.34)	0.73 (538.78)	0.49 (598.02)
Control 2 average	0.74 (1.32)	0.55 (-22.15)	0.77 (726.06)	0.66 (702.42)
Total site-year average	**0.75 (1.28)**	**0.58 (-91.43)**	**0.78 (808.32)**	**0.66 (707.63)**
*Calibration run: gddmat*0.8, jday*0.8 vcmx= 80 slatop=0.06 fleafi=0.68*				
Calibration:				
US-Bo1(1998,2000)	0.97 (-0.08)	0.83 (-46.72)	0.86 (534.36)	0.67 (484.44)
US-Ne3(2002,2004,2006)	0.91 (0.10)	0.62 (123.45)	0.83 (-99.7)	0.85 (23.57)
US-Ro1(2008,2010)	0.69 (0.15)	0.81 (-38.34)	0.9 (238.25)	0.76 (199.87)
Calibration average	0.87 (0.06)	0.74 (28.61)	0.86 (178.02)	0.77 (205.62)
Validation:				
US-Bo1(2002,2004,2006)	0.95 (0.11)	0.93 (137.09)	0.97 (120.16)	0.86 (255.13)
US-Ne3(2008,2010,2012)	0.8 (0.10)	0.65 (87.62)	0.86 (-23.87)	0.85 (62.75)
US-Ro3(2009)	0.86 (0.04)	0.75 (113.65)	0.91 (197.80)	0.7 (311.04)
Validation average	0.87 (0.10)	0.78 (112.54)	0.91 (69.52)	0.83 (180.67)
Total site-year average	**0.87 (0.08)**	**0.76 (70.57)**	**0.89 (123.77)**	**0.8 (193.15)**

Table 3.5 Calibration of soybean simulation, part two. Numbers in the table are correlation coefficients and bias (μmol·m^{-2}s^{-1}, in parenthesis) of the simulated weekly net radiation (*Rn*), sensible heat flux (*H*) and latent heat flux (*LE*).

Model run	*Rn*	*H*	*LE*
Control run: gddmat=default vcmx=100 slatop=0.07 fleafi=0.85			
Control 1:			
US-Bo1(1998,2000)	0.98 (-5.92)	0.43 (-0.55)	0.92 (-4.71)
US-Ne3(2002,2004,2006)	0.97 (-5.92)	0.23 (4.19)	0.85 (-0.57)
US-Ro1(2008,2010)	0.94 (-34.71)	0.51 (-18.40)	0.9 (2.37)
Control 1 average	0.97 (-14.15)	0.36 (-3.62)	0.88 (-0.91)
Control 2:			
US-Bo1(2002,2004,2006)	0.9 (-2.83)	0.33 (5.45)	0.9 (-3.11)
US-Ne3(2008,2010,2012)	0.98 (-3.62)	0.2 (7.51)	0.88 (1.15)
US-Ro3(2009)	0.93 (-17.8)	0.63 (-13.97)	0.87 (1.28)
Control 2 average	0.94 (-5.31)	0.32 (3.56)	0.89 (-0.66)
Total site-year average	**0.95 (-9.73)**	**0.34 (-0.03)**	**0.89 (-0.78)**
*Calibration run: gddmat*0.8, jday*0.8 vcmx= 80 slatop=0.06 fleafi=0.68*			
Calibration:			
US-Bo1(1998,2000)	0.98 (-9.94)	0.49 (1.36)	0.91 (-10.44)
US-Ne3(2002,2004,2006)	0.98 (-13.87)	0.48 (7.35)	0.91 (-11.60)
US-Ro1(2008,2010)	0.95 (-39.19)	0.56 (-16.81)	0.88 (-4.06)
Calibration average	0.97 (-19.98)	0.5 (-1.26)	0.9 (-9.12)
Validation:			
US-Bo1(2002,2004,2006)	0.9 (-7.05)	0.5 (5.88)	0.95 (-7.59)
US-Ne3(2008,2010,2012)	0.98 (-11.35)	0.41 (10.33)	0.91 (-9.26)
US-Ro3(2009)	0.93 (-21.01)	0.72 (-14.72)	0.93 (-1.26)
Validation average	0.94 (-10.89)	0.49 (4.85)	0.93 (-7.40)
Total site-year average	**0.96 (-15.43)**	**0.5 (1.79)**	**0.91 (-8.26)**

Table 4.1 List of PFTs in CLM4-CN and CLM4-Crop (CLM4-CropM)

CLM-CN	CLM-Crop and CLM-CropM
Same PFTs	
1. needle-leaf evergreen temperate tree	
2. needle-leaf evergreen boreal tree	
3. needle-leaf deciduous boreal tree	
4. broadleaf evergreen tropical tree	
5. broadleaf evergreen temperate tree	
6. broadleaf deciduous tropical tree	
7. broadleaf deciduous temperate tree	
8. broadleaf deciduous boreal tree	
9. broadleaf evergreen shrub	
10. broadleaf deciduous temperate shrub	
11. broadleaf deciduous boreal shrub	
12. c3 arctic grass	
13. c3 non-arctic grass	
14. c4 grass	
15. corn	
Different PFTs	
16. wheat(place holder)	16. C3 unmanaged crop
	17. C3 irrigated crop
	18. Temperate Cereals
	19. Winter cereals (place holder)
	20. Soybean

Table 4.2 57-year (1948-2004) averaged carbon budgets over the conterminous United States. Unit is *PgC* yr^{-1}.

	NEE	NPP	GPP	ER
		Steady CO2		
CLM4-CN	-0.091±0.034	3.122±0.027	8.570±0.053	8.350±0.048
CLM4-Crop	-0.135±0.021	3.797±0.022	8.645±0.042	8.400±0.040
CLM4-CropM	-0.037±0.024	3.271±0.024	7.770±0.044	7.623±0.038
		Transient CO2		
CLM4-CN	-0.139±0.034	3.238±0.028	8.898±0.061	8.631±0.057
CLM4-Crop	-0.191±0.020	3.992±0.026	9.044±0.055	8.742±0.053
CLM4-CropM	-0.094±0.024	3.460±0.028	8.155±0.056	7.951±0.049

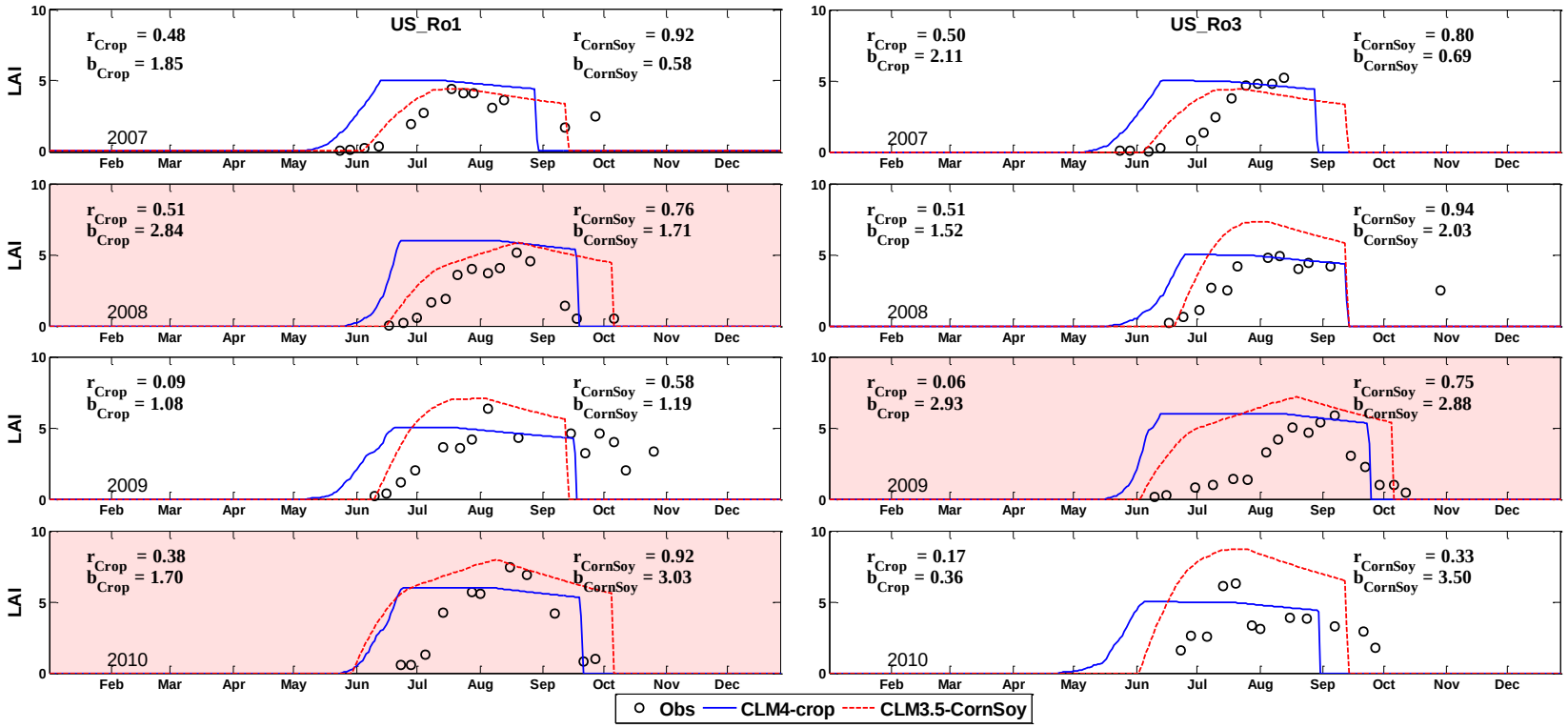

Figure 1.1 Simulated LAI compared with field observations. Circles represent observed values. The red line represents CLM3.5-CornSoy and the blue line represents CLM4-Crop. The white backgrounds represent corn years and the shaded background represents soybean years. The correlation coefficients (*r*) and bias (*b*) are calculated based on weekly averaged values. The subscript Crop stands for CLM-Crop and CornSoy stands for CLM3.5-CornSoy.

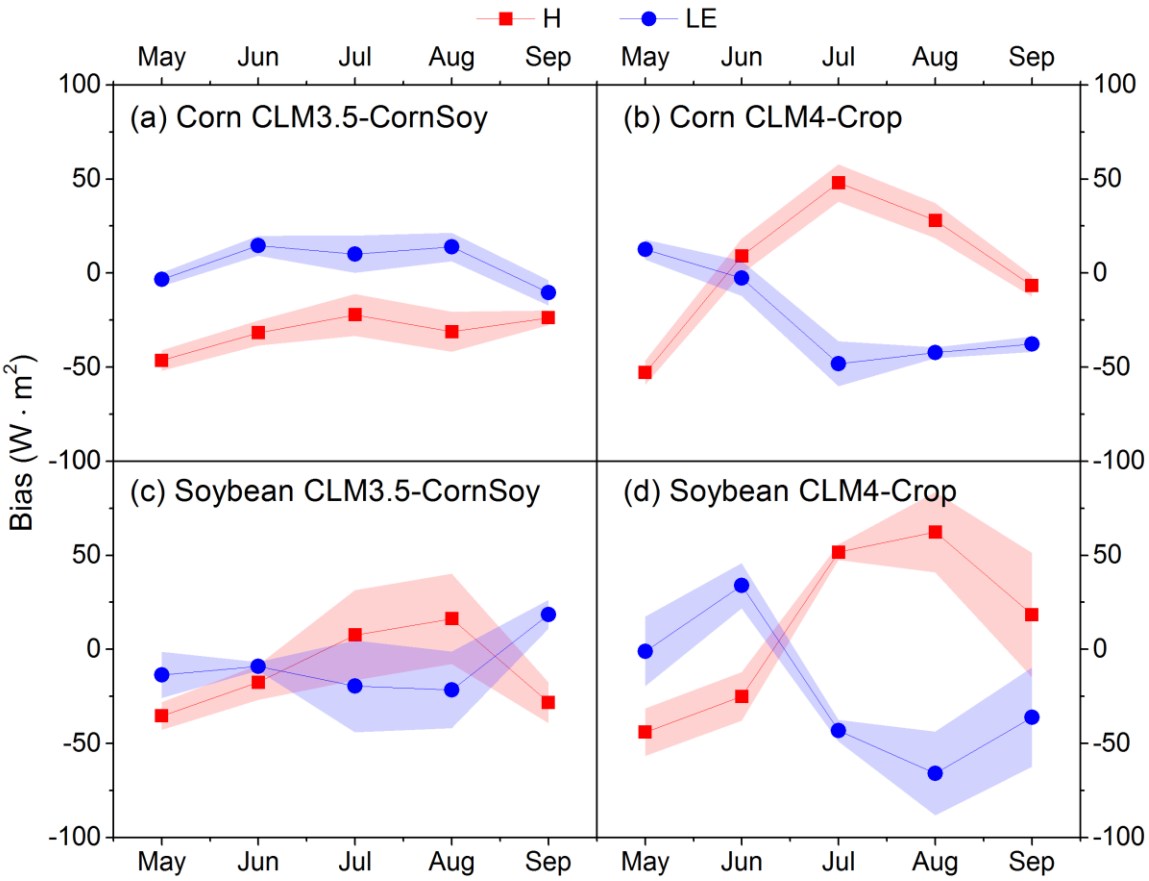

Figure 2.1 The 2007-2010 monthly average bias (model-observation) of two models simulated *H* and *LE*. For corn, it is averaged over 5 model years. For soybean, it is averaged over 3 model years. The shaded regions represent the standard errors of the monthly biases.

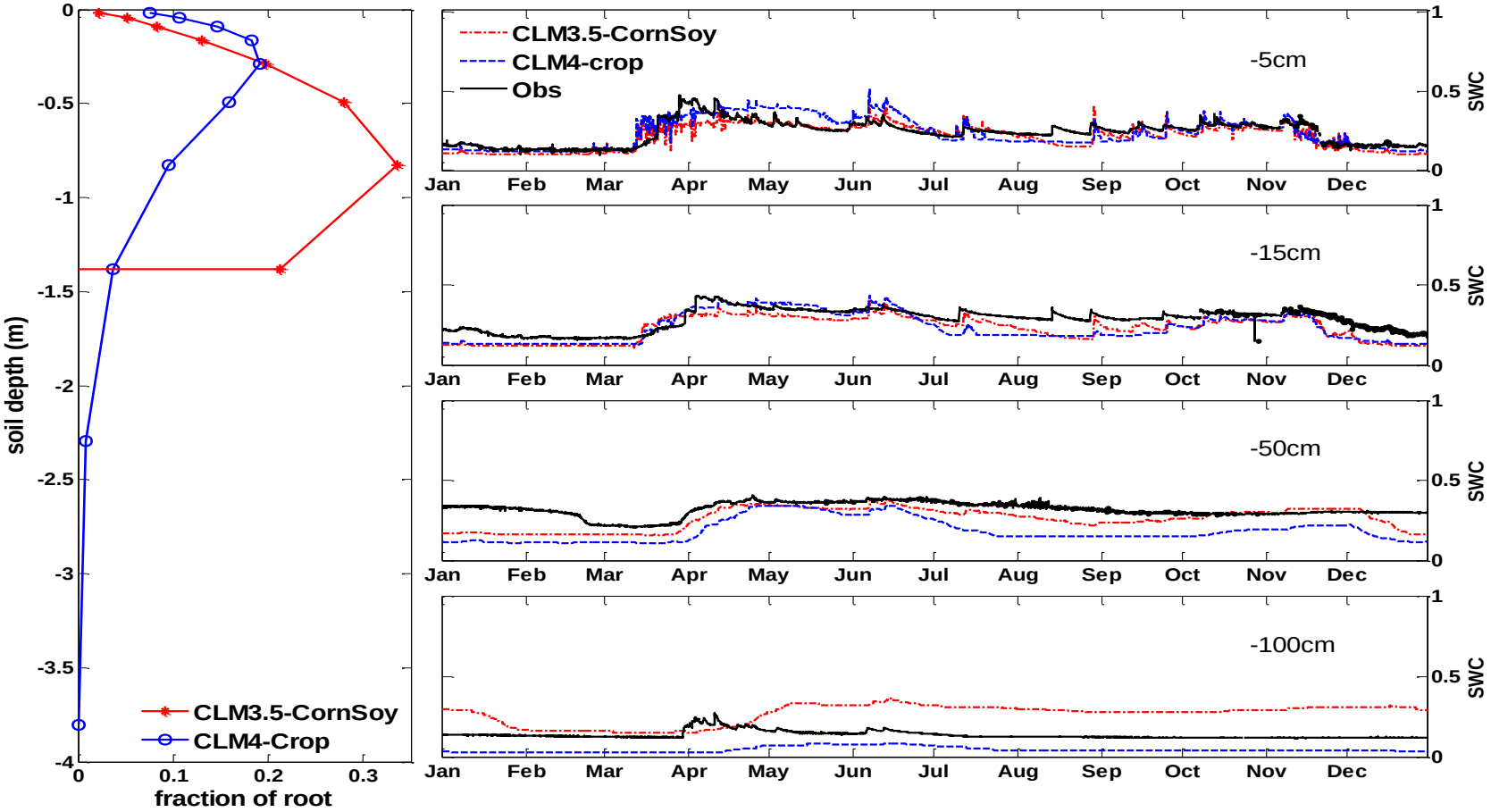

Figure 2.2 Crop root distribution and evaluation of soil liquid water content simulations at different soil depths in 2008, site US-Ro1, which was in a soybean phase. CLM simulated soil water contents are linearly interpolated to the observation depths -5 cm, -15 cm, -50 cm and -100 cm.

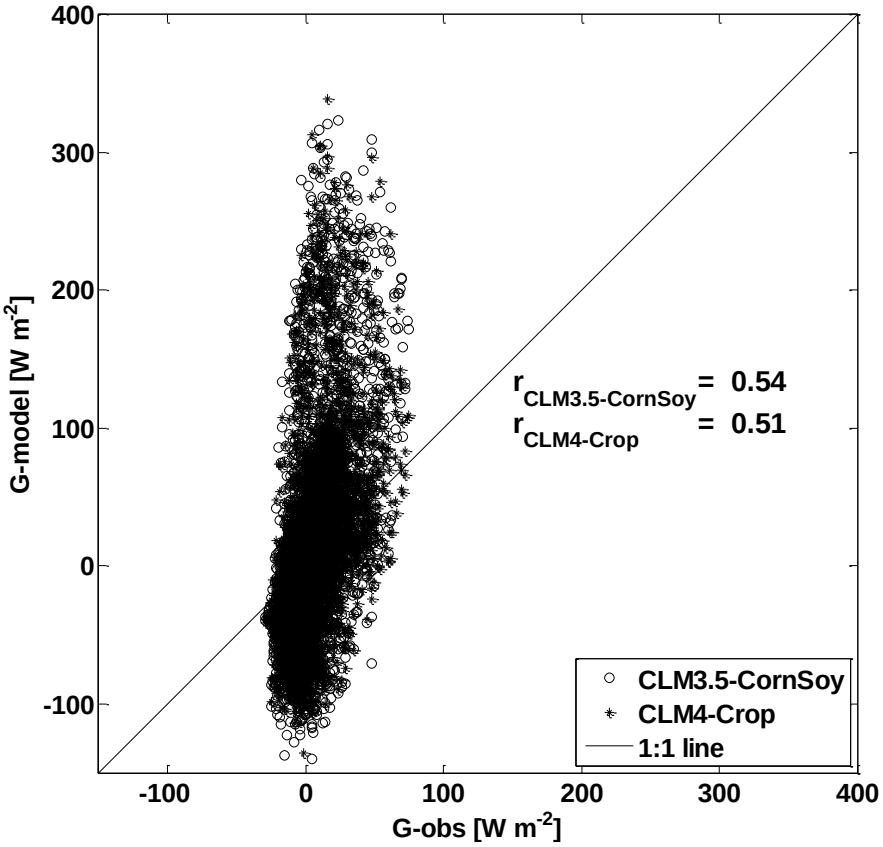

Figure 2.3 Evaluation of model simulated *G*. The data used in this figure are from US-Ro3 in 2008, which was in the corn phase of the crop rotation.

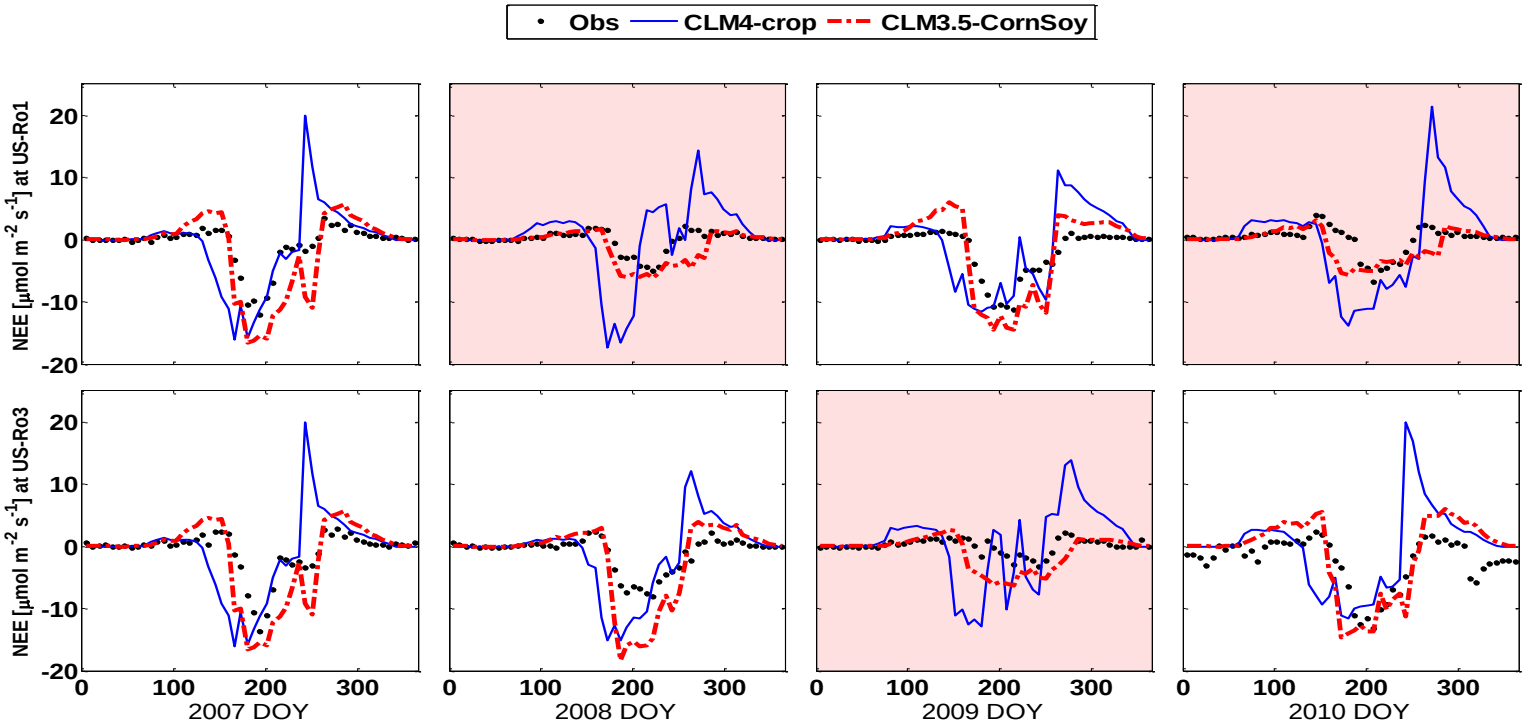

Figure 2.4 (a) Weekly averaged NEE at the two sites from 2007 to 2010. The white backgrounds represent corn years, and the shaded background represents soybean years. The red dashed lines represent CLM3.5-CornSoy, the blue solid lines represent CLM4-Crop, and the black dots represent observations.

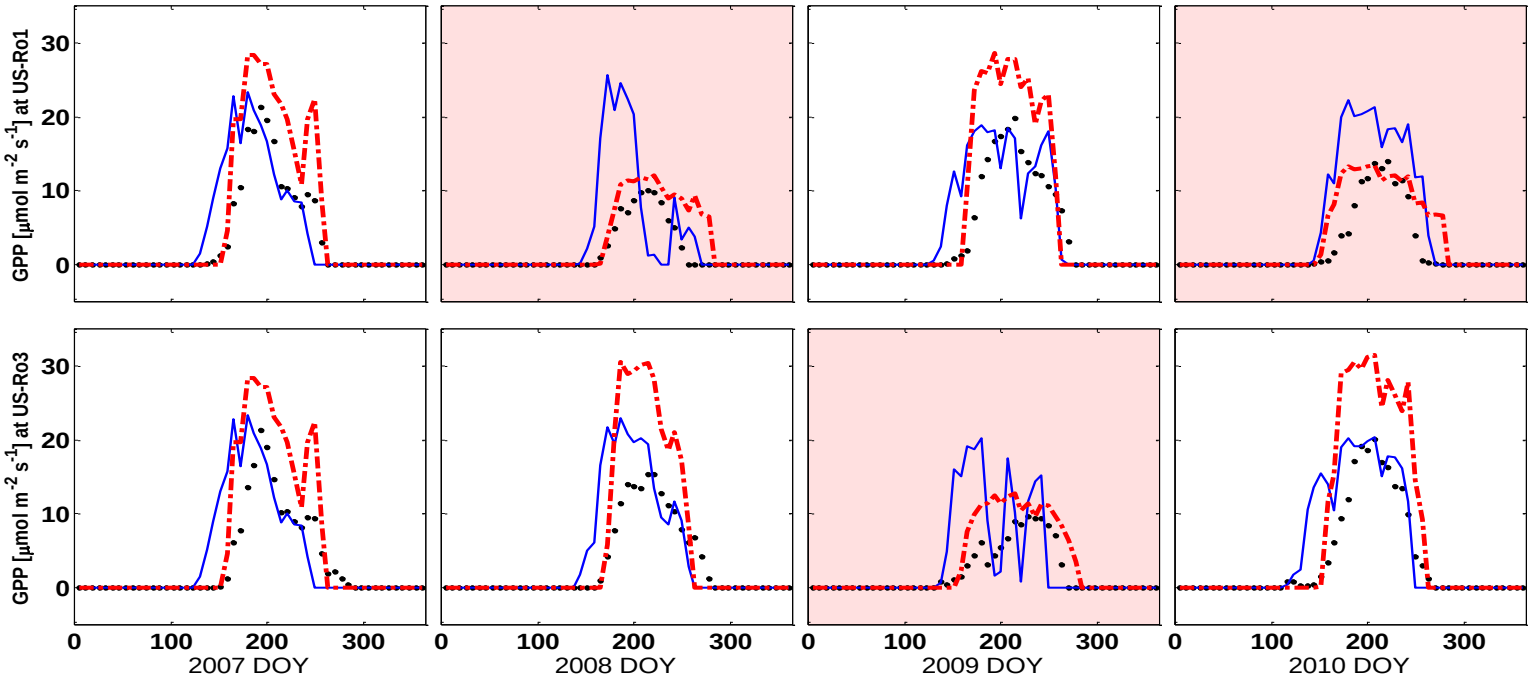

Figure 2.4 (b) Weekly averaged GPP at the two sites from 2007 to 2010. The white backgrounds represent corn years, and the shaded background represents soybean years. The red dashed lines represent CLM3.5-CornSoy, the blue solid lines represent CLM4-Crop, and the black dots represent observations.

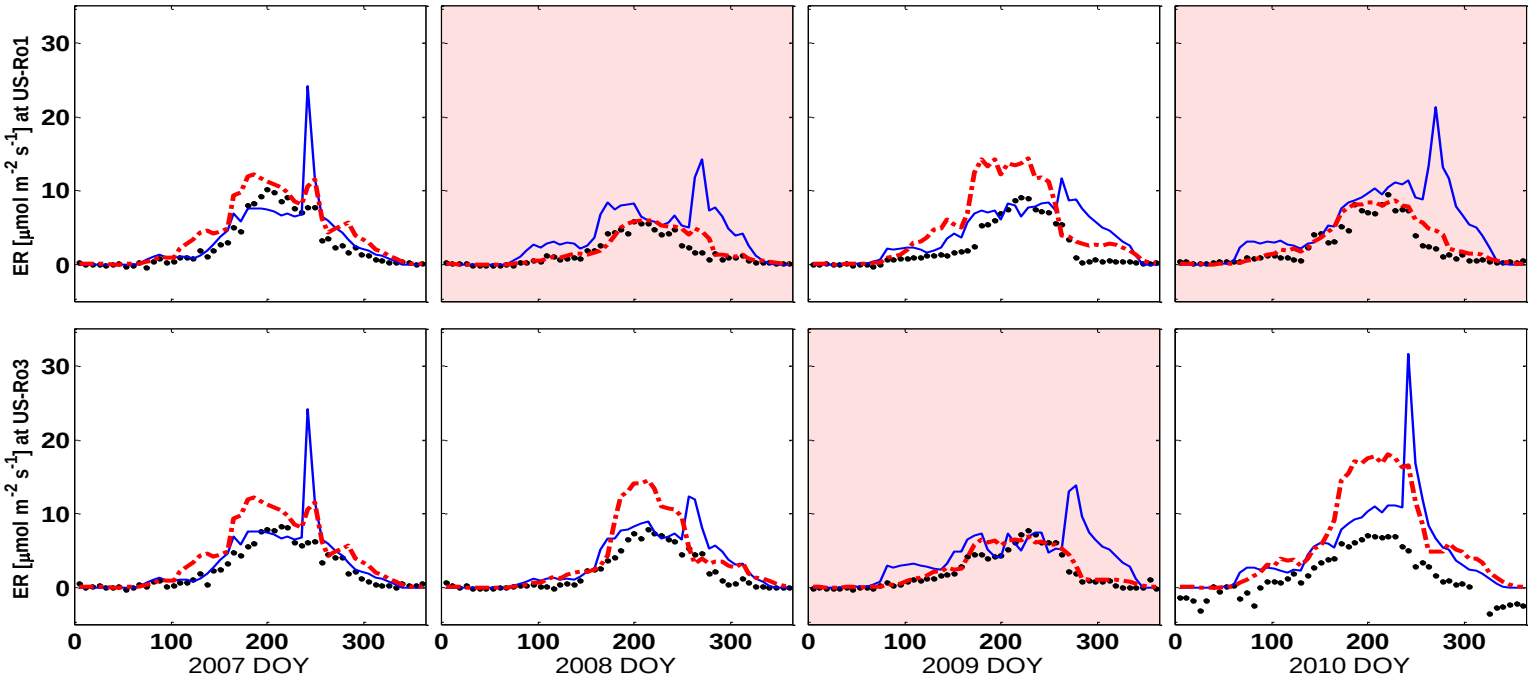

Figure 2.4 (c) Weekly averaged ER at the two sites from 2007 to 2010. The white backgrounds represent corn years, and the shaded background represents soybean years. The red dashed lines represent CLM3.5-CornSoy, the blue solid lines represent CLM4-Crop, and the black dots represent observations.

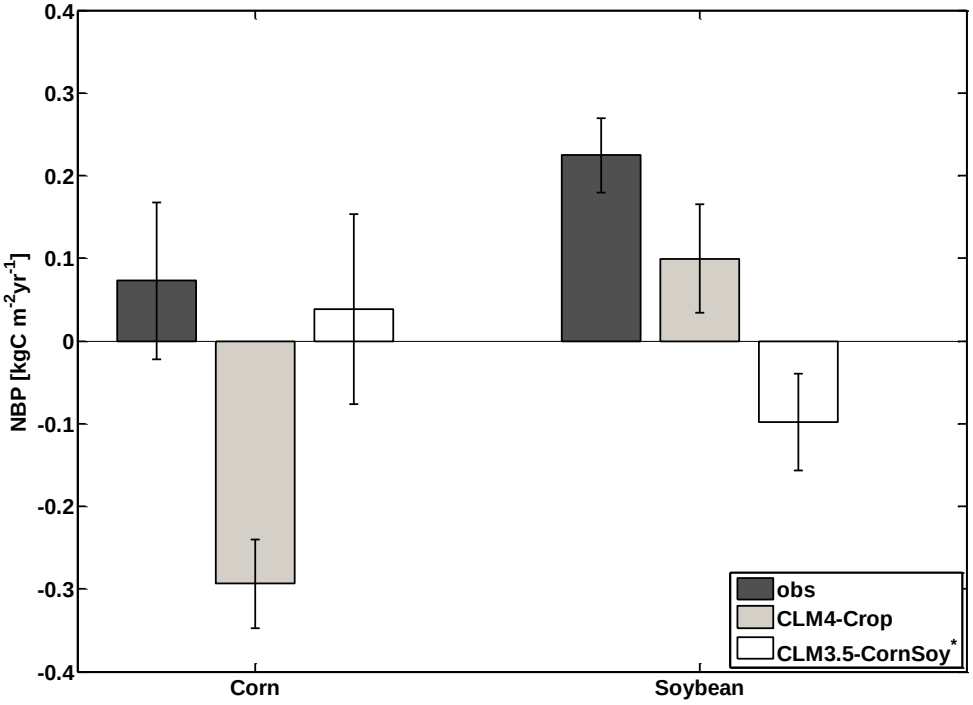

Figure 2.5 Evaluation of the simulated annual NBP budgets for corn and soybean. The error bars represent the standard errors of the annual NBP. The NBP of CLM3.5-CornSoy is estimated using the NEE of CLM3.5-CornSoy plus the harvested carbon calculated from yield data at the sites.

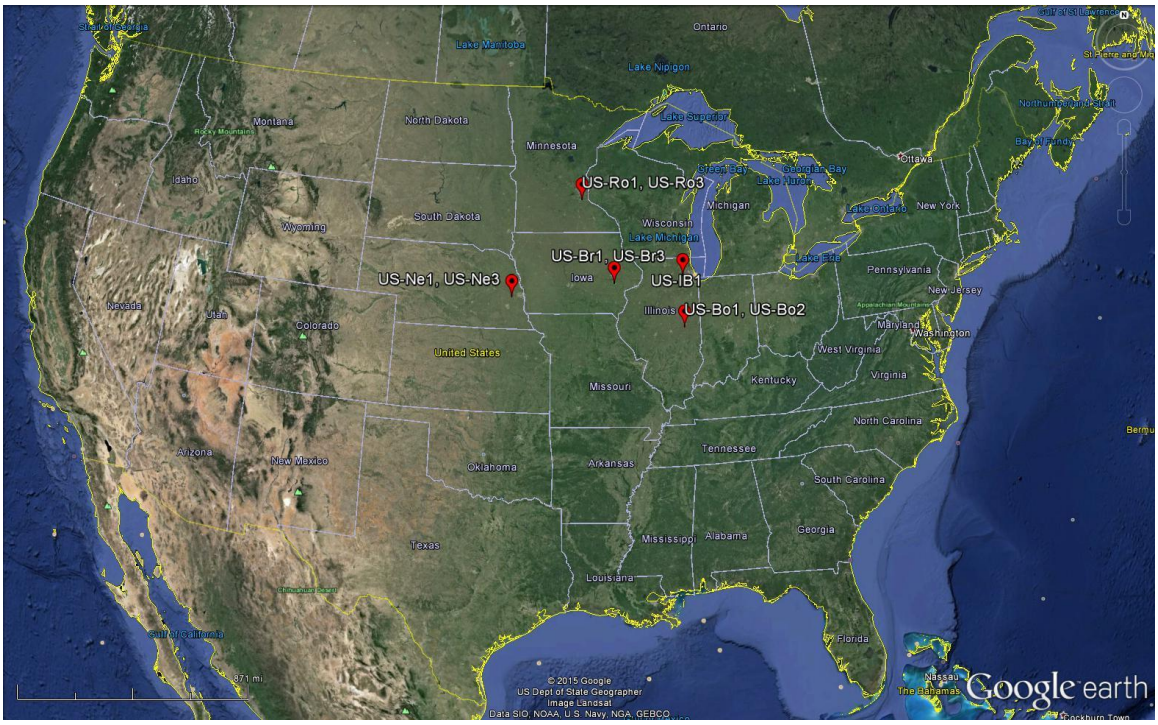

Figure 3.1 Nine AmeriFlux crop sites within the US Corn Belt

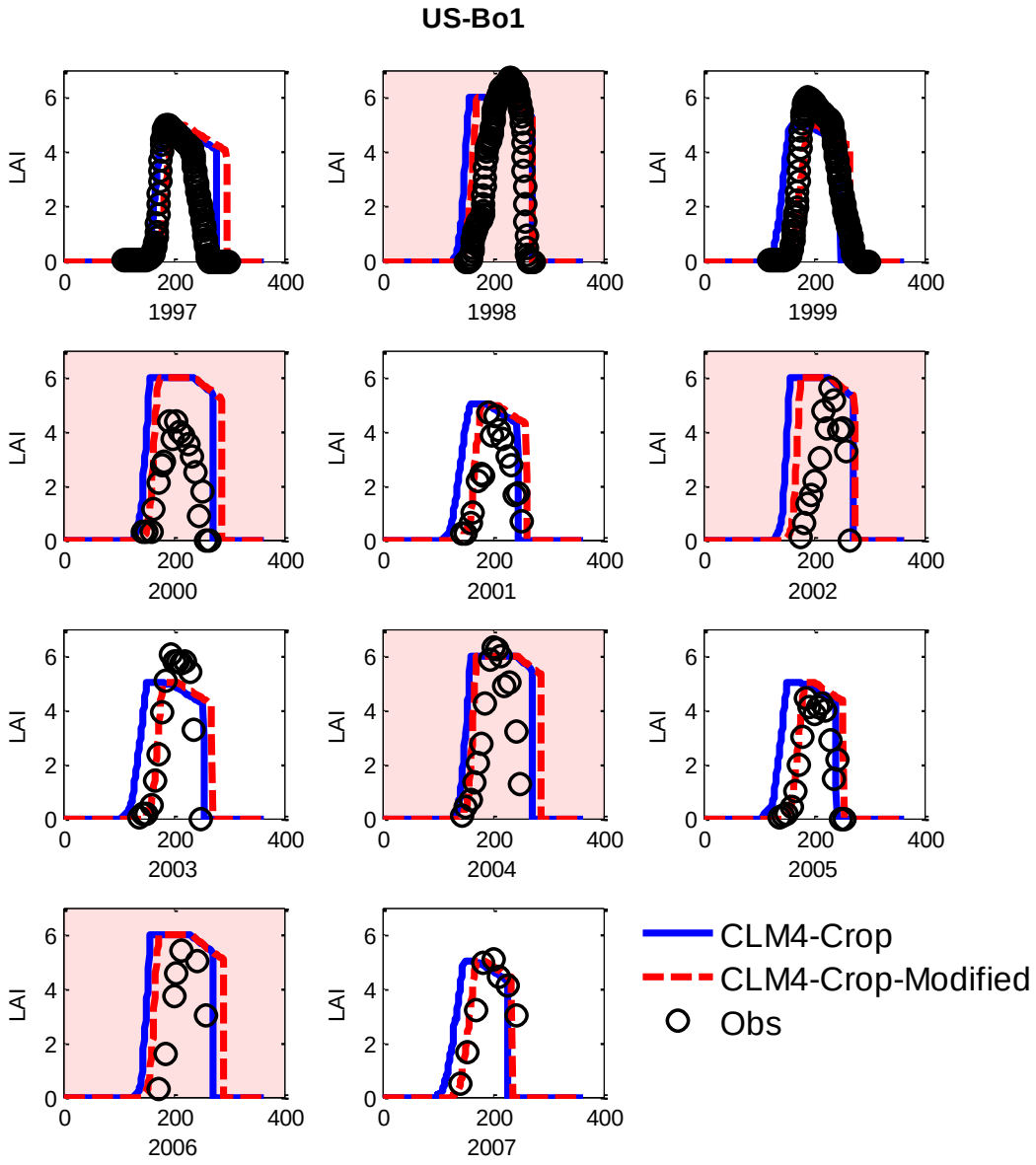

Figure 3.2 Evaluation of the simulated phenology for corn (white background) and soybean (red background) at AmeriFlux site Bondville (US-Bo1). The blue line represents default CLM4-Crop simulation and the red dashed line represents CLM4-Crop with modified phenology according to chapter two.

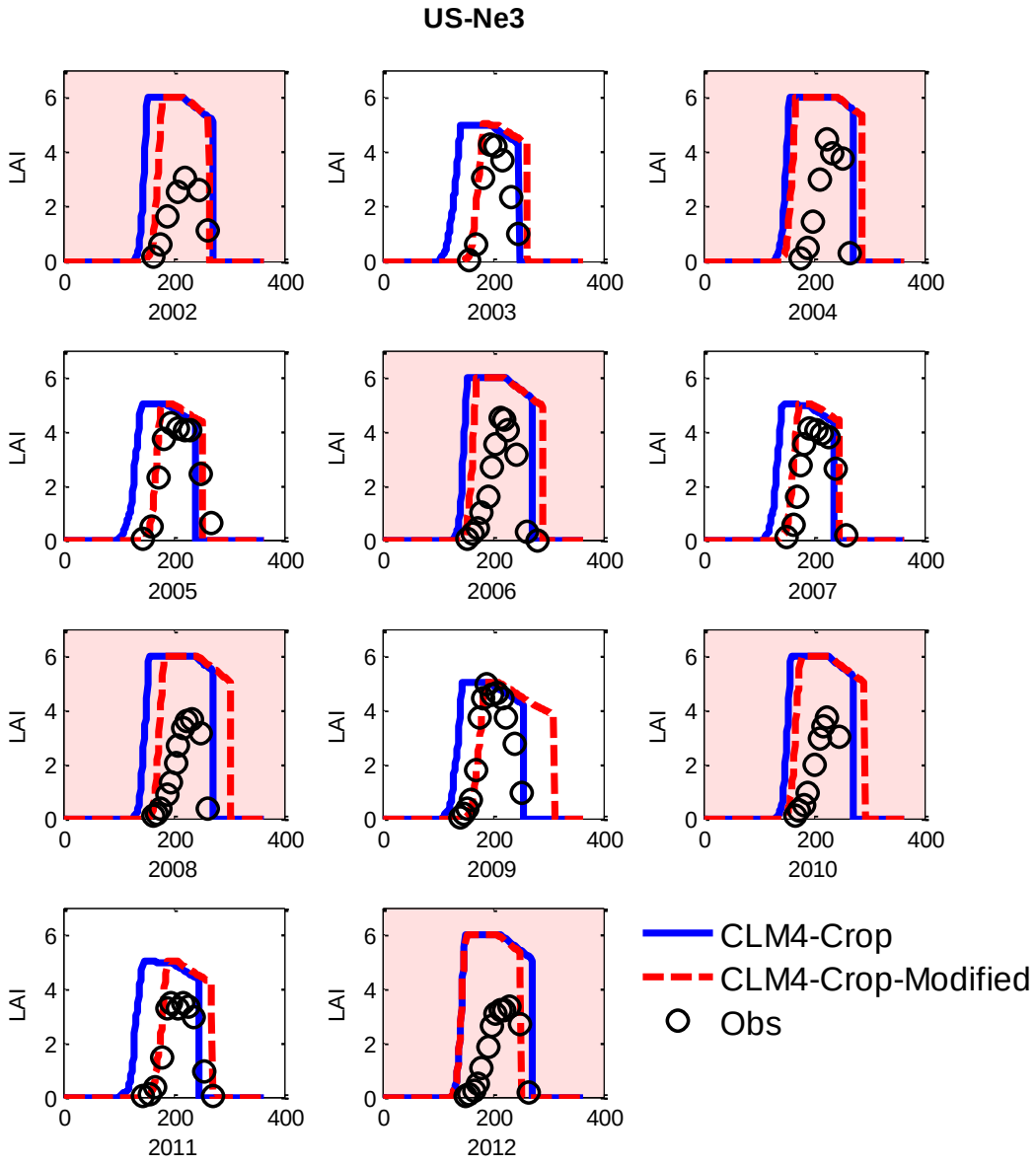

Figure 3.3 Evaluation of the simulated phenology for corn (white background) and soybean (red background) at a rainfed AmeriFlux site Mead (US-Ne3). The blue line represents default CLM4-Crop simulation and the red dashed line represents CLM4-Crop with modified phenology according to chapter two.

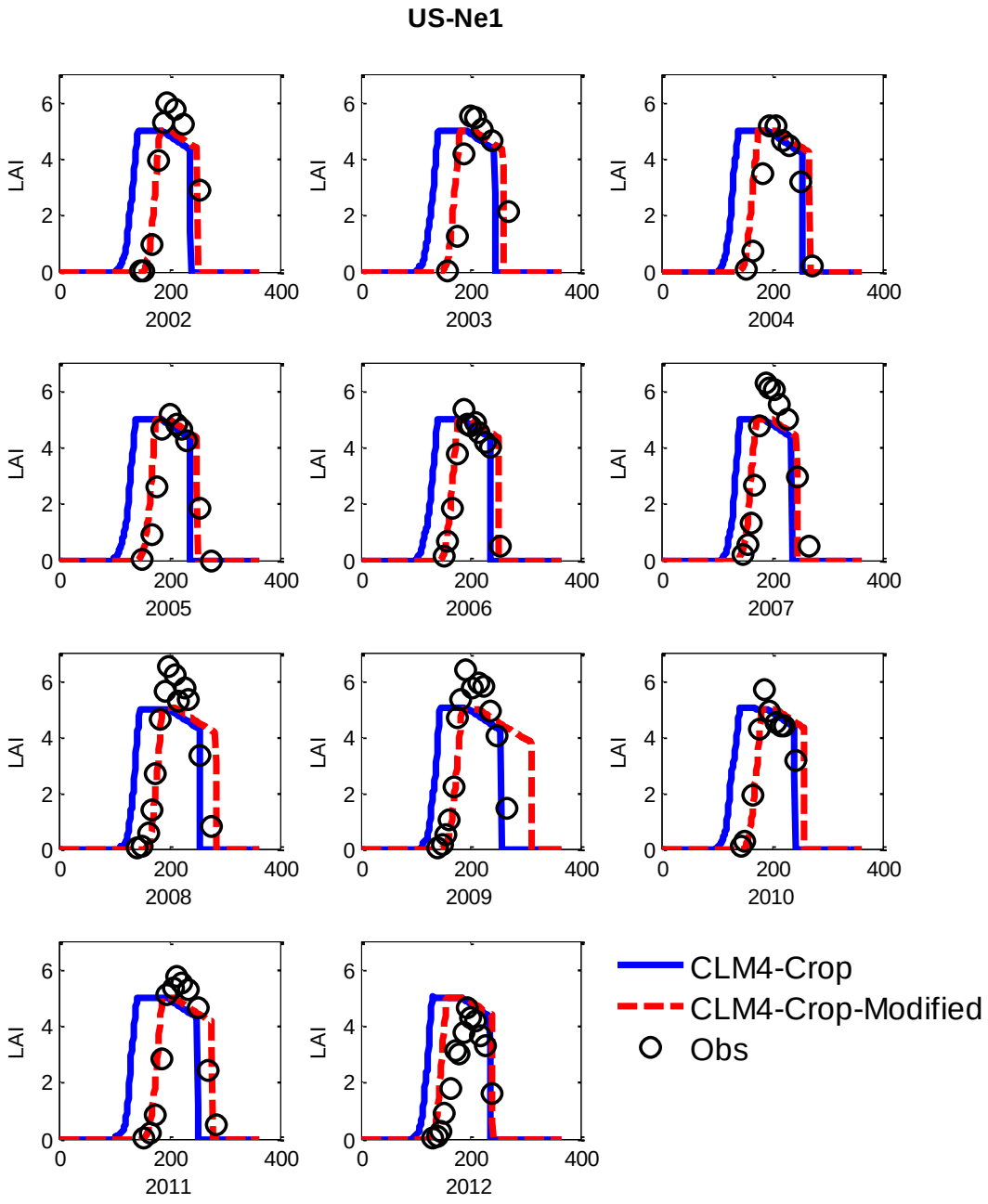

Figure 3.4 Evaluation of the simulated phenology for corn at an irrigated AmeriFlux site Mead (US-Ne1). The blue line represents default CLM4-Crop simulation and the red dashed line represents CLM4-Crop with modified phenology according to chapter two.

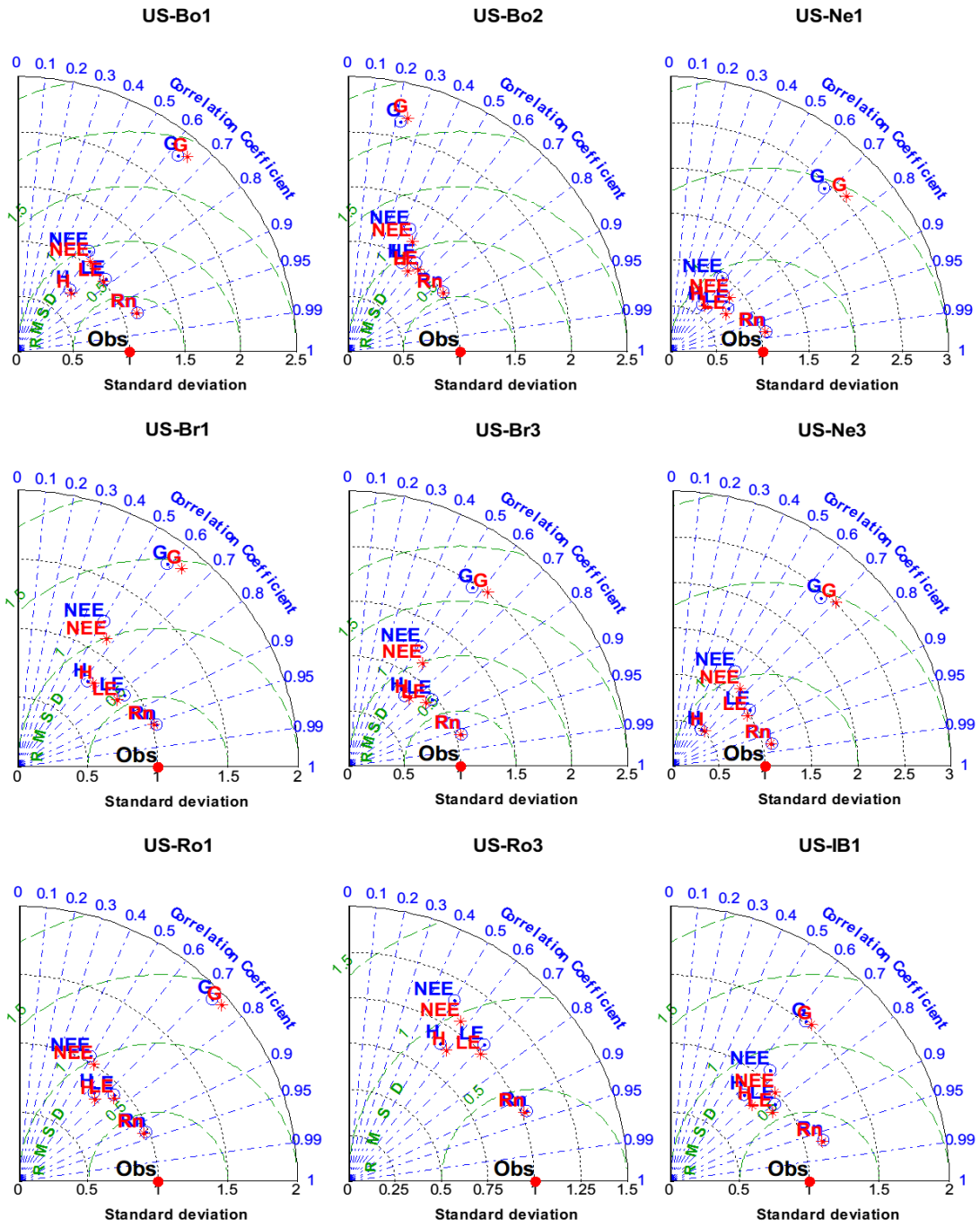

Figure 3.5 Across sites evaluation of the hourly energy fluxes and NEE simulation. Results are shown in Taylor diagrams. The standard deviations are normalized by the standard deviations of the observed values. The blue colored variables are the default CLM4-Crop simulations. The red colored variables are CLM4-CropM simulations.

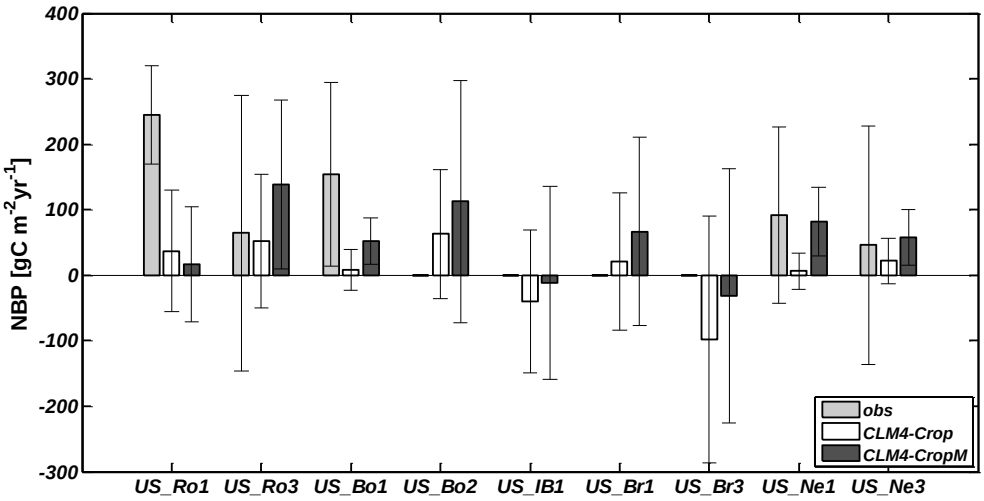

Figure 3.6 Cross-site comparison of the GDD and GDT methods simulated annual carbon budgets (NBP) at the nine AmeriFlux sites. The err bar is standard deviation of the annual mean NBP. At the sites US-Ro1, US-Ro3, US-Bo1, US-Ne1 and US-Ne3, yield data are available. Thus at those sites the measured annual carbon budgets were shown to be compred with the modeled values.

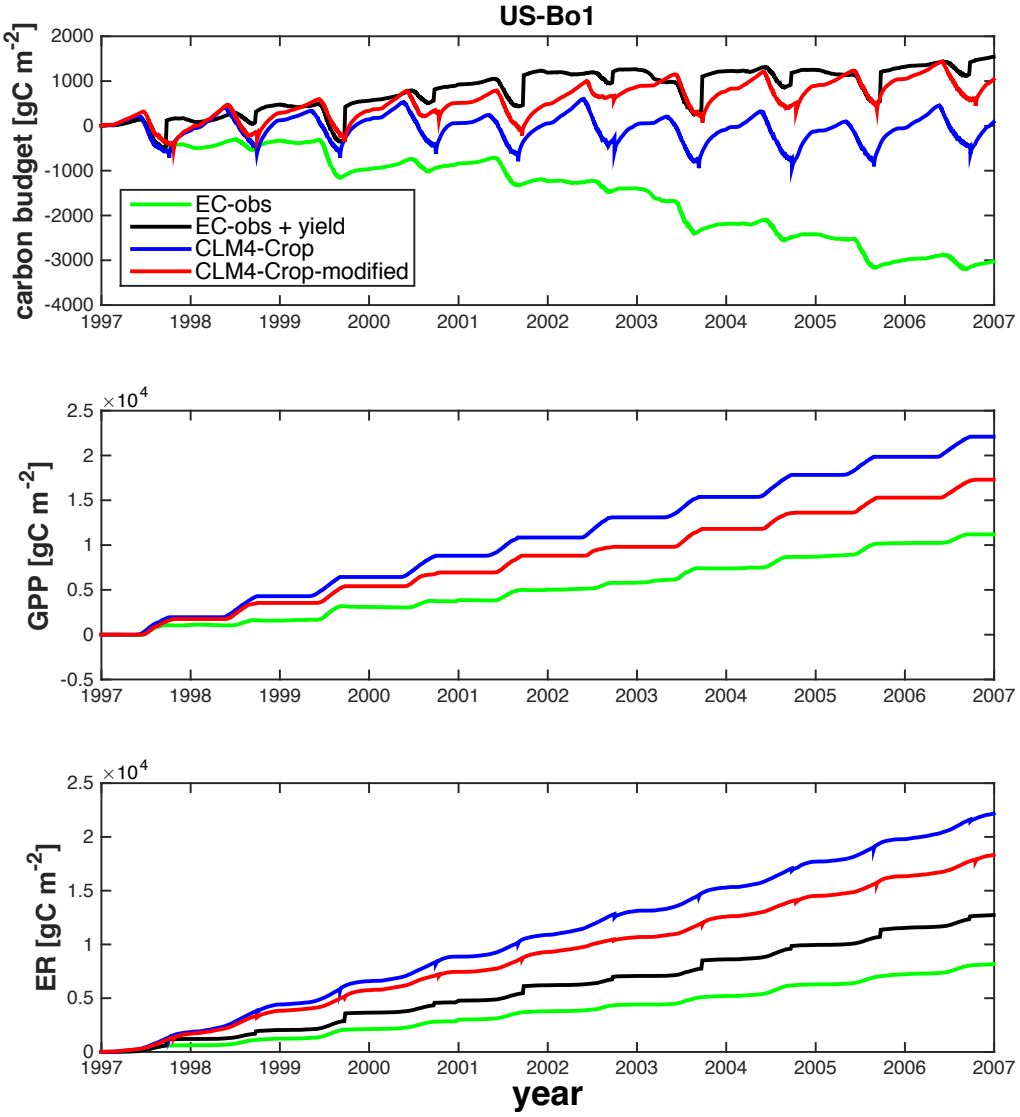

Figure 3.7 Long-term carbon budget simulation at site US-Bo1. The green line represents carbon fluxes calculated using the eddy covariance measured carbon fluxes. The black line is the eddy covariance measured carbon fluxes plus annual yield grain carbon from the field. The blue line is the default CLM4-Crop simulation and the red line is CLM4-CropM simulation.

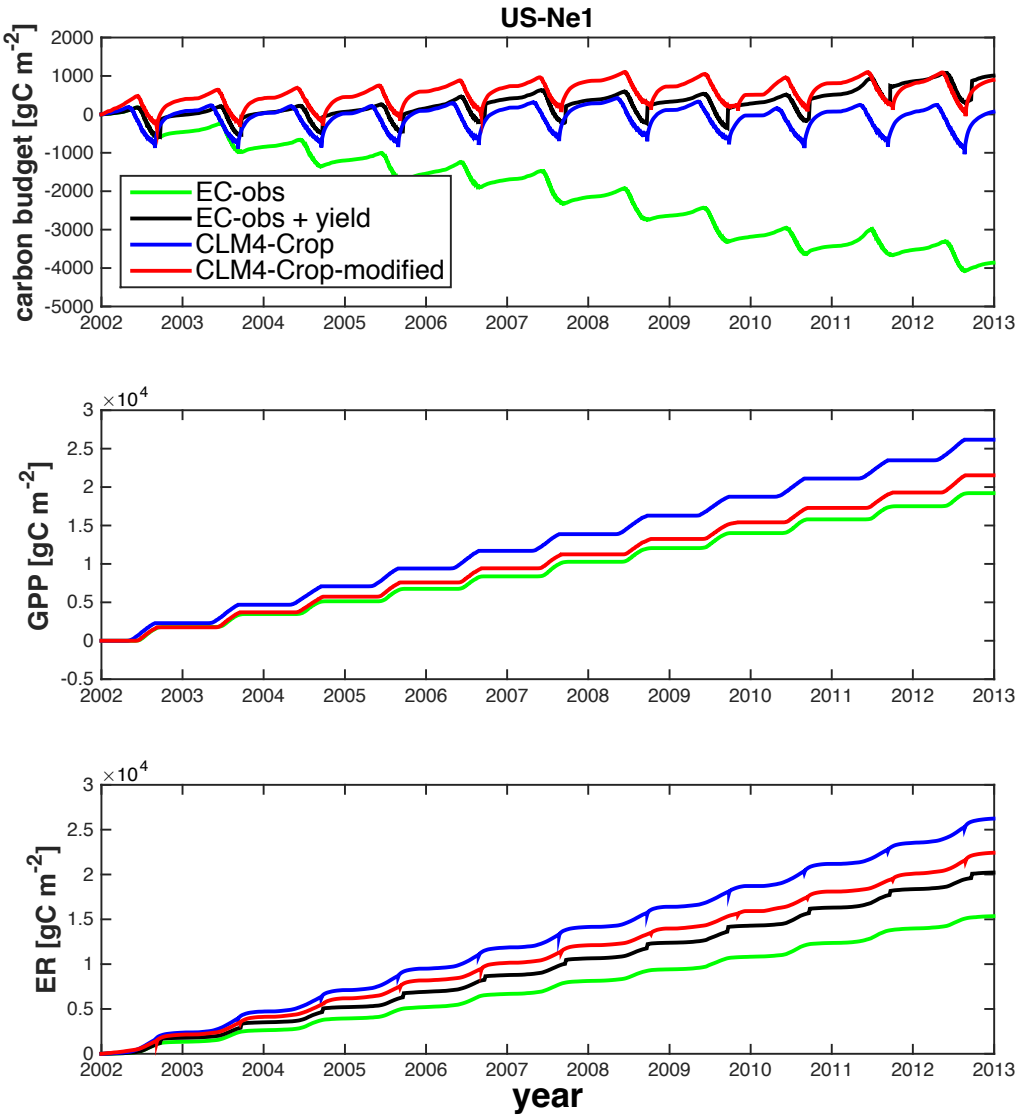

Figure 3.8 Long-term carbon budget simulation at site US-Ne1. The green line represents carbon fluxes calculated using the eddy covariance measured carbon fluxes. The black line is the eddy covariance measured carbon fluxes plus annual yield grain carbon from the field. The blue line is the default CLM4-Crop simulation and the red line is CLM4-CropM simulation.

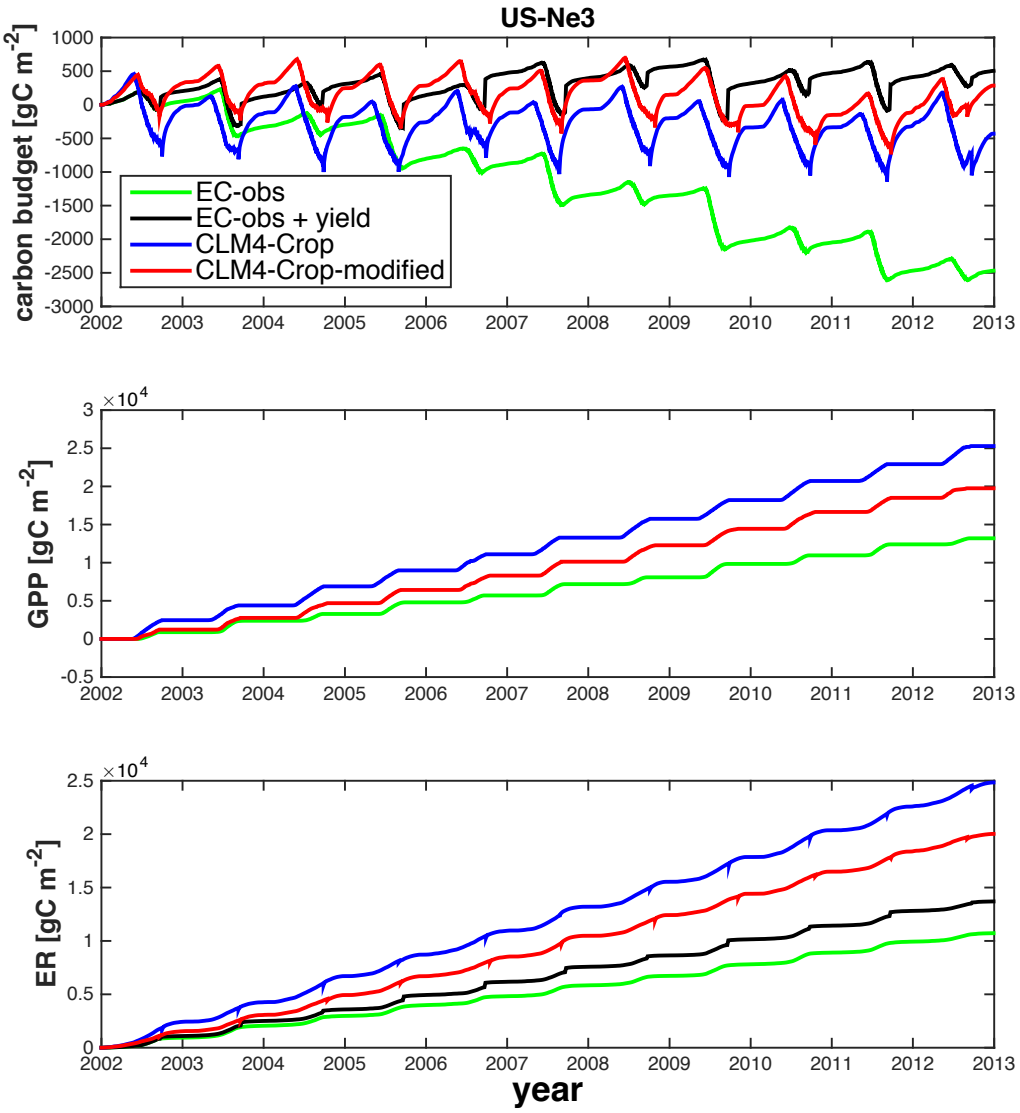

Figure 3.9 Long-term carbon budget simulation at site US-Ne3. The green line represents carbon fluxes calculated using the eddy covariance measured carbon fluxes. The black line is the eddy covariance measured carbon fluxes plus annual yield grain carbon from the field. The blue line is the default CLM4-Crop simulation and the red line is CLM4-CropM simulation.

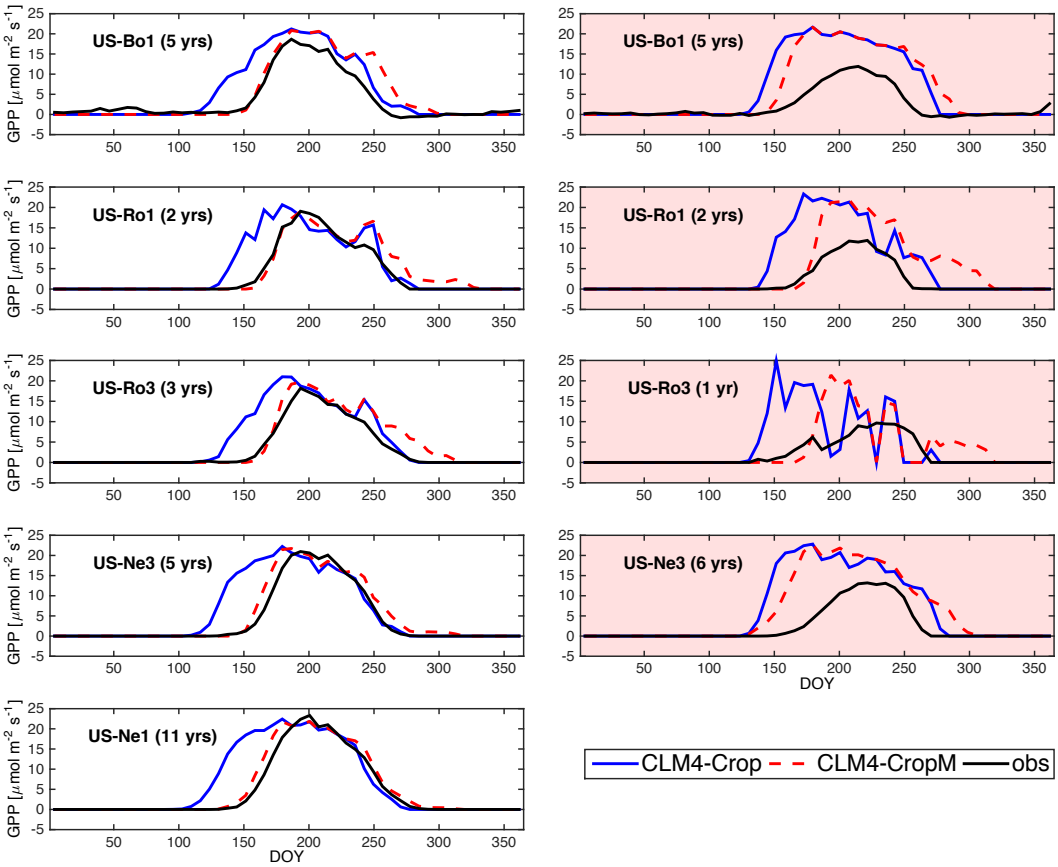

Figure 3.10 Annually averaged weekly GPP simulation for Corn and Soybean years respectively across sites. White background indicates corn years and red background indicates soybean years.

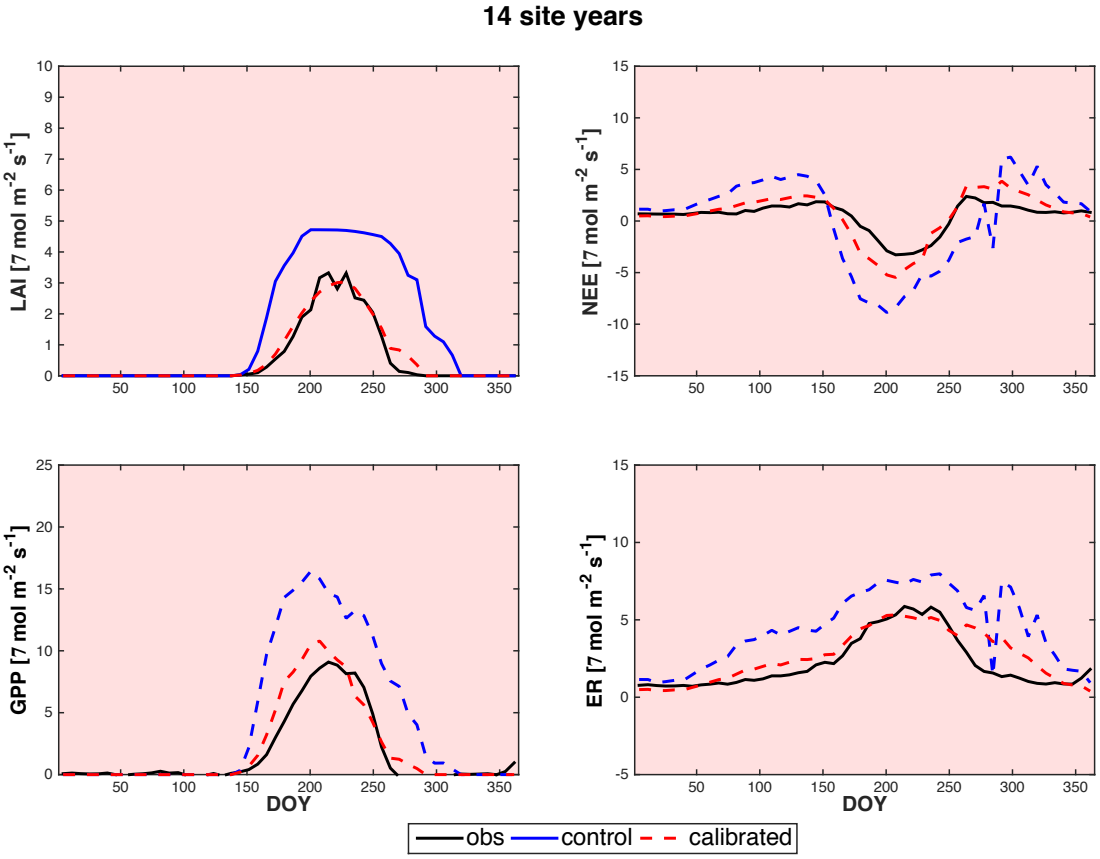

Figure 3.11 Calibration of the model simulated soybean LAI, NEE, GPP and ER. All values are weekly average of the variables over 14 site years. Parameters used in the control run and the calibration run can be found in table 3.5.

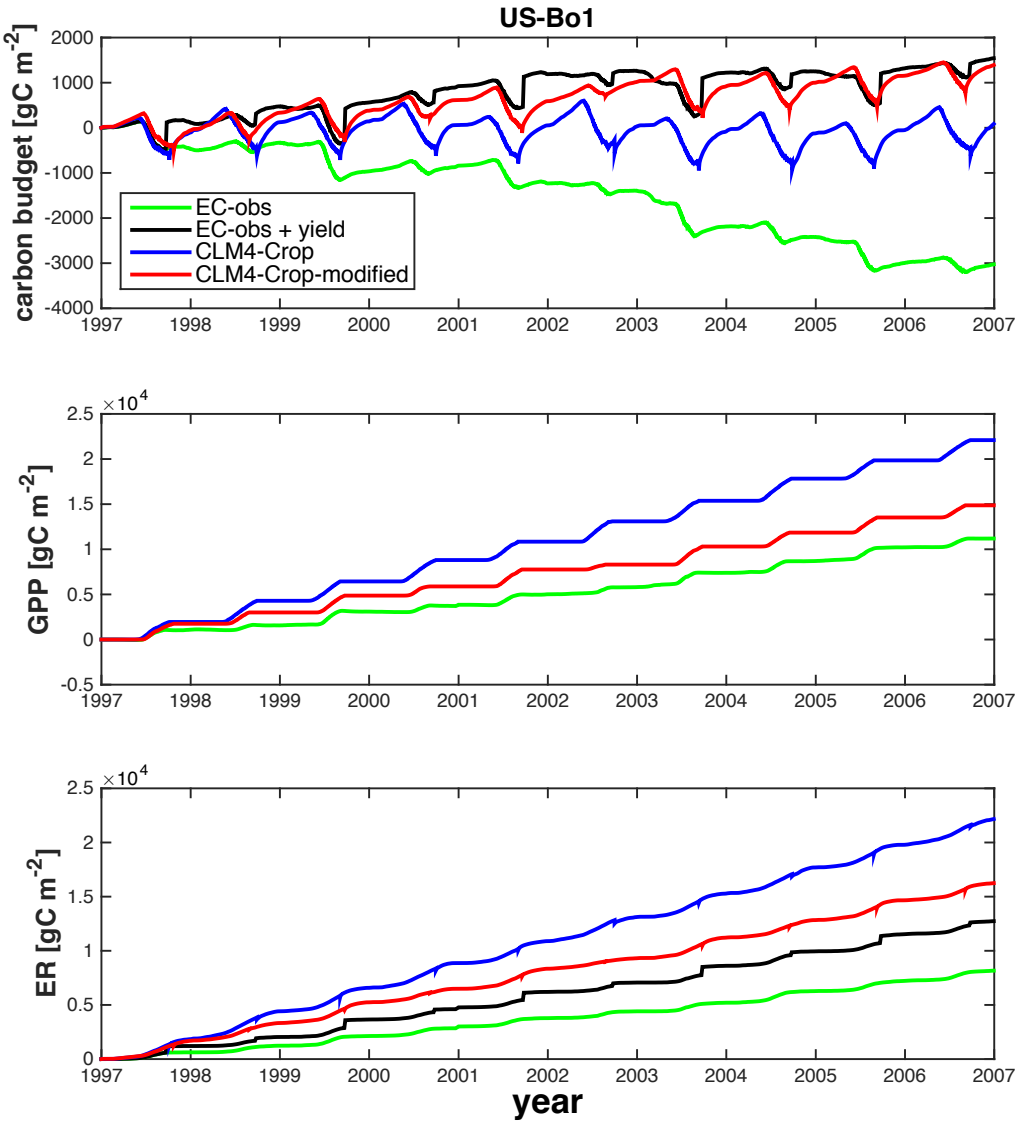

Figure 3.12 Long-term carbon budget simulation at site US-Bo1 (after calibration). The red line is the calibrated CLM4-CropM simulation. The green line represents carbon fluxes calculated using the eddy covariance measured carbon fluxes. The black line is the eddy covariance measured carbon fluxes plus annual yield grain carbon from the field. The blue line is the default CLM4-Crop simulation.

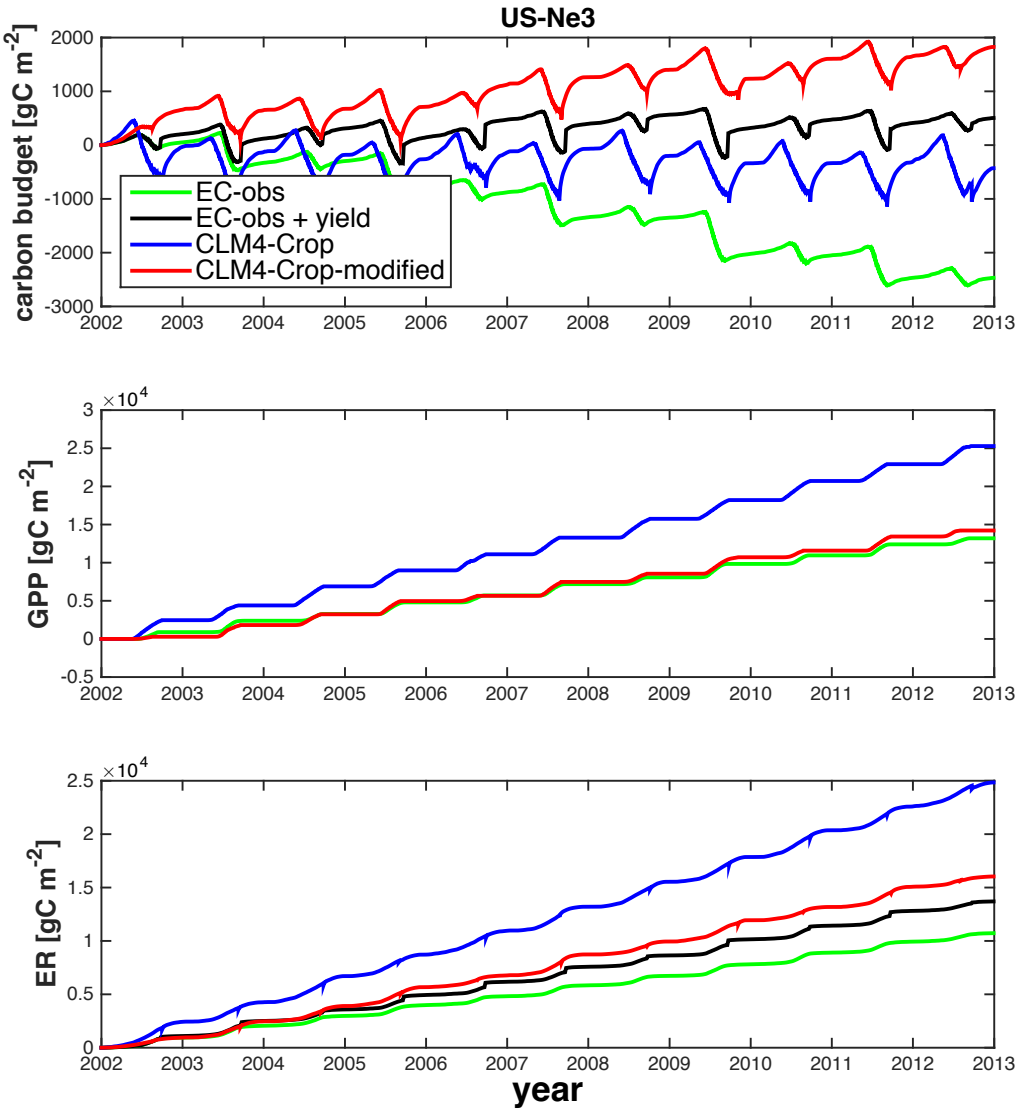

Figure 3.13 Long-term carbon budget simulation at site US-Ne3 (after calibration). The red line is the calibrated CLM4-CropM simulation. The green line represents carbon fluxes calculated using the eddy covariance measured carbon fluxes. The black line is the eddy covariance measured carbon fluxes plus annual yield grain carbon from the field. The blue line is the default CLM4-Crop simulation.

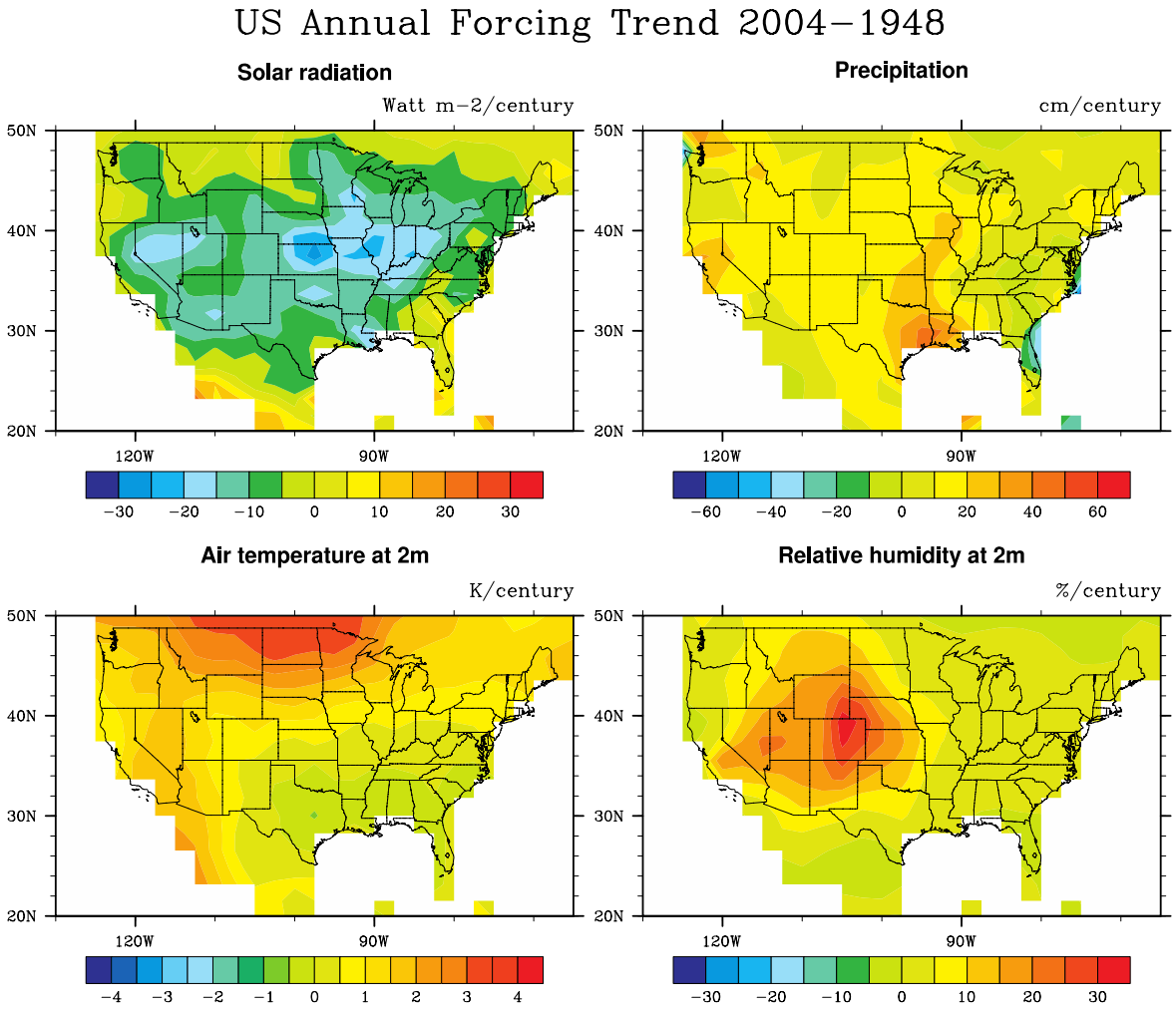

Figure 4.1 Trend of meteorological forcing in the United States from 1948 to 2004.

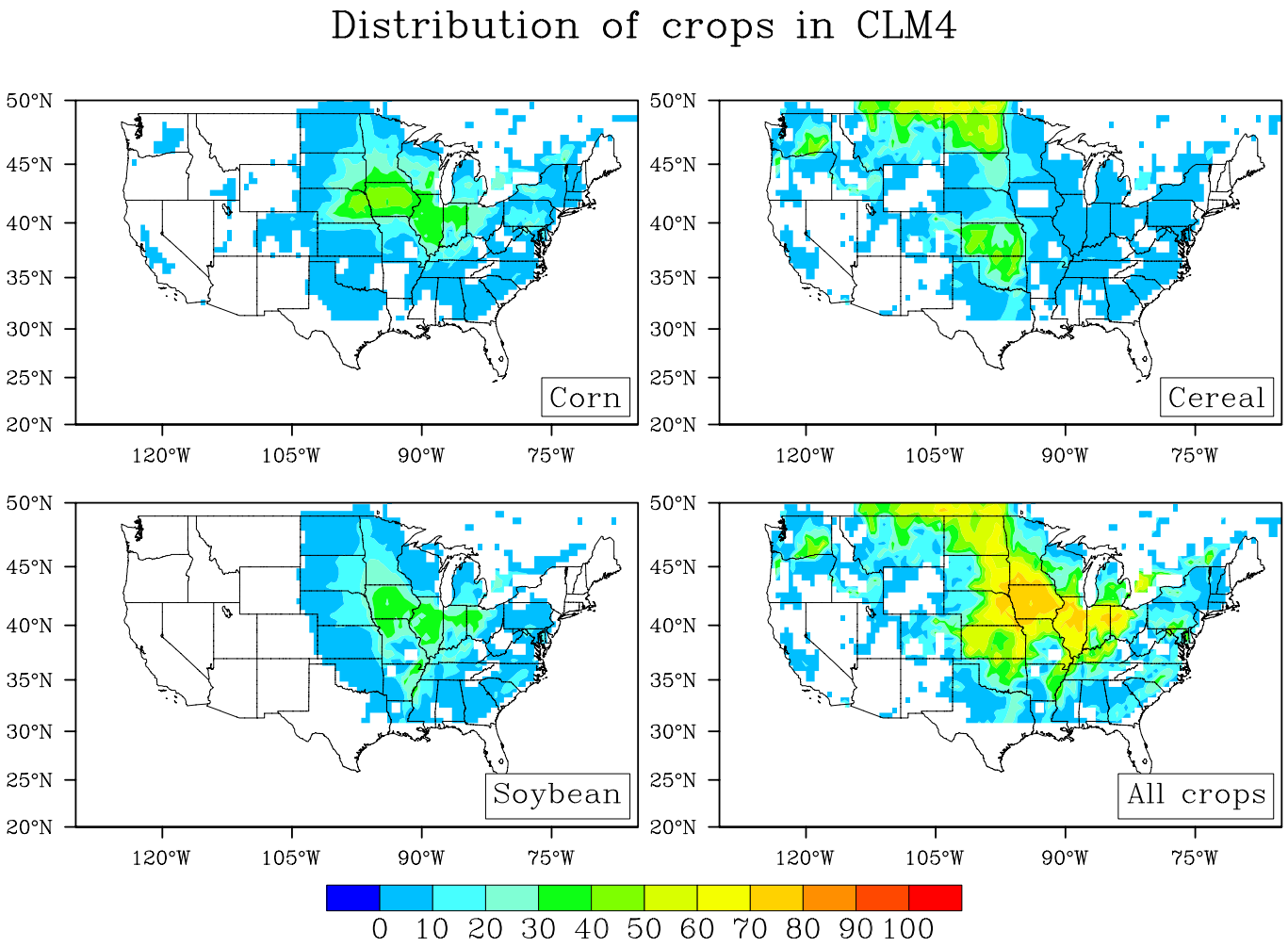

Figure 4.2 Crop distributions in CLM4-Crop. Colors represent the percentage (%) of the crop PFT in a grid cell.

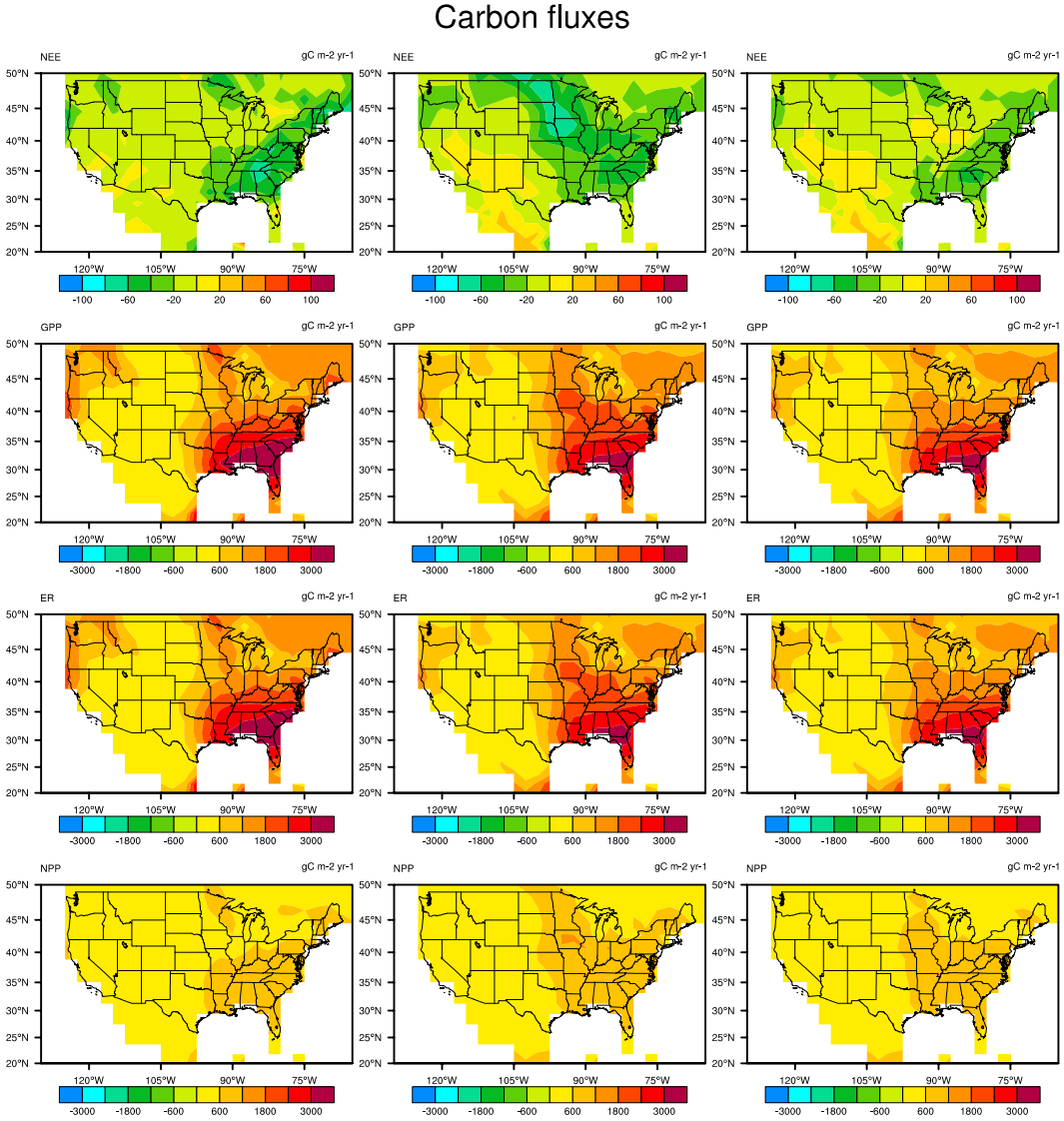

Figure 4.3 Averaged NEE, GPP, ER and NPP for the period 1948 to 2004 simulated by CLM4-CN (first column), CLM4-Crop (second column) and CLM4-CropM (third column).

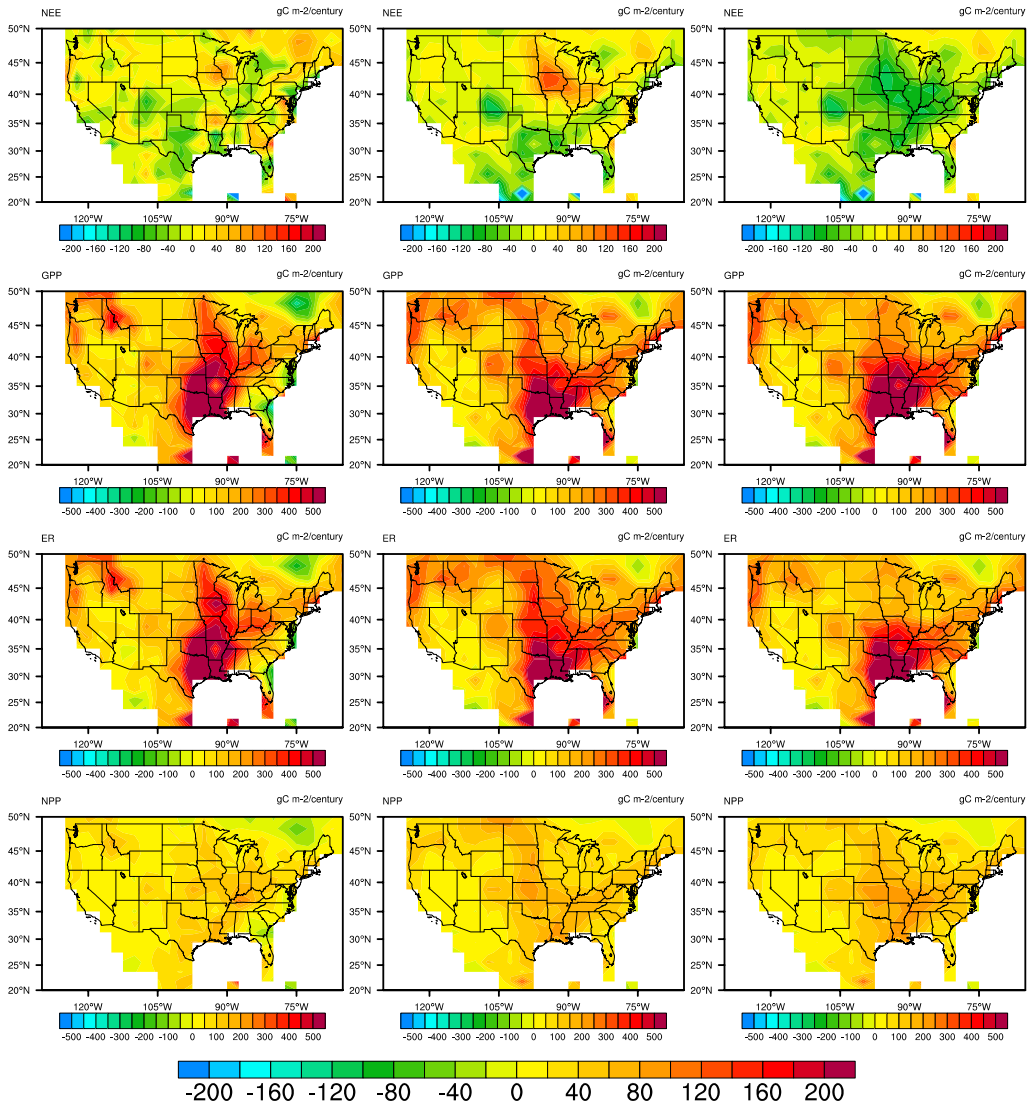

Figure 4.4 Trend of NEE, GPP, ER and NPP for the period 1948 to 2004 simulated by CLM4-CN (first column), CLM4-Crop (second column) and CLM4-CropM (third column).

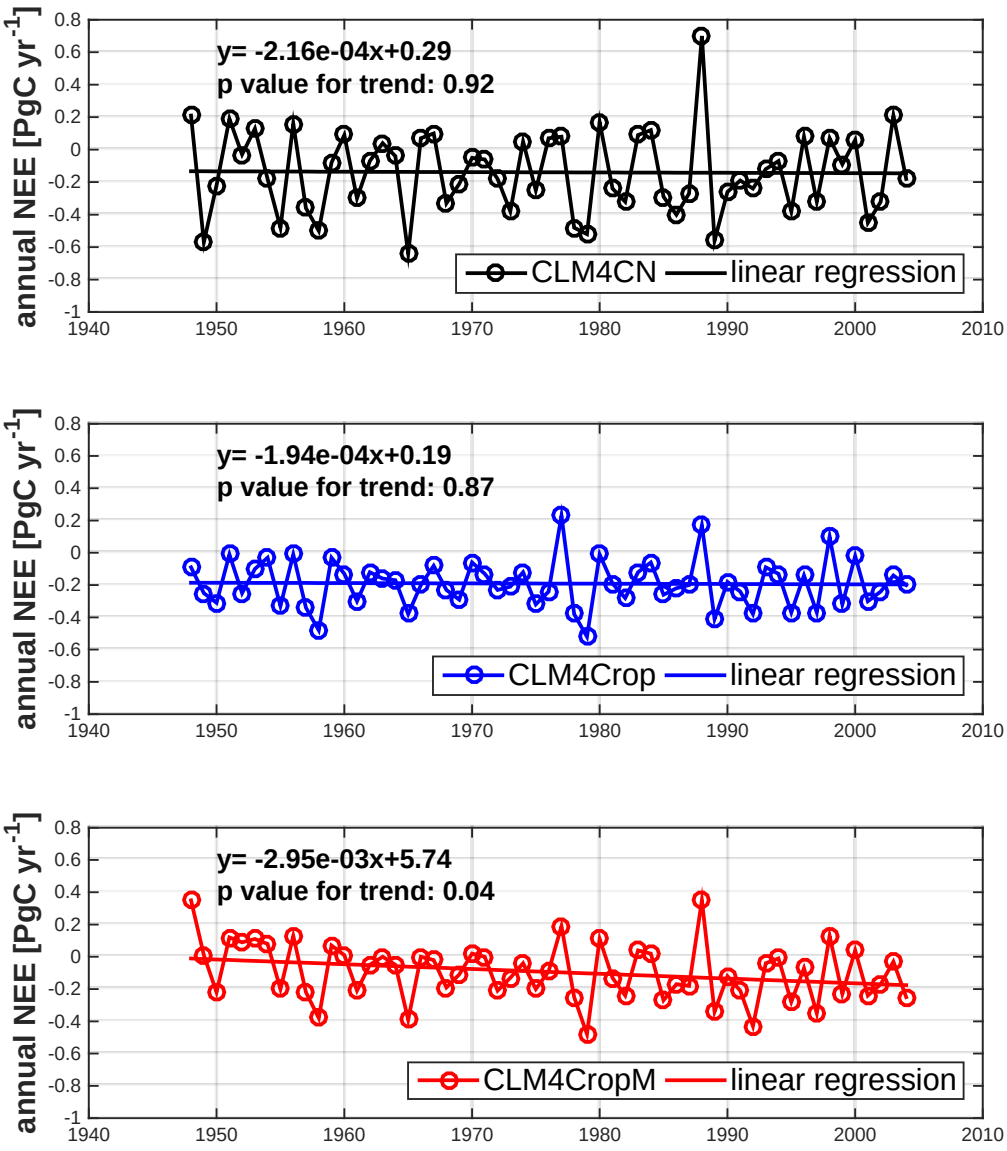

Figure 4.5 Time series of annual NEE for the conterminous United States from 1948 to 2004 simulated by CLM4-CN, CLM4-Crop and CLM4-CropM.